THE ROLE OF PDIA3 IN VITAMIN D SIGNALING IN OSTEOBLASTS

A Dissertation
Presented to
The Academic Faculty

By

Jiaxuan Chen

In Partial Fulfillment
of the Requirements for the Degree
Doctor of Philosophy in the
Department of Biomedical Engineering

Georgia Institute of Technology
December 2012

THE ROLE OF PDIA3 IN VITAMIN D SIGNALING IN OSTEOBLASTS

Thesis committee members:

Dr. Barbara D. Boyan, Advisor
Department of Biomedical Engineering
Georgia Institute of Technology

Dr. Todd C. McDevitt
Department of Biomedical Engineering
Georgia Institute of Technology

Dr. Zvi Schwartz
Department of Biomedical Engineering
Georgia Institute of Technology

Dr. Kirill S. Lobachev
School of Biology
Georgia Institute of Technology

Dr. Hong Chen
School of Medicine
Emory University

ACKNOWLEDGEMENTS

First, I would like to thank my advisors Dr. Barbara D. Boyan and Dr. Zvi Schwartz. In 2007, I came from China to Georgia Tech to pursue my Ph.D. Dr.Boyan was kind enough to take a young international student with little related research experience. Through my five year period of Ph.D. study, Dr. Boyan has exposed me to many different perspectives of being a good researcher. I have learned how to properly interpret the data, critique a paper, make a presentation, give a talk, submit a manuscript, respond to reviewers, and many other skills. For this, I am very thankful. Besides the field of research, Dr.Boyan always gave me support to pursuit what is the best of my interests. I am very grateful for her and Dr.Schwartz's support on my transferring my field of study to become a biomedical engineer, so I have the opportunity to establish my career in the field I am most interested in. Dr.Schwartz is the person who was involved in the design of every experiment conducted in this thesis. He has taught me how to make a hypothesis, how to design an experiment and how to set up proper controls when I was still an inexperienced graduate student. Ever since then, we have been going through both the good results and the bad ones and experiencing the exciting moments and the frustrating ones. He has always been inspiring me, challenging me and demanding more from me. Because of him, I was able to accomplish this thesis today, for which I am greatly appreciative. I would also like to thank my thesis committee members. Dr. Lobachev has been a great collaborator and has given me much help in establishing the site-directed mutations. Dr. McDevitt and Dr. Chen have provided their time and insight, and I am very appreciative to them for that.

I would also like to thank the members of Boyan and Schwartz's lab. They have been really helpful throughout the years. I would like to thank Leang Chhun, Crystal

Branan, Sri Vemula and Lauren Carson for their help in cell culture. Ms. Brentis Henderson and Shannon Sullivan have made the administration process so much easier. Reyhaan Chaudhri, Sharon Hyzy, Dr. Rene Olivares-Navarrete and Dr. Yun Wang have taught me from how to use a pipette to many other useful lab techniques. Without their help, this study would not have been possible. All of the Boyan laboratory graduate students have made my life here more enjoyable: Jiaying Guo, Reyhaan Chaudhri, Bryan Bell, Tracy Denison, Chris Lee, Andrew Raines, Khairat El- Baradie, Jennifer Hurst-Kennedy, Jamie Lazin, Maya Fisher, Ming Zhong, Tanya Farooque, Chris Hermann, Rolando Gittens, Jennie Park, Maryam Doroudi, Brandy Rogers, Shirae Leslie, Meredith Myers, Qingfen Pan, Erin Hewitt, James Wade, Alice Cheung, and Srishti Bhutani. I would also like to thank my parents. Although they are oversea in China, they have always been there to support, motivate and comfort me. Without their help, I would not get to where I am today.

TABLE OF CONTENTS

LIST OF TABLES

LIST OF FIGURES

SUMMARY

1α,25-Dihydroxyvitamin D3 (1α,25$(OH)_2D_3$) is a major functional metabolic form of vitamin D. 1α,25$(OH)_2D_3$ is traditionally known for maintaining calcium homeostasis. Over the past decade, increasingly new functions of 1α,25$(OH)_2D_3$ have been dicovered in bone, cartilage, muscle, immune system, neural system, and cancer. In order to maximize the pharmaceutical potential of 1α,25$(OH)_2D_3$, a better understanding its cell signaling pathway is necessary. 1α,25$(OH)_2D_3$ regulates osteoblasts through both classical nuclear vitamin D receptor (nVDR) mediated genomic effects and plasma membrane receptor-mediated rapid responses. The identity of the plasma membrane receptor for 1α,25$(OH)_2D_3$ is controversial. Protein disulfide isomerase family A, member 3 (Pdia3) has been hypothesized as one of the putative plasma membrane receptors for 1α,25$(OH)_2D_3$. The *overall goal* of this thesis was to understand the general role and the molecular mechanism of Pdia3 in 1α,25$(OH)_2D_3$-initiated rapid responses, and to determine the role of Pdia3 and its dependent signalings in osteoblast biology. This was evaluated in three specific aims: 1) to determine the role of Pdia3 in membrane-mediated responses of 1α,25$(OH)_2D_3$. 2) to determine the molecular mechanism of Pdia3 function in membrane-mediated responses of 1α,25$(OH)_2D_3$ and 3) to determine the role of Pdia3 in osteoblast mineralization. The results showed that Pdia3 is required for membrane-mediated responses of 1α,25$(OH)_2D_3$. Moreover, both Pdia3 and nVDR are critical components of the plasma membrane receptor complex for 1α,25$(OH)_2D_3$. Finally, Pdia3 and signaling via Pdia3 regulate osteoblast differentiation and mineralization. Taken together, this study demonstrates the role of Pdia3 in rapid responses to 1α,25$(OH)_2D_3$ and osteoblast biology, reveals the unexpected complexity of the 1α,25$(OH)_2D_3$ plasma receptor complex and opens the new target, Pdia3, and its asscociated signaling, for pharmaceutical application and tissue engineering.

CHAPTER 1. Introduction

1.1 The significance of vitamin D research.

Over the past decade, vitamin D has become the most popular vitamin in the research field. According to Pubmed, as of today, using vitamin D as a key word returns 56130 hits, which is greater than any single vitamin. Over 40% of the hits were published in the last decade. From 2007 to 2012, there was an average annual increase of 15% in the number of vitamin D related publications. This is exceptional in comparison to other vitamins. For vitamin A, there is no increase for the number of publications per year for the past twenty years. Therefore, vitamin D has drawn an exceptional amount of attention in recent years.

This trend is mainly due to the broad range of novel functions that have been discovered for vitamin D aside from its classical role in maintaining calcium and phosphate homeostasis. For normal tissue function, vitamin D has a direct role in regulation of cartilage matrix production (1), osteoblast mineralization (2), heart muscle contraction (3), stem cell differentiation (4, 5), immune responses (6) and skin cell survivability (7). In pathological conditions, vitamin D has shown beneficial effects in treating various types of cancer, diabetes, and multiple sclerosis (8-12) besides its well known efficacy in treating rickets and preventing osteoporosis. The reasons for its broad functions in a variety of cell types could be explained from its unexpected complicity in downstream signaling pathways, many of which are not well understood. This gap between fundamental mechanisms to clinical application largely limits its pharmaceutical potential. The scope of this thesis is to investigate a novel plasma membrane vitamin D receptor and its associated pathway and how they are crucial to vitamin D function and basic cellular physiology. The knowledge gained form this study can have a board impact in clinical applications, from directing normal tissue development in tissue

engineering to offering new pharmaceutical targets.

1.2 Vitamin D Family

Vitamin D is the name of a group of fat soluble, steroid hormones. All vitamin D family members, as many other steroid hormones, are composed of the basic four ring structure of cholesterol (A ring, B ring, C ring and D ring). Different from other steroids, one of the bonds in the B-rings is broken in vitamin D. Molecules with this characteristic chemical structure are named as secosteroids. These include vitamin D1, D2, D3, D4 and D5 in the vitamin D family. They all share a similar basic secosteroid structure with differences in the side chains. The generic name of vitamin D usually referrers to vitamin D2 and vitamin D3. Among these different forms, Vitamin D3, also called cholecalciferol is the only form of vitamin D that vertebrate animals naturally produce. Vitamin D2 or ergocalciferol, is produced only in phytoplankton, invertebrates and fungi. It is also used as a common form of vitamin D supplement for its highly similar physiological function to vitamin D3, although some controversy remains as to whether it could completely replace vitamin D3 (13).

1.3 The metabolic pathway of vitamin D

In the human body, 7-dehydrocholesterol is the precursor of vitamin D3. In the skin, under UV-B light irradiation, the B-ring of 7-dehydrocholesterol is broken and pre-vitamin D3 is formed, which will naturally isomerize to vitamin D3. However, vitamin D3 is not yet in its functional form and it needs further modifications. In the blood stream, the vitamin D binding protein (DBP), which binds with hydrophobic vitamin D3 either formed in the skin or absorbed from oral ingestion, helps vitamin D3 circulating in the blood stream. When vitamin D3 travels into the liver, it is catalytically processed with an extra hydroxyl group on the 25^{th} carbon of the side chain by vitamin D 25-hydroxylase

(CYP2R1) (Figure 1-1). This metabolite is called 25 hydroxyvitamin D3 (25(OH)D3) and it is the major form of circulating vitamin D3 metabolites in the body by abundance. Although liver cells are the principle cell type producing 25(OH)D3, other cells such as keratinocytes and macrophages have CYP2R1 activity too. 25(OH)D3 will be further catalyzed into 1α,25 dihydroxyvitamin D3 (1α,25(OH)2D3) in the kidney by the enzyme 25-hydroxyvitamin D-1 alpha hydroxylase (CYP27B1) (Figure 1-1). 1α,25(OH)2D3 has one more hydroxyl group at the 1α position of the A-ring and it is a major functional metabolite of vitamin D3. It has broad functions in many tissues and organs in the human body, which will be introduced later.

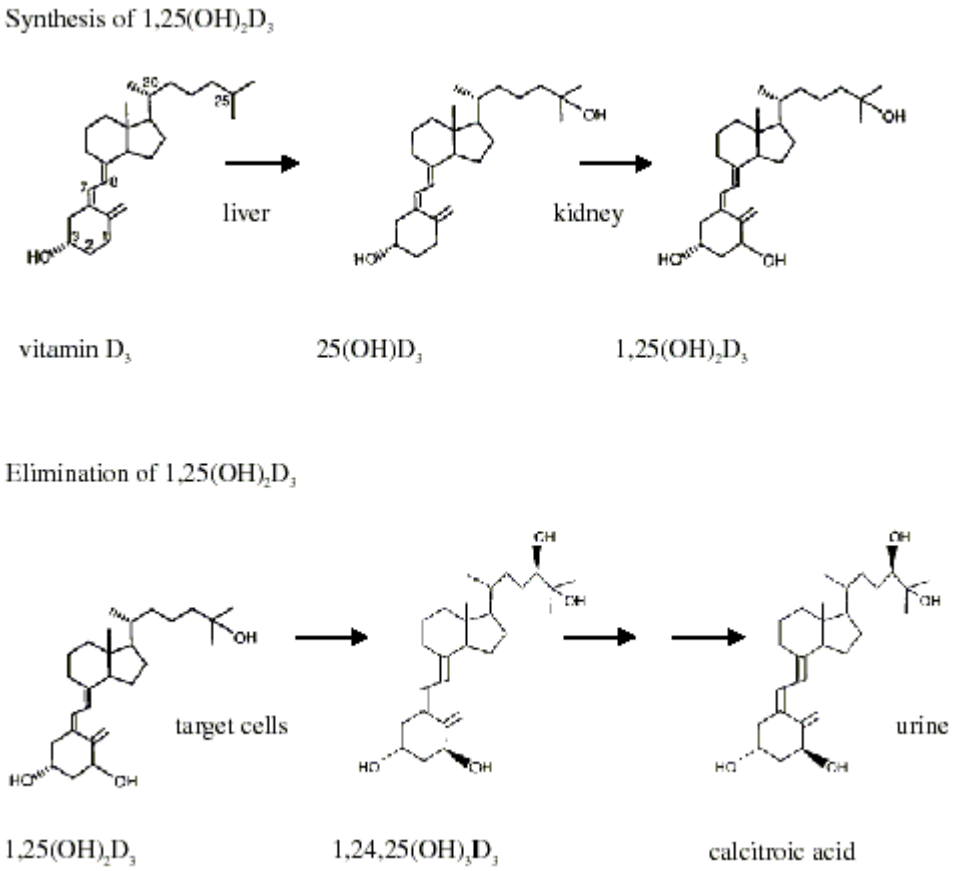

Figure 1-1. The schematic representation of key metabolic and catabolic steps of vitamin D3.

In order to adjust the concentration of 1α,25(OH)2D3 and avoid toxicity, many 1α,25(OH)2D3 targeted tissues such as kidney, intestine and bones, have vitamin D 24-hydroxylase (CYP24A1). This enzyme can add another hydroxyl group onto the 24th carbon on both 25(OH)D3 and 1α,25(OH)2D3 and correspondingly generates 24, 25-dihydroxyvitamin D3 (24,25(OH)2D3) and 1α,24,25-trihydroxyvitamin D3 (1α,24,25(OH)3D3) (Figure 1-1). While 24,25(OH)2D3 and 1α,24,25(OH)3D3 are traditionally considered as inactive catabolic byproducts, newer studies reveal that 24,25(OH)2D3 has its own specific physiological functions, especially in growth plate cartilage (1, 14). Kidney cells actively re-absorb 1α,25(OH)2D3 but not the 24th carbon hydroxylated metabolites. Therefore, 24,25(OH)2D3 and 1α,24,25(OH)3D3 would eventually leave the body through the excretory system.

1.4 The function of 1α,25(OH)2D3

The functional metabolite, 1α,25(OH)2D3, is well known for its role in maintaining calcium and phosphate homeostasis. In the intestine, 1α,25(OH)2D3 can stimulate the absorption of calcium and phosphate from the gut lumen into the blood stream (15). Similar to the intestine, calcium re-absorption in the distal tubes of the kidney is also promoted by 1α,25(OH)2D3 (16). In the area of bone and mineralization, 1α,25(OH)2D3 deficiency has been associated with rickets and osteoporosis (17, 18). 1α,25(OH)2D3 and calcium supplements have been prescribed as a treatment to rickets and osteoporosis (17, 19, 20). Recently, increasing amount of new function of 1α,25(OH)2D3 have been discovered, many of which have been described in session 1.1.

1.5 The genomic pathways and nuclear vitamin D receptor

Shortly after the discovery of 1α,25(OH)2D3 and its function in the absorption of calcium in the intestine, the signaling pathways and receptor that mediate its function

were intensively studied. Inhibitors were used to block new mRNA and protein synthesis. Calcium absorption was partially blocked indicating the requirement for new protein synthesis (15). Radio-labeled 1α,25(OH)2D3 was also found to travel into the nucleus of bone cells in a rachitic chick model, which further supports the role of gene expression in this function (21). In 1969, a 1α,25(OH)2D3 nuclear vitamin D receptor (VDR) was purified from the nuclear chromatin of the mucosa of the rachitic chicks (22). It was further found to be present in cytosol and to translocate into nucleus after binding with 1α,25(OH)2D3. In the nucleus, the receptor-ligand complex forms a heterodimer with retinoid X receptor (RXR), and together they bind to specific sequences called vitamin D responsive elements (VDRE) to regulate gene expression (23). Using gene expression microarray, and VDRE predictions, 1α,25(OH)2D3 have been found to regulate the expression of many genes in cell signaling, matrix composition, differentiation and proliferation (24-26).

1.6 Rapid responses and plasma membrane vitamin D receptor

Besides genomic regulation, which can take from hours to days, 1α,25(OH)2D3 can also activate a series of signaling changes on the order of seconds to minutes. These changes are considered to be too fast to be mediated by genomic regulation (27, 28). They are named after rapid responses to be distinguished from the VDR mediated genomic changes. Several cell models have been used to elucidate the role of rapid signaling by 1α,25(OH)2D3. In growth plate chondrocytes, 1α,25(OH)2D3 rapidly regulates phospholipase A_2 (PLA_2) activity, phospholipase C (PLC) activity, intracellular Ca^{2+} mobilization and protein kinase C (PKC) activity (29-31). Moreover, experiments using matrix vesicles isolated from these cells, which do not contain RNA or DNA, and therefore no gene expression or protein synthesis, demonstrated clearly that rapid actions of the steroid hormone could have consequences independent from the

traditional nuclear receptor-mediated outcomes (30). In osteoblasts, 1α,25(OH)2D3 has also been shown to rapidly activate PLC and PKC, regulating voltage gated Ca^{2+} and Cl^- channels, and increase PLA_2 activity and prostaglandin (PGE_1 and PGE_2) production (32-35). Besides the musculoskeletal system, rapid response to 1α,25(OH)2D3 were also found to regulate a broad range of cellular physiology in other cells. Some of the examples include intestinal absorption of calcium, secretion of insulin by pancreatic β cells, photo-protection against UV damage in skin and tailoring the contraction of heart muscle cells (36-39).

Besides their direct physiological consequences, rapid responses such as ion influx and enzymatic activity changes may eventually modulate gene transcription. 1α,25(OH)2D3 regulates gene expression in rat growth zone chondrocytes via PKC and extracellular signal-regulated kinases 1 and 2 (ERK1/2) in a Pdia3-dependent pathway leading to extracellular matrix protein production (40). Microarray analysis of rat osteoblastic ROS 17/2.8 cells treated with a 1α,25(OH)2D3 analogue with low binding affinity to VDR also demonstrated regulation of a large number of genes through an intracellular calcium-dependent mechanism (41, 42).

Today, the rapid responses of 1α,25(OH)2D3 are well accepted. But regarding the plasma membrane receptor to 1α,25(OH)2D3, there is still controversy. Protein disulfide isomerase family A, membrane 3 (Pdia3; also known as ERp60, ERp57, Grp58, and 1,25-MARRS) has been identified as a potential membrane-associated receptor for 1α,25(OH)2D3. It has been intensively studied as a chaperone protein in glycoprotein folding (43) and major histocompatibility complex I loading (44). Unlike other protein disulfide isomerase family members, Pdia3 exists not only in the endoplasmic reticulum but also in the nucleus, plasma membrane, and extracellular matrix, suggesting it has additional functions (45). In the field of 1α,25(OH)2D3, key observations using chick intestinal epithelial cells indicated that a receptor for 1,25(OH)2D3 was on the plasma

membrane and that it was distinct from the VDR (46). The presence of this novel receptor was confirmed using osteoblasts and growth plate chondrocytes, as well as extracellular matrix vesicles produced by these cells (47, 48). Later, this novel plasma membrane receptor was indentified to be the same protein as Pdia3 (49). More recently, antibody-blocking and knock down experiments have further linked this protein to rapid responses to 1α,25(OH)2D3 in rat chondrocytes, rat osteoblasts, and chick intestinal epithelial cells (48-50). In 2010, an *in vivo* study showed the epithelial cells isolated from Pdia3-conditional knockout mice lost the surface binding and rapid responses to 1α,25(OH)2D3 (39). These data have demonstrated the role of Pdia3 in 1α,25(OH)2D3 rapid responses.

Besides Pdia3, traditional VDR has also been found in the caveolae fraction of plasma membranes and has been showed to bind with 1α,25(OH)2D3 *in vivo* and *in vitro* (51). In 2004, an alternative 1α,25(OH)2D3 binding pocket in VDR was found, which is proposed for initiating rapid responses (52, 53). Later, a functional VDR was also shown to be necessary to initiate rapid responses in different studies (32, 54-56).

Some controversy over the requirement of VDR in rapid responses has been due to differences in animal models. The genetic lesion in the two major VDR knockout mouse strains is different (57, 58). Moreover, the same outcomes are not investigated by different laboratories. Intestinal epithelial cells isolated from one strain of VDR-/- mice, which was generated in the laboratory of Kato, lack the ability to transport Ca^{2+} in response to 1,25(OH)2D3 (59), indicating that VDR is required for transcaltachia via modulation of voltage gated ion channels in this cell type. In contrast, a different strain of VDR-/- mice generated in the laboratory of Marie DeMay (57) showed 1,25(OH)2D3-dependent rapid PKC activation remained not only in its growth plate chondrocytes (34, 60), but also in its osteoblasts, as does transcaltachia (34).

1.7 Thesis objective

Vitamin D has drawn intense attention in the fields of skeletal development, cancer prevention, and immunology. A deeper understanding of vitamin D signaling, especially the less known rapid signaling, will be especially valuable to provide new approaches to vitamin D supplement and treatment of diseases. Moreover, elucidating the mechanism of how Pdia3, a well known chaperone protein, functions as or as a part of a 1α,25(OH)2D3 plasma membrane receptor would be a breakthrough in the field of steroid hormone membrane receptors. It would not only increase our basic knowledge about the function of chaperone proteins and steroid hormone receptors but also provide new promising cell surface targets for pharmaceutical applications. Lastly, understanding the effect of Pdia3 regulation on osteoblast differentiation and mineralization would provide a new angle to enhance bone formation in tissue engineering.

The overall objective of this thesis was to understand the general role and the molecular mechanism of Pdia3 in 1α,25(OH)2D3-initiated rapid responses, and to determine the role of Pdia3 and its dependent signaling pathway in osteoblast physiology. The first specific aim was to determine the role of Pdia3 in membrane-mediated responses of 1α,25(OH)2D3 in osteoblasts. In this aim, we used an RNA silencing technique to knock down Pdia3 and a plasmid to overexpress Pdia3 and we found rapid responses could either be turned off or augmented. In this aim, we also examined the 1α,25(OH)2D3-regulated gene expression and *in vitro* 2D mineralization and we showed Pdia3 also affects these downstream physiological changes.

The second aim was to determine the molecular mechanism of Pdia3 in membrane-mediated responses to 1α,25(OH)2D3. In this study, we focus on comparing the relative role of Pdia3 and VDR as plasma membrane receptor. We found that both Pdia3 and VDR exist in caveolae where they connect with downstream mediators. Silencing either receptor cause a block on signaling mediators as well as rapid

response-induced physiological changes. We also mutated specific amino acids that are important for the chaperone role of Pdia3 and found that these amino acids are also important for rapid responses.

The third aim was to determine the role of Pdia3 in osteoblast mineralization in a 3D poly-caprolactone *in vitro* model. Besides the role of 1α,25(OH)2D3, we also examined the interaction between 1α,25(OH)2D3 and the bone morphogenetic protein 2 (BMP-2) in osteoblast mineralization. We found that 1α,25(OH)2D3 and BMP-2 have a synergistic effect on osteoblast maturation in 2D and mineralization in 3D. Furthermore, the effect of 1α,25(OH)2D3 and the synergistic effect between 1α,25(OH)2D3 and BMP-2 are mediated by both Pdia3 and VDR.

Taken together, this thesis demonstrates the role of Pdia3 in rapid responses to 1α,25(OH)2D3 and osteoblast physiology, reveals the unexpected complexity of plasma receptor complex and opened the new target, Pdia3, and its associated signaling for pharmaceutical application and tissue engineering.

1.8 References

1. Schwartz Z, Schlader DL, Ramirez V, Kennedy MB, Boyan BD. Effects of vitamin D metabolites on collagen production and cell proliferation of growth zone and resting zone cartilage cells in vitro. J Bone Miner Res.4:199-207. 1989.
2. Chen J, Olivares-Navarrete R, Wang Y, Herman TR, Boyan BD, Schwartz Z. Protein-disulfide isomerase-associated 3 (Pdia3) mediates the membrane response to 1,25-dihydroxyvitamin D3 in osteoblasts. J Biol Chem.285:37041-50. 2010.
3. Tishkoff DX, Nibbelink KA, Holmberg KH, Dandu L, Simpson RU. Functional vitamin D receptor (VDR) in the t-tubules of cardiac myocytes: VDR knockout cardiomyocyte contractility. Endocrinology.149:558-64. 2008.
4. Piek E, Sleumer LS, van Someren EP, Heuver L, de Haan JR, de Grijs I, et al. Osteo-transcriptomics of human mesenchymal stem cells: accelerated gene expression and osteoblast differentiation induced by vitamin D reveals c-MYC as an enhancer of BMP2-induced osteogenesis. Bone.46:613-27. 2010.
5. Song I, Kim BS, Kim CS, Im GI. Effects of BMP-2 and vitamin D3 on the osteogenic differentiation of adipose stem cells. Biochem Biophys Res Commun.408:126-31. 2011.
6. Lagishetty V, Liu NQ, Hewison M. Vitamin D metabolism and innate immunity. Mol Cell Endocrinol.347:97-105. 2011.
7. Sequeira VB, Rybchyn MS, Tongkao-On W, Gordon-Thomson C, Malloy PJ, Nemere I, et al. The role of the vitamin D receptor and ERp57 in photoprotection by 1alpha,25-dihydroxyvitamin D3. Mol Endocrinol.26:574-82. 2012.
8. Becklund BR, Hansen DW, Jr., Deluca HF. Enhancement of 1,25-dihydroxyvitamin D3-mediated suppression of experimental autoimmune encephalomyelitis by calcitonin. Proc Natl Acad Sci U S A.106:5276-81. 2009.
9. Mathieu C, Waer M, Casteels K, Laureys J, Bouillon R. Prevention of type I diabetes in NOD mice by nonhypercalcemic doses of a new structural analog of 1,25-dihydroxyvitamin D3, KH1060. Endocrinology.136:866-72. 1995.
10. Yudoh K, Matsuno H, Kimura T. 1alpha,25-dihydroxyvitamin D3 inhibits in vitro invasiveness through the extracellular matrix and in vivo pulmonary metastasis of B16 mouse melanoma. The Journal of laboratory and clinical medicine.133:120-8. 1999.
11. Lee HJ, Paul S, Atalla N, Thomas PE, Lin X, Yang I, et al. Gemini vitamin D analogues inhibit estrogen receptor-positive and estrogen receptor-negative mammary tumorigenesis without hypercalcemic toxicity. Cancer Prev Res (Phila).1:476-84. 2008.
12. Wali RK, Bissonnette M, Khare S, Hart J, Sitrin MD, Brasitus TA. 1 alpha,25-Dihydroxy-16-ene-23-yne-26,27-hexafluorocholecalciferol, a noncalcemic analogue of 1 alpha,25-dihydroxyvitamin D3, inhibits azoxymethane-induced colonic tumorigenesis. Cancer Res.55:3050-4. 1995.
13. Chen PS, Jr., Bosmann HB. EFFECT OF VITAMINS D2 AND D3 ON SERUM CALCIUM AND PHOSPHORUS IN RACHITIC CHICKS. The Journal of nutrition.83:133-9. 1964.
14. Schwartz Z, Sylvia VL, Liu Y, Dean DD, Boyan BD. Treatment of resting zone chondrocytes with bone morphogenetic protein-2 induces maturation into a phenotype characteristic of growth zone chondrocytes by downregulating responsiveness to 24,25(OH)2D3 and upregulating responsiveness to 1,25-(OH)2D3. Endocrine.9:273-80. 1998.
15. Favus MJ. Factors that influence absorption and secretion of calcium in the small intestine and colon. Am J Physiol.248:G147-57. 1985.
16. Hofmeister MV, Fenton RA, Praetorius J. Fluorescence isolation of mouse late distal convoluted tubules and connecting tubules: effects of vasopressin and vitamin D3 on Ca2+ signaling. Am J Physiol Renal Physiol.296:F194-203. 2009.

17. Holick MF. Resurrection of vitamin D deficiency and rickets. J Clin Invest.116:2062-72. 2006.
18. Holick MF. Vitamin D deficiency. N Engl J Med.357:266-81. 2007.
19. Jackson RD, LaCroix AZ, Gass M, Wallace RB, Robbins J, Lewis CE, et al. Calcium plus vitamin D supplementation and the risk of fractures. N Engl J Med.354:669-83. 2006.
20. Larsen ER, Mosekilde L, Foldspang A. Vitamin D and calcium supplementation prevents osteoporotic fractures in elderly community dwelling residents: a pragmatic population-based 3-year intervention study. J Bone Miner Res.19:370-8. 2004.
21. Weber JC, Pons V, Kodicek E. The localization of 1,25-dihydroxycholecalciferol in bone cell nuclei of rachitic chicks. The Biochemical journal.125:147-53. 1971.
22. Haussler MR, Norman AW. Chromosomal receptor for a vitamin D metabolite. Proc Natl Acad Sci U S A.62:155-62. 1969.
23. Ozono K, Sone T, Pike JW. The genomic mechanism of action of 1,25-dihydroxyvitamin D3. J Bone Miner Res.6:1021-7. 1991.
24. Lin R, Nagai Y, Sladek R, Bastien Y, Ho J, Petrecca K, et al. Expression profiling in squamous carcinoma cells reveals pleiotropic effects of vitamin D3 analog EB1089 signaling on cell proliferation, differentiation, and immune system regulation. Mol Endocrinol.16:1243-56. 2002.
25. Akutsu N, Lin R, Bastien Y, Bestawros A, Enepekides DJ, Black MJ, et al. Regulation of gene Expression by 1alpha,25-dihydroxyvitamin D3 and Its analog EB1089 under growth-inhibitory conditions in squamous carcinoma Cells. Mol Endocrinol.15:1127-39. 2001.
26. Wang TT, Tavera-Mendoza LE, Laperriere D, Libby E, MacLeod NB, Nagai Y, et al. Large-scale in silico and microarray-based identification of direct 1,25-dihydroxyvitamin D3 target genes. Mol Endocrinol.19:2685-95. 2005.
27. Langston GG, Swain LD, Schwartz Z, Del Toro F, Gomez R, Boyan BD. Effect of 1,25(OH)2D3 and 24,25(OH)2D3 on calcium ion fluxes in costochondral chondrocyte cultures. Calcif Tissue Int.47:230-6. 1990.
28. Civitelli R, Kim YS, Gunsten SL, Fujimori A, Huskey M, Avioli LV, et al. Nongenomic activation of the calcium message system by vitamin D metabolites in osteoblast-like cells. Endocrinology.127:2253-62. 1990.
29. Schwartz Z, Graham EJ, Wang L, Lossdorfer S, Gay I, Johnson-Pais TL, et al. Phospholipase A2 activating protein (PLAA) is required for 1alpha,25(OH)2D3 signaling in growth plate chondrocytes. J Cell Physiol.203:54-70. 2005.
30. Schwartz Z, Sylvia VL, Larsson D, Nemere I, Casasola D, Dean DD, et al. 1alpha,25(OH)2D3 regulates chondrocyte matrix vesicle protein kinase C (PKC) directly via G-protein-dependent mechanisms and indirectly via incorporation of PKC during matrix vesicle biogenesis. J Biol Chem.277:11828-37. 2002.
31. Schwartz Z, Gilley RM, Sylvia VL, Dean DD, Boyan BD. Prostaglandins mediate the effects of 1,25-(OH)2D3 and 24,25-(OH)2D3 on growth plate chondrocytes in a metabolite-specific and cell maturation-dependent manner. Bone.24:475-84. 1999.
32. Zanello LP, Norman AW. Electrical responses to 1alpha,25(OH)2-Vitamin D3 and their physiological significance in osteoblasts. Steroids.69:561-5. 2004.
33. Baran DT. Nongenomic actions of the steroid hormone 1 alpha,25-dihydroxyvitamin D3. J Cell Biochem.56:303-6. 1994.
34. Wali RK, Kong J, Sitrin MD, Bissonnette M, Li YC. Vitamin D receptor is not required for the rapid actions of 1,25-dihydroxyvitamin D3 to increase intracellular calcium and activate protein kinase C in mouse osteoblasts. J Cell Biochem.88:794-801. 2003.
35. Matthews L, Berry A, Ohanian V, Ohanian J, Garside H, Ray D. Caveolin

mediates rapid glucocorticoid effects and couples glucocorticoid action to the antiproliferative program. Mol Endocrinol.22:1320-30. 2008.
36. Zhao G, Simpson RU. Interaction between vitamin D receptor with caveolin-3 and regulation by 1,25-dihydroxyvitamin D3 in adult rat cardiomyocytes. J Steroid Biochem Mol Biol.121:159-63. 2010.
37. Sequeira VB, Rybchyn MS, Tongkao-On W, Gordon-Thomson C, Malloy PJ, Nemere I, et al. The Role of the Vitamin D Receptor and ERp57 in Photoprotection by 1alpha,25-Dihydroxyvitamin D3. Mol Endocrinol. 2012.
38. Kajikawa M, Ishida H, Fujimoto S, Mukai E, Nishimura M, Fujita J, et al. An insulinotropic effect of vitamin D analog with increasing intracellular Ca2+ concentration in pancreatic beta-cells through nongenomic signal transduction. Endocrinology.140:4706-12. 1999.
39. Nemere I, Garbi N, Hammerling GJ, Khanal RC. Intestinal cell calcium uptake and the targeted knockout of the 1,25D3-MARRS (membrane-associated, rapid response steroid-binding) receptor/PDIA3/Erp57. J Biol Chem.285:31859-66. 2010.
40. Schwartz Z, Ehland H, Sylvia VL, Larsson D, Hardin RR, Bingham V, et al. 1alpha,25-dihydroxyvitamin D(3) and 24R,25-dihydroxyvitamin D(3) modulate growth plate chondrocyte physiology via protein kinase C-dependent phosphorylation of extracellular signal-regulated kinase 1/2 mitogen-activated protein kinase. Endocrinology.143:2775-86. 2002.
41. Farach-Carson MC, Bergh JJ, Xu Y. Integrating rapid responses to 1,25-dihydroxyvitamin D3 with transcriptional changes in osteoblasts: Ca2+ regulated pathways to the nucleus. Steroids.69:543-7. 2004.
42. Farach-Carson MC, Xu Y. Microarray detection of gene expression changes induced by 1,25(OH)(2)D(3) and a Ca(2+) influx-activating analog in osteoblastic ROS 17/2.8 cells. Steroids.67:467-70. 2002.
43. Jessop CE, Chakravarthi S, Garbi N, Hammerling GJ, Lovell S, Bulleid NJ. ERp57 is essential for efficient folding of glycoproteins sharing common structural domains. EMBO J.26:28-40. 2007.
44. Peaper DR, Wearsch PA, Cresswell P. Tapasin and ERp57 form a stable disulfide-linked dimer within the MHC class I peptide-loading complex. EMBO J.24:3613-23. 2005.
45. Khanal RC, Nemere I. The ERp57/GRp58/1,25D3-MARRS receptor: multiple functional roles in diverse cell systems. Curr Med Chem.14:1087-93. 2007.
46. Nemere I, Dormanen MC, Hammond MW, Okamura WH, Norman AW. Identification of a specific binding protein for 1 alpha,25-dihydroxyvitamin D3 in basal-lateral membranes of chick intestinal epithelium and relationship to transcaltachia. J Biol Chem.269:23750-6. 1994.
47. Nemere I, Schwartz Z, Pedrozo H, Sylvia VL, Dean DD, Boyan BD. Identification of a membrane receptor for 1,25-dihydroxyvitamin D3 which mediates rapid activation of protein kinase C. J Bone Miner Res.13:1353-9. 1998.
48. Boyan BD, Bonewald LF, Sylvia VL, Nemere I, Larsson D, Norman AW, et al. Evidence for distinct membrane receptors for 1 alpha,25-(OH)(2)D(3) and 24R,25-(OH)(2)D(3) in osteoblasts. Steroids.67:235-46. 2002.
49. Nemere I, Farach-Carson MC, Rohe B, Sterling TM, Norman AW, Boyan BD, et al. Ribozyme knockdown functionally links a 1,25(OH)2D3 membrane binding protein (1,25D3-MARRS) and phosphate uptake in intestinal cells. Proc Natl Acad Sci U S A.101:7392-7. 2004.
50. Wang Y, Chen J, Lee CS, Nizkorodov A, Riemenschneider K, Martin D, et al. Disruption of Pdia3 gene results in bone abnormality and affects 1alpha,25-dihydroxy-vitamin D3-induced rapid activation of PKC. J Steroid Biochem Mol Biol.121:257-60.

2010.
51. Huhtakangas JA, Olivera CJ, Bishop JE, Zanello LP, Norman AW. The vitamin D receptor is present in caveolae-enriched plasma membranes and binds 1 alpha,25(OH)2-vitamin D3 in vivo and in vitro. Mol Endocrinol.18:2660-71. 2004.
52. Mizwicki MT, Keidel D, Bula CM, Bishop JE, Zanello LP, Wurtz JM, et al. Identification of an alternative ligand-binding pocket in the nuclear vitamin D receptor and its functional importance in 1alpha,25(OH)2-vitamin D3 signaling. Proc Natl Acad Sci U S A.101:12876-81. 2004.
53. Norman AW. Minireview: vitamin D receptor: new assignments for an already busy receptor. Endocrinology.147:5542-8. 2006.
54. Zhang X, Zanello LP. Vitamin D receptor-dependent 1 alpha,25(OH)2 vitamin D3-induced anti-apoptotic PI3K/AKT signaling in osteoblasts. J Bone Miner Res.23:1238-48. 2008.
55. Buitrago C, Boland R. Caveolae and caveolin-1 are implicated in 1alpha,25(OH)2-vitamin D3-dependent modulation of Src, MAPK cascades and VDR localization in skeletal muscle cells. J Steroid Biochem Mol Biol.121:169-75. 2010.
56. Vertino AM, Bula CM, Chen JR, Almeida M, Han L, Bellido T, et al. Nongenotropic, anti-apoptotic signaling of 1alpha,25(OH)2-vitamin D3 and analogs through the ligand binding domain of the vitamin D receptor in osteoblasts and osteocytes. Mediation by Src, phosphatidylinositol 3-, and JNK kinases. J Biol Chem.280:14130-7. 2005.
57. Li YC, Pirro AE, Amling M, Delling G, Baron R, Bronson R, et al. Targeted ablation of the vitamin D receptor: an animal model of vitamin D-dependent rickets type II with alopecia. Proc Natl Acad Sci U S A.94:9831-5. 1997.
58. Yoshizawa T, Handa Y, Uematsu Y, Takeda S, Sekine K, Yoshihara Y, et al. Mice lacking the vitamin D receptor exhibit impaired bone formation, uterine hypoplasia and growth retardation after weaning. Nat Genet.16:391-6. 1997.
59. Zanello LP, Norman AW. Rapid modulation of osteoblast ion channel responses by 1alpha,25(OH)2-vitamin D3 requires the presence of a functional vitamin D nuclear receptor. Proc Natl Acad Sci U S A.101:1589-94. 2004.
60. Boyan BD, Sylvia VL, McKinney N, Schwartz Z. Membrane actions of vitamin D metabolites 1alpha,25(OH)2D3 and 24R,25(OH)2D3 are retained in growth plate cartilage cells from vitamin D receptor knockout mice. J Cell Biochem.90:1207-23. 2003.

CHAPTER 2

Pdia3 mediates the membrane response to 1α,25-Dihydroxyvitamin D3 in osteoblasts

Chapter 2 was published as [Chen J, Olivares-Navarrete R, Wang Y, Herman TR, Boyan BD, Schwartz Z (2010) Protein-disulfide isomerase-associated 3 (Pdia3) mediates the membrane response to 1,25-dihydroxyvitamin D3 in osteoblasts. J Biol Chem 285:37041-37050]

2.1 Introduction

Protein disulfide isomerase associated 3 (Pdia3) is a multifunctional protein hypothesized to be a membrane receptor for $1,25(OH)_2D_3$. In intestinal epithelium and chondrocytes, $1,25(OH)_2D_3$ stimulates rapid membrane responses that are different from genomic effects via the vitamin D receptor (VDR). In this study, we show that $1,25(OH)_2D_3$ stimulates phospholipase A_2 (PLA_2)-dependent rapid release of prostaglandin E_2 (PGE_2), activation of protein kinase C (PKC), and regulation of bone related gene transcription and mineralization in osteoblast-like MC3T3-E1 cells (WT) via a mechanism involving Pdia3. Pdia3 was present in caveolae based on co-localization with lipid rafts and caveolin-1. In Pdia3-silenced (Sh-Pdia3) cells, $1,25(OH)_2D_3$ failed to stimulate PKC and PGE_2 responses; in Pdia3-overexpressing cells (Ov-Pdia3), responses to $1,25(OH)_2D_3$ were augmented. Downstream mediators of Pdia3, PLA_2 activating protein (PLAA) and arachidonic acid, stimulated similar PKC activation in wild type, Sh-Pdia3 and Ov-Pdia3 cells supporting the hypothesis that Pdia3 mediates the membrane action of $1,25(OH)_2D_3$. Treatment of MC3T3-E1 cells with $1,25(OH)_2D_3$ for 9minutes stimulated rapid phosphorylation of extracellular signal-regulated kinases 1 and 2 (ERK1/2) and increased expression of alkaline phosphatase, MMP-13, and

osteopontin but decreased expression of osteocalcin, osteoprotegerin (mRNA and protein) and smad2. These effects were attenuated in Sh-Pdia3 cells. Sh-Pdia3 cells produced higher numbers of von Kossa-positive nodules and alizarin red-positive nodules compared to WT cells with or without 1,25$(OH)_2D_3$ treatment while Ov-Pdia3 did not show any mineralization. Our data suggest Pdia3 is an important initiator of 1,25$(OH)_2D_3$ stimulated membrane signaling pathways, which have both genomic and non genomic effects during osteoblast maturation.

The secosteroid 1,25-dihydroxy vitamin D_3 [1α,25$(OH)_2D_3$] regulates osteoblasts through both the classic vitamin D receptor (VDR) mediated genomic pathway and through membrane receptor mediated rapid responses (1-3). In osteoblasts, the VDR acts by binding with vitamin D response elements (VDRE) to modulate gene transcription (4,5). Rapid membrane signaling has been shown to regulate calcium, phosphate and chloride transport though ion channels (6-8). The VDR has been implicated in these rapid responses to 1α,25$(OH)_2D_3$ (9,10). However, studies using analogues to the secosteroid with low VDR binding affinities indicate that the structural features of 1α,25$(OH)_2D_3$ are important in stimulating the membrane response, suggesting the existence of a specific membrane receptor (8).

Protein disulfide isomerase associated 3 (Pdia3, also known as ERp60, ERp57, Grp58, and 1,25-MARRS) has been identified as a potential candidate as an alternate membrane-associated receptor for 1α,25$(OH)_2D_3$ (11). It has been intensively studied as a chaperone protein in glycoprotein folding (12) and major histocompatibility complex I loading (13). Unlike other protein disulfide isomerase family members, Pdia3 exists not only in the endoplasmic reticulum but also in the nucleus, extracellular matrix, and plasma membrane, suggesting additional functions (3). Pdia3 purified from chick intestinal epithelium (14) exhibits saturable binding to 1α,25$(OH)_2D_3$. More recently, antibody-blocking and ribosome-knock down experiments have further linked this protein

to rapid responses to 1α,25$(OH)_2D_3$ both in rat chondrocytes and chick intestinal epithelial cells (11,15). Taken together, these observations support a role for Pdia3 as a membrane receptor for the secosteroid.

Multiple cell models have been used to elucidate the role of membrane signaling by 1α,25$(OH)_2D_3$. In growth plate chondrocytes, 1α,25$(OH)_2D_3$ regulates phospholipase A_2 (PLA_2), phospholipase C (PLC), intracellular Ca^{++} and protein kinase C (PKC) (16-18). In osteoblasts, 1α,25$(OH)_2D_3$ has also been shown to activate PLC and PKC as well as regulating voltage gated ion channels and increasing PLA_2 activity and prostaglandin production (PGE_1 and PGE_2) (10,19-21). These data suggest that the rapid membrane signaling pathway discovered in chondrocytes may also function in osteoblasts.

One function of membrane signaling is to modulate gene transcription. 1α,25$(OH)_2D_3$ regulates rat growth zone chondrocytes via PKC and extracellular signal-regulated kinases 1 and 2 (ERK1/2) in a Pdia3-dependent pathway (22). Microarray analysis of rat osteoblastic ROS 17/2.8 cells treated with a 1,25$(OH)_2D_3$ analogue with low binding affinity to VDR also demonstrated regulation of a large number of genes through an intracellular calcium dependent mechanism (23,24). Whether Pdia3 mediates 1α,25$(OH)_2D_3$ dependent gene expression in osteoblasts is not known, nor are the overall physiological consequences of rapid responses to the secosteroid clear.

In this study, we first examined 1α,25$(OH)_2D_3$ stimulated rapid membrane signaling in osteoblasts. Second, we showed Pdia3 is required to initiate this rapid signaling. Third, we showed that 1α,25$(OH)_2D_3$ stimulated Pdia3 dependent non-genomic effects eventually control genomic changes affecting mineralization

2.2 Material and Methods

2.2.1 Pdia3 Knock Down and Overexpression

Pdia3 shRNA probes were designed to target the mouse Pdia3 mRNA

(NM_007952). Five different sequences were generated and incorporated into lentivirus particles (SHCLNV-NM 007592, Sigma-Aldrich, St. Louis, MO). To select the optimal shRNA, mouse MC3T3-E1 osteoblasts (CRL-2593, ATCC, Manassas, VA) were plated at a density of 20,000 cells/cm^2 in a 24-well plate in α-MEM supplemented with 10% fetal bovine serum (FBS), and 1% penicillin/streptomycin (P/S). After 24 hours, media were changed to α-MEM supplemented with 10% FBS, 1%P/S and 8μg/mL hexadimethrine bromide and transduced with lentivirus particles at multiplicity of infection (MOI) of 7.5. Cells containing shRNAs or empty vectors were selected by culturing the cells for two weeks in media containing 2.0 μg/ml puromycin. Loss of Pdia3 expression was quantified by real-time PCR and verified by western blot using anti-Pida3 antibody (Alpha Diagnostic International Inc., San Antonio, Texas). A stable transduced cell line with 80% knockdown of Pdia3 was chosenThe shRNA targeted the 3'UTR region of Pdia3 mRNA (ggaccagtttatgtttgtggttt, #N0000011436, Sigma-Aldrich).

To overexpress Pdia3, MC3T3-E1 cells were plated at a density of 20,000 cells/cm^2 in a 24 well plate in α-MEM supplied with 10%FBS. After 24 hours, 100μl of Opti-MEM (Invitrogen, Carlsbad, CA) containing 2.0μl lipofectamine 2000 (Invitrogen) and 0.8μg pCMV6-Kan/Neo empty vector (OriGene, Rockville, MD) or overexpression plasmid (#MC200134, OriGene) that contained full length of mouse Pdia3 cDNA (BC003285.1) was added into each well. After 48 hours, cells were selected in media containing 550 μg/ml G418 for two weeks. mRNA and protein were quantified by real-time PCR and western blot as described above. A stable transfected cell line with 100% overexpression of Pdia3 was chosen.

2.2.2 Cell Culture

Wild type MC3T3-E1 cells, MC3T3-E1 cells silenced for Pdia3 (Sh-Pdia3), and MC3T3-E1 cells overexpressing Pdia3 (Ov-Pdia3) were plated in T75 flasks (10,000

cells/cm^2) and cultured in α-MEM containing 10% FBS and 1% P/S. Puromycin (2μg/ml) was included in the media of Sh-Pdia3 cells and G418 (550μg/ml) was included in the media of Ov-Pdia3 cells. At confluence, cells were subcultured at the same plating density. 48 hours after plating the media were replaced with α-MEM supplemented with 5%FBS, 1% P/S and 1% vitamin C. After 12 days in culture, the cells were treated with media containing either the 1α,25$(OH)_2D_3$ vehicle (ethanol) alone or with the appropriate dose of 1α,25$(OH)_2D_3$.

2.2.3 Plasma Membranes and Caveolae

A detergent-free method of plasma membrane and caveolae isolation was used as described previously (25). MC3T3-E1 cells were cultured for 12 days and harvested by scraping in isolation buffer (0.25M sucrose, 1mM EDTA, 20mM tricine, PH=7.8). Samples were homogenized using a tissue grinder for twenty strokes. Homogenates were centrifuged at 20,000g for 10mins to pellet cell debris, including nucleus, mitochondria, and endoplasmic reticulum. The supernatant was collected, placed on top of 30% Percoll (GE Healthcare, Piscataway, NJ) in isolation buffer, and then centrifuged for 30 mins at 84,000g. The plasma membranes formed a visible band and were collected by aspiration. Plasma membranes were layered on a 10%-20% OptiPrep gradient (Sigma-Aldrich) and centrifuged at 52,000g for 90mins. The top layer was collected, overlaid with 5% OptiPrep, and centrifuged at 52,000g for another 90mins. Fractions were collected from the top to the bottom in thirteen fractions. The caveolae existed as an opaque band, which was collected in Fraction 3, based on the presence of caveolin-1 as described below.

2.2.4 Western Blot

Gel electrophoresis was performed using NuSep 4-20% LongLife Gels (NuSep,

Lawrenceville, GA). Proteins were transferred from gels to nitrocellulose membrane using an iBlot Dry Blotting System (Invitrogen). The membrane was subsequently blotted in 1% bovine serum albumin (BSA) in phosphate buffered saline (PBS) for one hour. Next, samples were incubated overnight with antibodies against Pdia3 (Alpha Diagnostic International); caveolin-1 (Sc-894, Santa Cruz Biotechnology, Santa Cruz, CA); or glyceraldehyde 3-phosphate dehydrogenase (GAPDH) (MAB374, Millipore, Billerica, MA). After washing three times with PBS containing 0.05% Tween-20, the membrane was incubated with goat anti-rabbit or goat anti-mouse horse radish peroxidase conjugated secondary antibodies (Bio-Rad, Hercules, CA) in PBS containing 5% dry milk and 0.05% Tween-20 for one hour. After three washes, the membrane was developed using SuperSignal West Pico Chemiluminescent System (Thermo Fisher Scientific, Rockford, IL) and imaged with VersaDoc imaging system (Bio-Rad, Hercules, CA).

2.2.5 Immunofluorescence

Immunofluorescence was used to assess Pdia3 protein in intact cells. Wild type, Sh-Pdia3 and Ov-Pdia3 MC3T3-E1 cells were plated at 10,000 cells/cm^2 on a glass chamber slide for 24 hours. The cells were fixed in 4% paraformaldehyde for 20mins and permeabilized with 0.01% Triton-X 100 for 10mins. Cells were then incubated with 1:100 dilution of Hoechst 33342 (Invitrogen), Pdia3 primary antibody, and 1:40 dilution of Alexa Fluor 555 phalloidin (Invitrogen) in a PBS containing 1%BSA. After washing, cells were incubated with goat anti-rabbit Alexa 488 (Invitrogen) in 1%BSA-PBS.

In order to determine if Pdia3 was associated with a specific plasma membrane compartment, co-localization experiments were performed. Cells in suspension were labelled with Vybrant Lipid Rafts Labeling Kits-Alexa Fluor 594 (Invitrogen). After labeling, cells were fixed in 4% paraformaldehyde for 20mins. Then, cells were further stained with Pdia3 primary antibody and 1:100 (v/v) Hoechst 33342 in 1%BSA-PBS.

After washing, cells were incubated with goat anti-rabbit Alexa 488 in 1%BSA-PBS, fixed with GEL/MOUNT (Biomeda Corp, Foster City, CA), and imaged using a Zeiss LSM 510 confocal microscope.

2.2.6 Signaling by 1α,25$(OH)_2D_3$

To study the effect of 1α,25$(OH)_2D_3$ on PKC activity, cells were treated with vehicle (ethanol) or 10^{-10}, 10^{-9} or 10^{-8}M 1α,25$(OH)_2D_3$ for 9mins, based on the observation that 1α,25$(OH)_2D_3$ activates PKC in chondrocytes at this time point (26). The effect of 1α,25$(OH)_2D_3$ on PKC is via a PLA_2-dependent pathway (16). To determine if this is also the case for MC3T3-E1 cells, one half of the cultures were treated with 10^{-5}M of the PLA_2 inhibitor quinacrine (Calbiochem, San Diego, *CA*). Quinacrine was added to media 30mins before and maintained during 1α,25$(OH)_2D_3$ treatment. Cells were also treated for 9min with 0, 10^{-8}, 10^{-7}, 10^{-6}M PLA_2 activating protein (PLAA) (Enzo Life Sciences International, Inc, Plymouth Meeting, PA) as well as with 0, 10^{-6}, 10^{-5}, or 10^{-4}M arachidonic acid (AA) (Calbiochem), which is the product of PLA_2 action. Media were collected and cell layers were washed twice with PBS and lysed in 300µl RIPA buffer (20mM Tris-HCl, 150mM NaCl, 5mM disodium EDTA, 1%NP-40). PKC activity was measured using a commercial kit (RPN77, GE Healthcare) and normalized by total protein. To measure rapid PGE_2 release into the media, cells were treated with vehicle (ethanol), 10^{-10}, 10^{-9}, or 10^{-8}M 1α,25$(OH)_2D_3$. After 30min treatment, the media were acidified and PGE_2 was measured using a commercial kit (Perkin Elmer, Waltham, MA) and normalized by cell number.

2.2.7 ERK1/2

To determine if the rapid responses to 1α,25$(OH)_2D_3$ result in ERK1/2 activation, phosphorylation of ERK1/2 was determined using an ELISA assay. After 12 day's

culture, cells were treated for 9mins with media containing vehicle (ethanol) or 10^{-8}M 1α,25$(OH)_2D_3$. Media were replaced and cells were harvested 0, 30 and 90mins later. Phospho-ERK1/2 was measured in cell layer lysate using a mouse Phospho-ERK1/2 ELISA kit (R&D system, Minneapolis, MN).

2.2.8 Gene Expression

After 12 day's culture, cells were treated with media containing vehicle (ethanol) or 10^{-8}M 1α,25$(OH)_2D_3$. After 9mins, media were replaced with fresh media for another 8 hours. RNA was extracted using TRIzol (Invitrogen) and reverse-transcribed into cDNA using the Omniscript RTkit (Qiagen, Valencia, CA) according to the manufacturer's directions. Real-time PCR was performed using SYBR Green SuperMix 170-8882 (Bio-Rad) for osteocalcin (OCN, NM_001032298), alkaline phosphatase (ALP, NM_007431), bone sialoprotein (BSP, NM_008318), matrix metalloproteinase 13 (MMP-13, NM_008607), osteopontin (OPN, NM_009263), osteoprotegerin (OPG, NM_011613), protein disulfide isomerase associated 3 (Pdia3, NM_007952), Runx2 (NM_009820), inositol 1,4,5-trisphosphate 3-kinase A (ITPKA, NM_146125), osteonectin (OTN, NM_009242), Smad2 (NM_010754), Vitamin D receptor (VDR, NM_009504), and glyceraldehyde 3-phosphate dehydrogenase (GAPDH, NM_008084). Oligonucleotide primers were designed using Beacon Designer 7.0 software (Table A-1). A homology blast search was performed within the mammalian genome to exclude the possibility of sequence similarity. Real-time PCR was performed using an iCycler PCR machine (Bio-Rad) with iCycler software. Data were normalized to the endogenous reference gene GAPDH.

2.2.9 Osteopontin

Changes in osteopontin secreted into the conditioned media were used as an

outcome measure of the rapid signaling pathway. The role of Ca^{++} ions was examined by incubating the cells with 10^{-4}M Ca^{++} chelator BAPTA-AM (Sigma-Aldrich) .The role of PLA_2 was assessed by treating the cells with 10^{-5}M quinacrine. For these experiments, cultures were treated with media containing the inhibitor vehicle (ddH_2O) or inhibitor for 30mins. Fresh media containing the 1,25$(OH)_2D_3$ vehicle (ethanol) or the inhibitor plus 10^{-8}M 1α,25$(OH)_2D_3$ were added. Nine mins later, the media were replaced by fresh media and these media were collected 24 hours later. Osteopontin in the conditioned media was determined by ELISA using a mouse osteopontin ELISA kit (R&D Systems).

2.2.10 Calcification

To determine if Pdia3 modulates terminal osteoblast differentiation, we assayed the ability of the cells to mineralize their extracellular matrix. Cells were plated in 24-well plates in full media and cultured as described above. At confluence, full media were changed for osteogenic media (α-MEM supplemented with 5% FBS, 1% P/S, 100µg/ml ascorbic acid, 10mM β-glycerol phosphate and 10^{-7}M dexamethasone) or growth media (α-MEM supplemented with 5% FBS, 1%P/S). Every 48 hours, the osteogenic media were replaced with growth media containing vehicle (ethanol) or 10^{-8} M 1α,25$(OH)_2D_3$ for 9mins; these media were then removed and replaced with osteogenic media. Growth media were replaced every two days without additional 1α,25$(OH)_2D_3$. On day 28 after plating, media were replaced with osteogenic media containing 10% alamar blue for 40 minutes to assess viability of the cells. In healthy cells, alamar blue is reduced by components of the electron transport chain, resulting in red fluorescence. The cultures were then fixed in 10% formalin and alizarin red and von Kossa staining were performed.

2.2.11 Statistical Analysis

For each experiment, each data point represents the means ± SEM for six

individual cultures. Each experiment was repeated two or more times to ensure the validity of the data. The data presented are from a single representative experiment. Significance was determined by analysis of variance and post hoc testing performed using Bonferroni's modification of Student's *t* test for multiple comparisons. $p \leq 0.05$ was considered to be significant.

2.3 Results

2.3.1 Rapid Membrane Response in MC3T3-E1 Cells

PKC activity in MC3T3-E1 cells was stimulated by 1α,25$(OH)_2D_3$ in a dose dependent-manner (Fig. 2-1a). This effect was rapid, occurring within 9 mins of treatment. 1α,25$(OH)_2D_3$ also caused a dose-dependent increase in PGE_2 content of the conditioned media at 30 mins (Fig. 2-1b), suggesting that PLA_2 had been activated. Inhibition of PLA_2 with quinacrine blocked the stimulating effect of 1α,25$(OH)_2D_3$ on PKC at all concentration treated. Moreover, the PLA_2 activator, PLAA, and the product of PLA_2 action, arachidonic acid both stimulated PKC activity to a similar extent. PLAA caused a dose-dependent increase in PKC activity at 10^{-7}M to 10^{-6}M (Fig. 2-1c); arachidonic acid increased PKC at 10^{-4}M (Fig. 2-1d). These results indicate that 1α,25$(OH)_2D_3$ regulated PKC via a mechanism that required PLA_2.

2.3.2 Subcellular Location of Pdia3

Western blots of whole cell lysates and isolated plasma membranes indicated that both Pdia3 and caveolin-1 were present (Fig. 2-2a). Pdia3 was present in factions 1, 2, 3 and 4 of the plasma membrane whereas caveolin-1 was present only in faction 3 (Fig. 2-2b). These observations were supported by confocal microscopy. Both Pdia3 and lipid rafts were distributed over the surface of non-permeabilized MC3T3-E1 cells. When the immunofluorescent images were merged, part of staining overlapped. However, a

small portion of fluorescently labeled Pdia3 was not associated with lipid rafts.

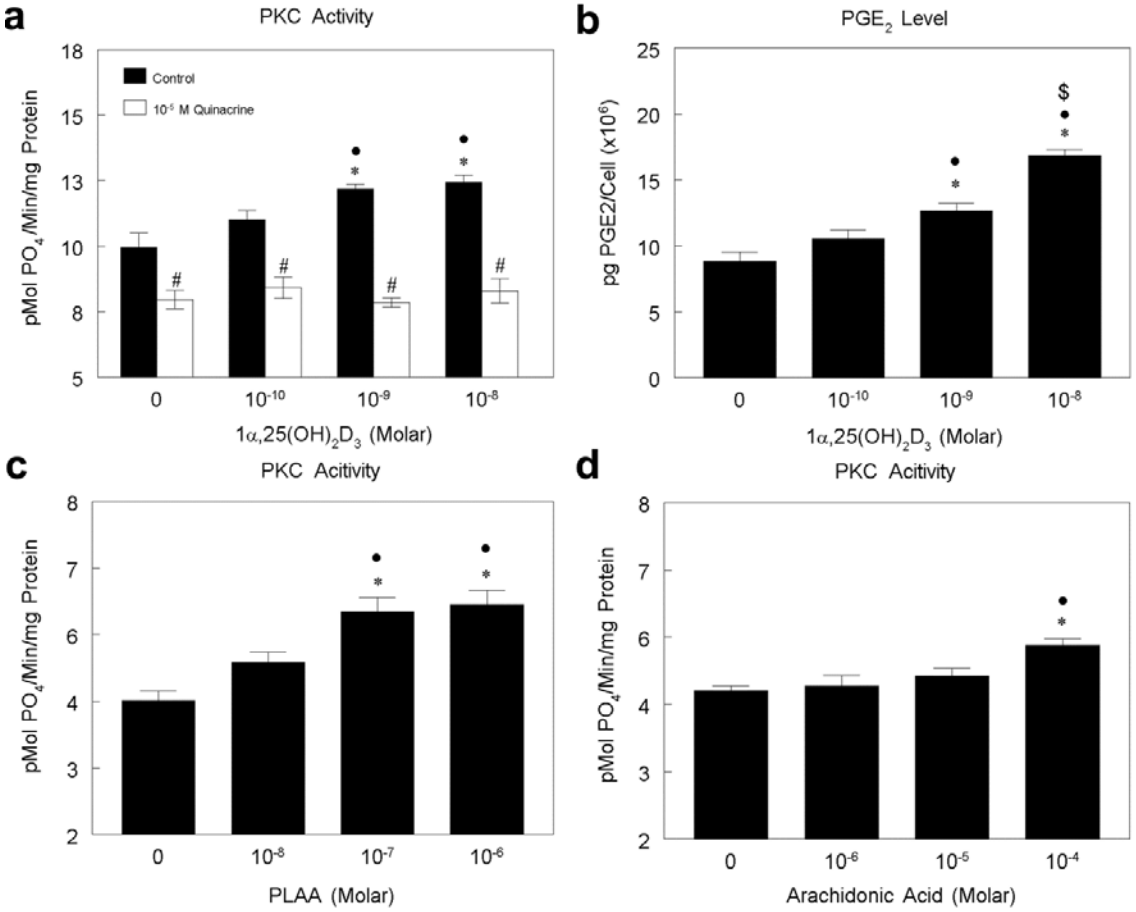

Fig. 2-1 Effect of 1α,25$(OH)_2D_3$ on PGE_2 production and PKC activity and role of PLA_2 in PKC activation in MC3T3-E1 cells. (A): MC3T3-E1 cells were treated with vehicle (ethanol) or 10^{-10}, 10^{-9} or 10^{-8}M 1α,25$(OH)_2D_3$ with or without 10^{-5}M quinacrine (PLA_2 inhibitor) for 9mins. PKC activity was normalized to total protein. (B): MC3T3-E1 cells were treated with vehicle (ethanol) or 10^{-10}, 10^{-9} or 10^{-8}M 1α,25$(OH)_2D_3$ for 30min. Conditioned media were collected and PGE_2 was measured and normalized to cell number. (C): MC3T3-E1 cells were treated with vehicle (ddH_2O) or 10^{-8}, 10^{-7} or 10^{-6}M PLAA for 9mins. PKC activity was normalized to total protein level. (D): MC3T3-E1 cells were treated with vehicle (media) or 10^{-6}, 10^{-5} or 10^{-4}M AA for 9mins. PKC activity was normalized to total protein level. * $p<0.05$, treatment vs. control; • $p<0.05$, 10^{-8}M and 10^{-9}M vs. 10^{-10}M, $ $p<0.05$, 10^{-8}M vs. 10^{-9}M; # $p<0.05$ quinacrine vs. control.

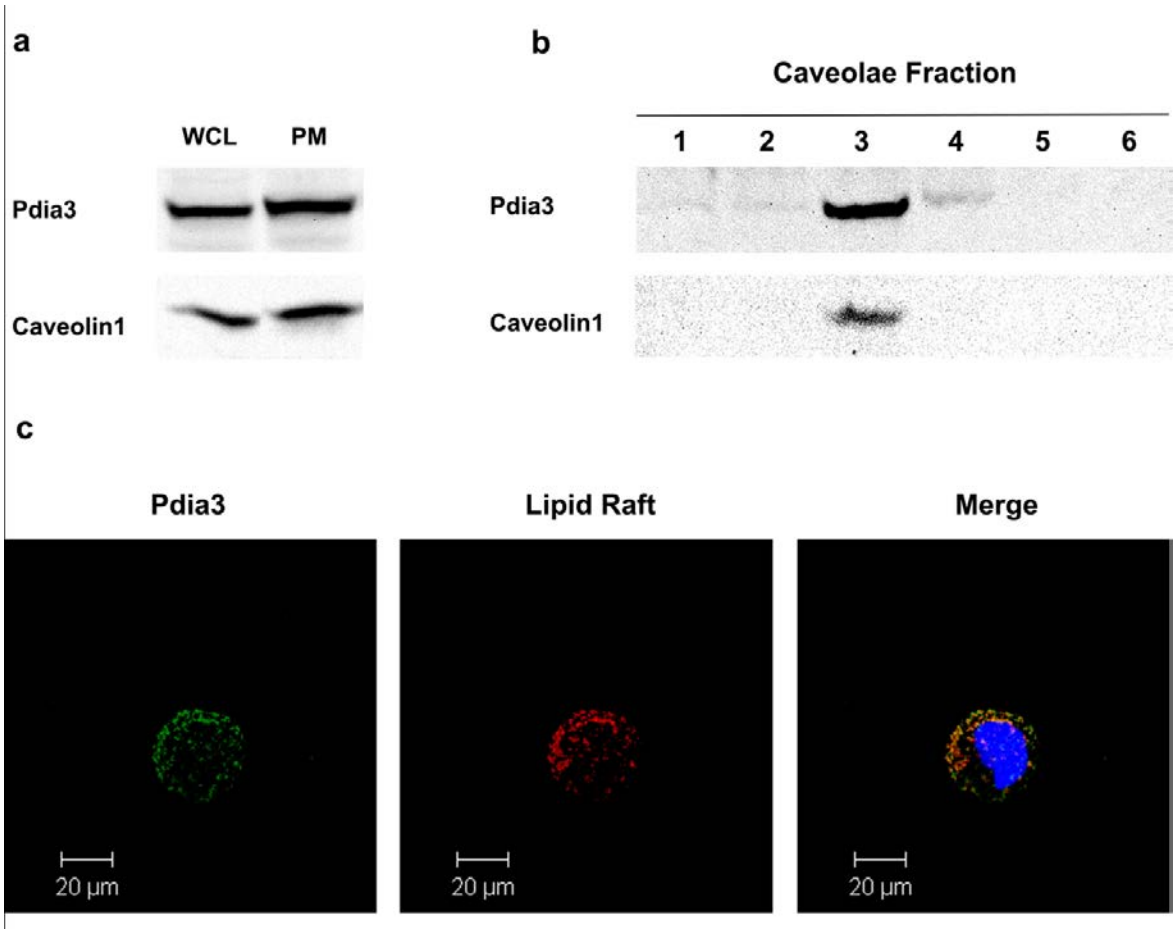

Fig. 2-2 Western blot and confocal microscope image of MC3T3-E1 cells. MC3T3-E1 cells were cultured as previously described. Whole cell lysates, plasma membrane fractions and caveolae fractions were collected separately. Western blots against caveolin-1 and Pdia3 were performed. (A) Western blot of whole cell lysates and membrane fractions. Thirteen fractions were collected; fractions one to six are shown. Caveolae exist in fraction three (B). (C) Confocal image of non-permeabilized MC3T3-E1 cells. Green: Pdia3; Red: lipid rafts; Yellow: merge of Pdia3 and lipid rafts.

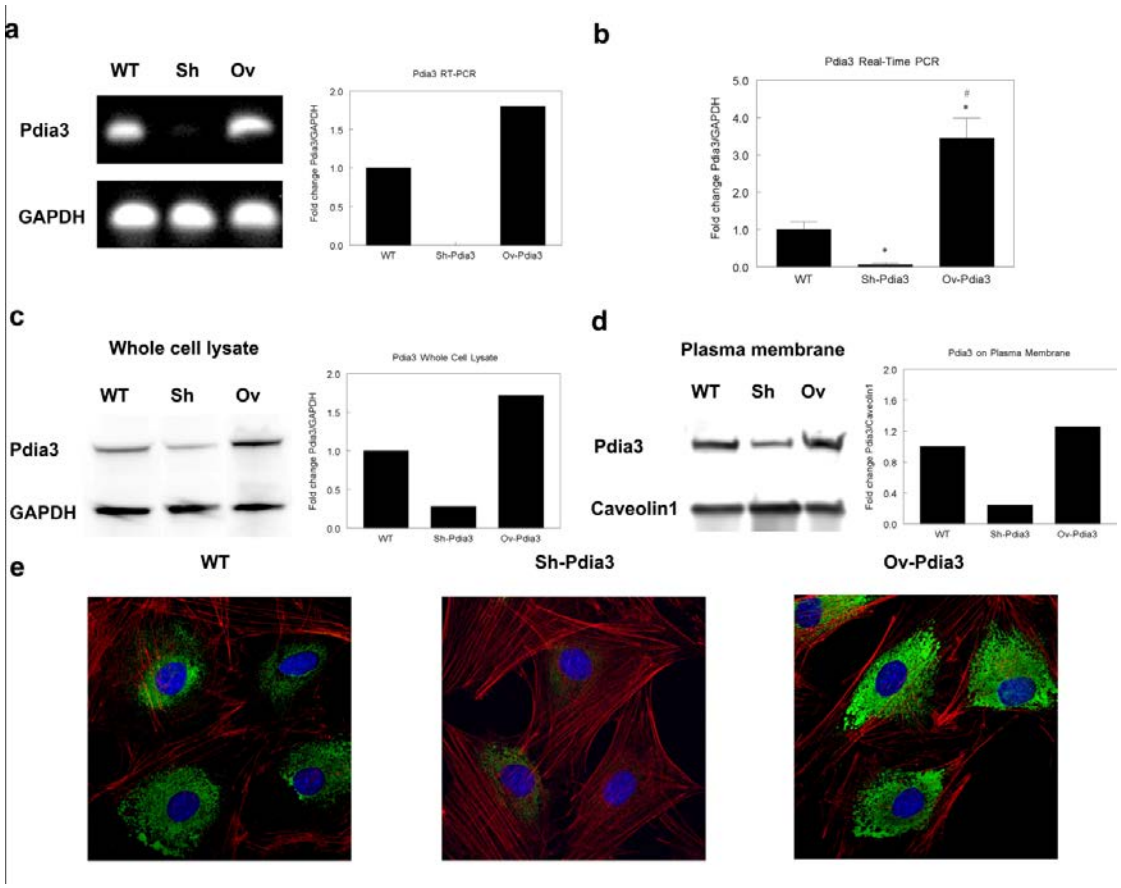

Fig. 2-3 Silencing and overexpression of Pdia3 in MC3T3-E1 cells: RT-PCR, real-time PCR, western blot and confocal microscopy. (A): RT-PCR. Left: Gel electrophoresis of RT-PCR product. Right: Quantitative RT-PCR for the fold change of Pdia3 levels relative to GAPDH control (B): Real-time PCR. Fold change of Pdia3 levels relative to GAPDH control. (C): Western blot of whole cell lysate. Left: Blotting image. Right: Quantitative western blot for the fold change of Pdia3 levels relative to GAPDH control. (D): Western blot of plasma membranes Left: Blotting image. Right: Quantitative western blot for the fold change of Pdia3 levels relative to GAPDH control. (E): Confocal microscopy of permeabilized cells. Red: actin; Green: Pdia3; Blue: nucleus. Cells were permeabilized before staining.

2.3.3 Pdia3 Expression in MC3T3-E1 Cells

Two MC3T3-E1 cell lines were established that were silenced for expression of Pdia3 or that over-expressed this protein. RT-PCR indicated that mRNA for Pdia3 was reduced in Sh-Pdia3 cells compared to wild type cells whereas expression was increased in Ov-Pdia3 cells (Fig. 2-3a). Real-time PCR analysis of six independent cultures showed Pdia3 expression was decreased by 80% in Sh-Pdia3 cells; it increased by 200% in Ov-Pdia3 cells (Fig. 2-3b). Western blots of whole cell lysates confirmed that Pida3 protein was affected in a comparable manner. Pdia3 protein was reduced by 75% in the Sh-Pdia3 cells and increased by 70% in Ov-Pdia3 cells (Fig. 2-3c). Western blots of plasma membranes showed similar results. Pdia3 protein was decreased by 80% in plasma membranes from Sh-Pdia3 cells and increased by 30% in plasma membranes from Ov-Pdia3 cells (Fig. 2-3d). Similarly, MC3T3-E1 cells exhibited intense immunofluorescence for Pdia3 surrounding the nucleus, but this staining was largely decreased in Sh-Pdia3 cells; it was augmented in Ov-Pdia3 cells (Fig. 2-3e).

2.3.4 Role of Pdia3 in the Rapid Response to 1α,25$(OH)_2D_3$

Pdia3 mediated the rapid response of MC3T3-E1 cells to 1α,25$(OH)_2D_3$. Whereas 1α,25$(OH)_2D_3$ increased PKC in wild type cells, it had no effect on PKC activity in Sh-Pdia3 cells (Fig. 2-4a). In contrast, in Ov-Pdia3 cells, 1α,25$(OH)_2D_3$ increased PKC activity over the stimulatory effect of the secosteroid in wild type cells. 10^{-8}M 1α,25$(OH)_2D_3$ caused a 1.8 fold increase of PKC activity in Ov-Pdia3 compared to a 1.3 fold increase in wild type cells (Fig. 2-4a). These effects were specific to Pdia3 since the cells transfected with empty vectors responded to 1α,25$(OH)_2D_3$ as the wild type MC3T3-E1 cells (Fig. A-1).

Pdia3 also mediated the 1α,25$(OH)_2D_3$-dependent PLA_2 signaling pathway resulting in PKC activation. Production of PGE_2, a downstream metabolite of PLA_2

action, was increased by 1α,25$(OH)_2D_3$ in MC3T3-E1 cells and this effect was enhanced in Ov-Pdia3 cells at all concentrations tested (Fig. 2-4b). In contrast, the stimulatory effect of 1α,25$(OH)_2D_3$ was reduced in Sh-Pdia3 cells. The PLA_2 pathway was functional in all three cell lines, however. Treatment of the cells with PLAA caused a dose-dependent increase in PKC that was comparable in all three cell types (Fig. 2-4c). Similarly arachidonic acid activated PKC to a comparable extent as 1α,25$(OH)_2D_3$ in all three cell lines (Fig. 2-4d).

2.3.5 Pdia3-Dependent Rapid Signaling Regulates Gene Expression

Gene expression was regulated, at least in part, by Pdia3-mediated signaling (Fig. 2-5). Treatment of MC3T3-E1 cells with 1α,25$(OH)_2D_3$ for 9mins resulted in changes in mRNA levels for bone related genes. OPN, ALP, and MMP-13 were up-regulated, while OPG, Smad2 and OCN were down-regulated. BSP, ITPKA, Runx2, OTN, VDR and Pdia3 showed no significant differences as a function of 1α,25$(OH)_2D_3$ treatment. 1α,25$(OH)_2D_3$ did not affect mRNA for BSP, IPTKA, Runx2, OTN VDR or Pdia3 in Sh-Pdia3 cells. However, genes that were down regulated in wild type cells (OPG, OCN and Smad2) were unaffected by 1α,25$(OH)_2D_3$ in Sh-Pdia3 cells. For the three up-regulated genes (OPN, ALK and MMP-13), the effects of 1α,25$(OH)_2D_3$ were reduced in the Sh-Pdia3 cells.

Pdia3 was required for 1α,25$(OH)_2D_3$ dependent activation of ERK1/2. 1α,25$(OH)_2D_3$ treatment caused phosphorylation of ERK1/2 by 30mins; this effect was lost by 90mins (Fig. 2-6a). In contrast, 1α,25$(OH)_2D_3$ had no effect on ERK1/2 phosphorylation in Sh-Pdia3 cells (Fig. 2-6b).

Changes in protein production correlated with changes in gene expression. Treatment of wild type MC3T3-E1 cells with 1α,25$(OH)_2D_3$ for 9mins caused a 200% increase in OPN mRNA at 8 hours (Fig. 2-5a) and a marked increase in OPN protein at

24 hours (Fig. 2-6c). This effect was attenuated in Sh-Pdia3 cells while Ov-Pdia3 cells showed an augmented increase. The basal level of OPN protein was also lower in Sh-Pdia3 cells and higher in Ov-Pdia3 cells. Inhibition of rapid membrane signaling using quinacrine or bapta-AM also blocked the 1α,25$(OH)_2D_3$–dependent increase in OPN protein in the conditioned media in cultures of wild type cells. Neither inhibitor affected the basal level of OPN, indicating they did not block the normal transcription and translation activity of this protein.

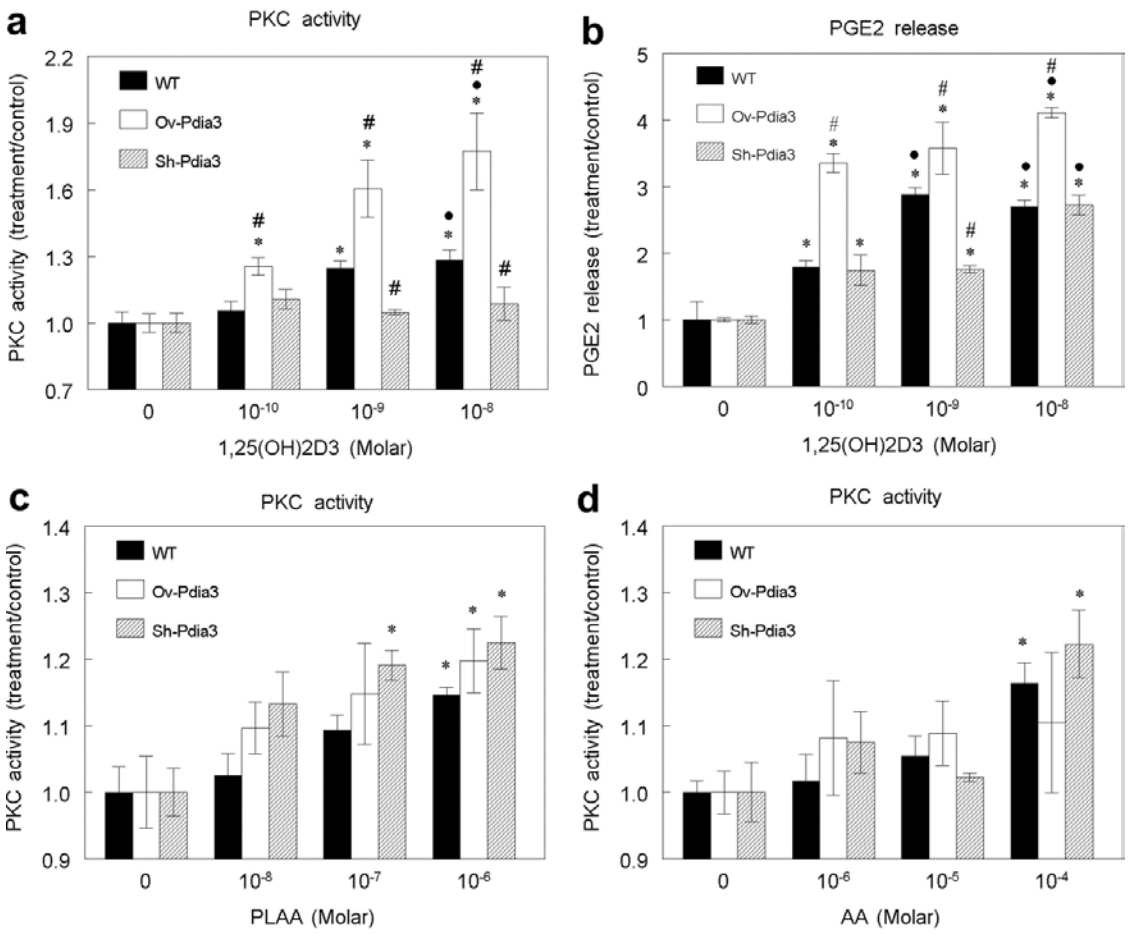

Fig. 2-4 Effect of $1\alpha,25(OH)_2D_3$, PLAA and AA on PKC activity and effect of $1\alpha,25(OH)_2D_3$ on PGE_2 release in wild type, Sh-Pdia3 and Ov-Pdia3 MC3T3-E1 cells. (A): the effect of $1\alpha,25(OH)_2D_3$ on PKC activity of WT, Sh-Pdia3 and Ov-Pdia3 MC3T3-E1 cells. MC3T3-E1 cells were treated with vehicle (ethanol) or 10^{-10}, 10^{-9} or 10^{-8}M $1\alpha,25(OH)_2D_3$ for 9mins. PKC activity was normalized to total protein. (B): $1\alpha,25(OH)_2D_3$ effect on PGE_2 release of WT, Sh-Pdia3 and Ov-Pdia3 MC3T3-E1. MC3T3-E1 cells were treated with vehicle (ethanol) or 10^{-10}, 10^{-9} or 10^{-8}M $1\alpha,25(OH)_2D_3$ for 30mins. PGE_2 in conditioned media was measured and normalized to cell number. (C): PLAA effect on PKC activity of WT, Sh-Pdia3 and Ov-Pdia3 MC3T3-E1 cells. MC3T3-E1 cells were treated with vehicle (ddH_2O) or 10^{-6}, 10^{-7} or 10^{-8}M PLAA for 9mins. PKC activity was measured and normalized to total protein. (D): AA effect on PKC activity of WT, Sh-Pdia3 and Ov-Pdia3 MC3T3-E1 cells. MC3T3-E1 cells were treated with vehicle (media) or 10^{-4}, 10^{-5} or 10^{-6}M AA for 9mins. PKC activity was measured and normalized by total protein. * $p<0.05$, treatment vs. control; • $p<0.05$, 10^{-8} and 10^{-9} vs. 10^{-10}; # $p<0.05$ Sh-Pdia3 and Ov-Pdia3 vs. WT for the same treatment.

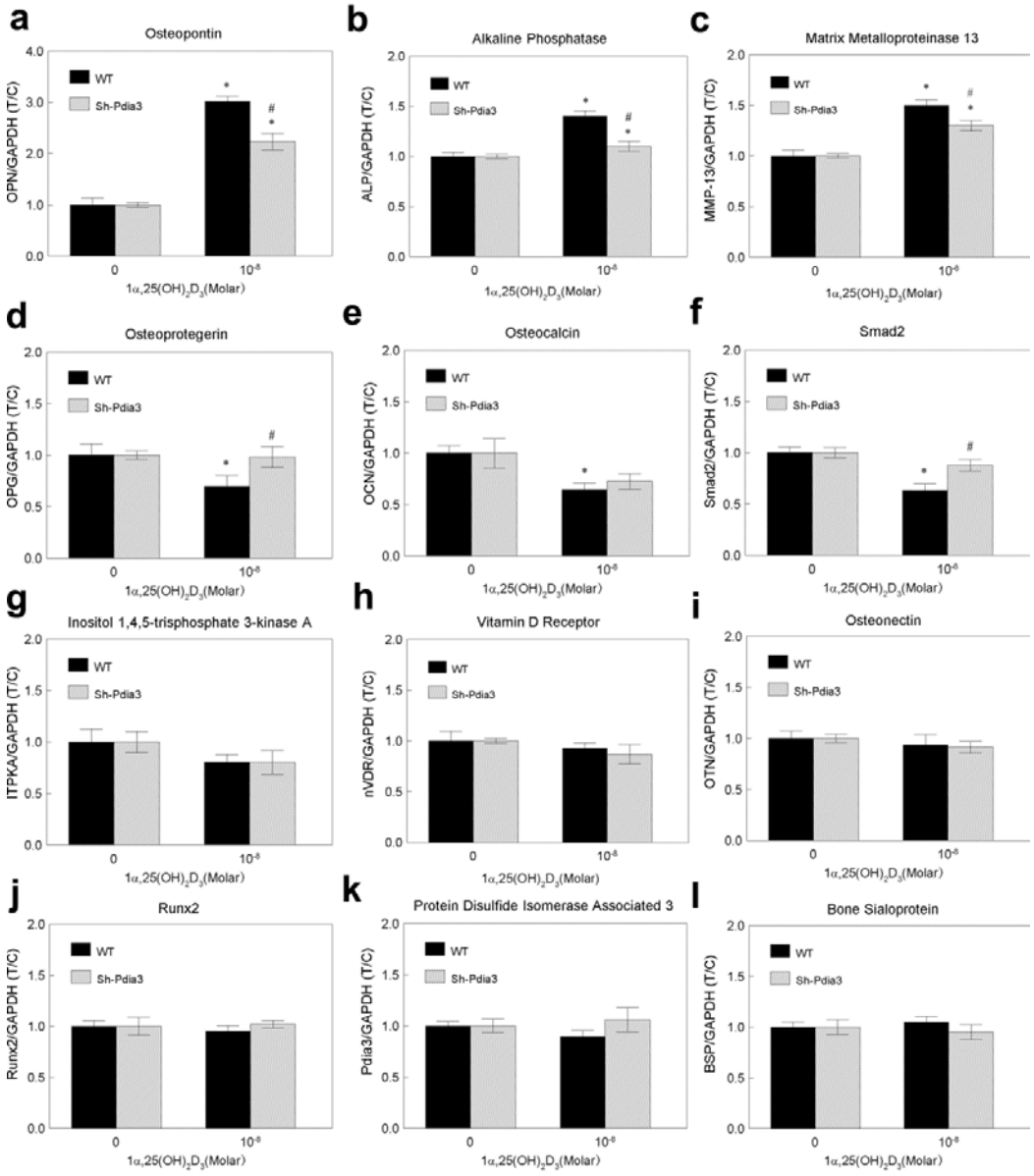

Fig. 2-5 Effect of $1\alpha,25(OH)_2D_3$ on gene transcription in wild type and Sh-Pdia3 MC3T3-E1 cells. Wild type and Sh-Pdia3 cells were treated with vehicle (ethanol) or 10^{-8}M $1\alpha,25(OH)_2D_3$. After 9mins, media were replaced with fresh media for another 8 hours before harvest. Real-time PCR was performed against twelve bone related genes: (A) osteopontin; (B) alkaline phosphatase; (C) matrix metalloproteinase 13; (D) osteoprotegerin; (E) osteocalcin; (F) Smad2; (G); inositol 1,4,5-trisphosphate 3-kinase A; (H) vitamin D receptor; (I) osteonectin; (J) Runx2; (K) protein disulfide isomerase associated 3; and (L) bone sialoprotein. T/C represents the treatment over control ratio. Absolute values of targeting genes were first normalized by GAPDH. Then the normalized values from treatment groups were further divided by the normalized values from vehicle (ethanol) control groups. * $p<0.05$, treatment vs. control; # $p<0.05$, Sh-Pdia3 vs. WT for the same treatment.

Figure 6

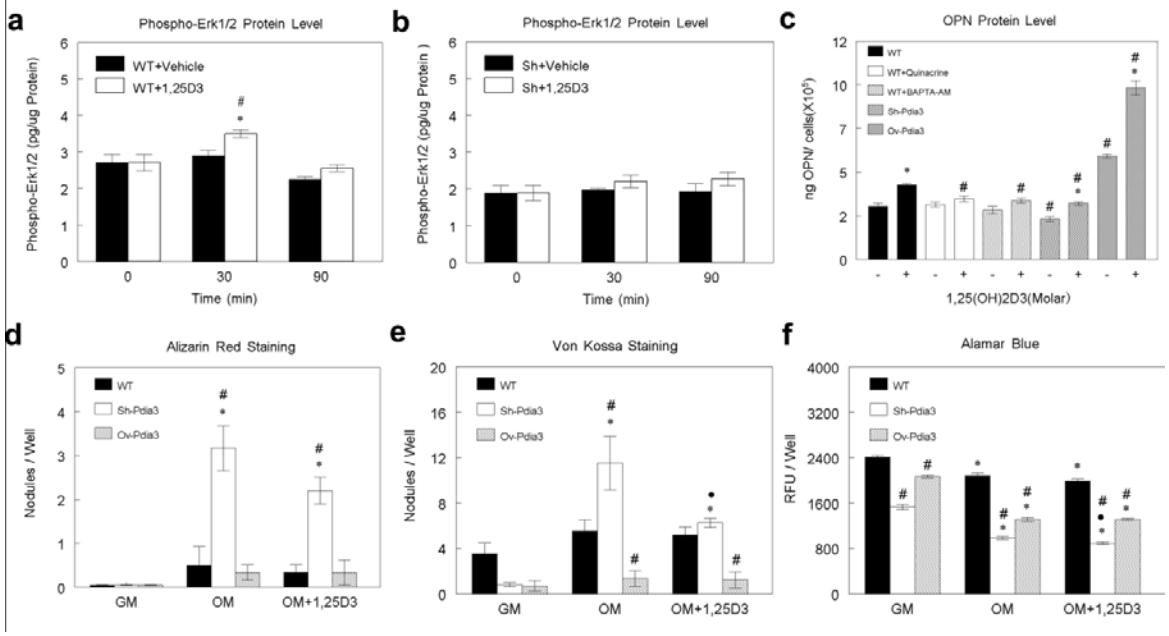

Fig. 2-6 Effect of 1α,25$(OH)_2D_3$ on ERK1/2 phosphorylation, OPN secretion and *in vitro* mineralization in wild type, Sh-Pdia3 and Ov-Pdia3 cells. (A) and (B): Wild type and Sh-Pdia3 MC3T3-E1 cells were treated with vehicle (ethanol) or 10^{-8}M 1α,25$(OH)_2D_3$ for 9mins. The media were replaced and cells were harvested at 0min (no treatment), 30min and 90min after treatment. Intracellular phospho-ERK1/2 was measured by ELISA and normalized to total protein. (C): Wild type, Ov-Pdia3 and Sh-Pdia3 MC3T3-E1 cells were treated with vehicle (ethanol) or 10^{-8}M 1α,25$(OH)_2D_3$ for 9mins with or without 10^{-5}M quinacrine or 10^{-6}M BAPTA-AM. After 9mins, the media were replaced and after 24 hours, OPN was measured in the conditioned media using an ELISA assay. OPN levels were normalized to cell number. (D) (E) and (F): Wild type, Ov-Pdia3 and Sh-Pdai3 cells were cultured in growth media or osteogenic media with or without pulse treatments (9 min) with 10^{-8}M 1α,25$(OH)_2D_3$ every 48 hours. Four weeks after seeding, cultures were examined by alamar blue, alizarin red and van Kossa staining. (D): Number of alizarin red positive nodules; (E): Number of von Kossa positive nodules. (F): Relative fluorescence units of alamar blue stain. Numbers indicate the cell viability. Each data point represents mean ± SEM for N = 6 independent cultures. * $p<0.05$, 30min and 90mins vs. 0 mins for A and B or 1α,25$(OH)_2D_3$ vs. vehicle (ethanol) for C or OM± 1α,25$(OH)_2D_3$ vs. GM for D, E and F; • $p<0.05$, OM+1α,25$(OH)_2D_3$ vs. OM-1α,25$(OH)_2D_3$ for D, E and F; # $p<0.05$, 1α,25$(OH)_2D_3$ vs. vehicle (ethanol) for A and B or Sh-Pdia3, Ov-Pdia3 and WT with inhibitors vs. WT for the same conditions for C, D, E and F.

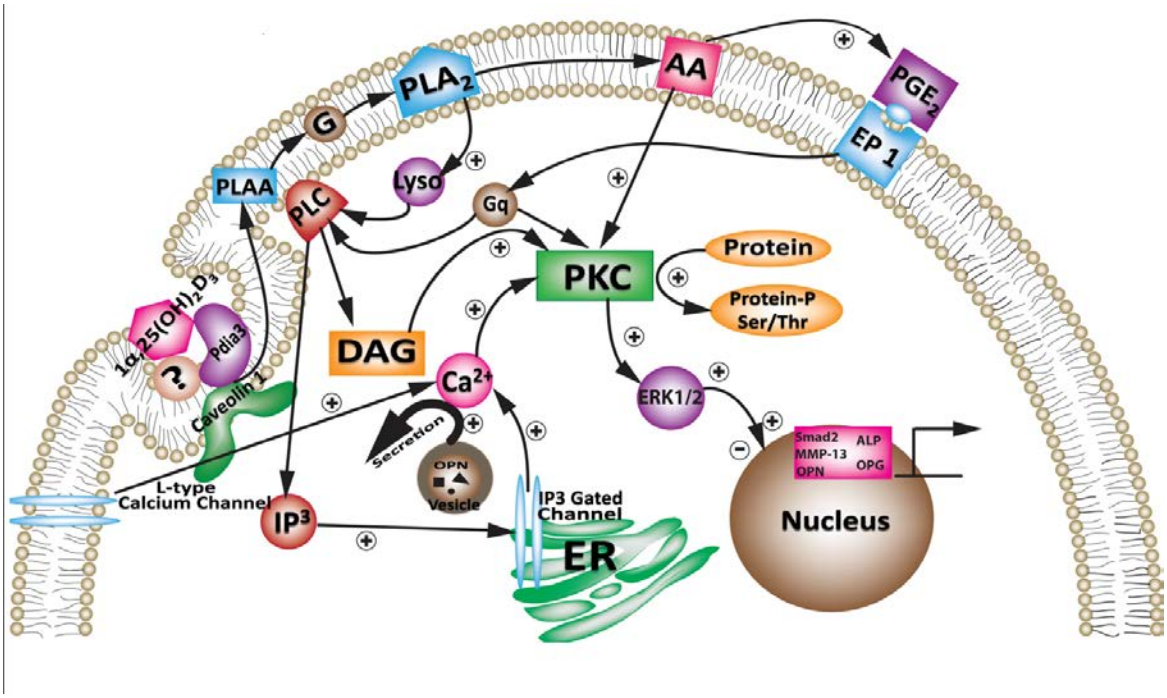

Fig. 2-7 Proposed mechanism of $1\alpha,25(OH)_2D_3$ stimulated rapid responses in osteoblasts.

.

2.3.6 Pdia3 Regulates Mineralization.

Wild type MC3T3-E1 cells, Sh-Pdia3 cells and Ov-Pdia3 cells all formed von Kossa positive nodules. The number of alizarin-red/von Kossa positive nodules formed by wild type cells were comparable in cultures grown in growth media, osteogenic media, or osteogenic media plus 1α,25$(OH)_2D_3$ (Fig. 2-6 d,e). In growth media, von Kossa positive nodule formation was reduced in Sh-Pdia3 and Ov-Pdia3 cultures compared to wild type cells although differences in Pdia3 expression did not affect the number of alizarin-red positive nodules. When Sh-Pdia3 cells were cultured in osteogenic media, the number of alizarin-red/von Kossa positive nodules was markedly increased in comparison to wild type cells. In contrast, von Kossa positive nodule formation was reduced in cultures of Ov-Pdia3 cells. Treatment with 1α,25$(OH)_2D_3$ blocked the stimulatory effect of the osteogenic media on von Kossa positive nodule formation in cultures of Sh-Pdia3 cells but had no effect on alizarin-red positive nodules. Moreover, treatment did not affect wild type or Ov-Pdia3 cultures. For all cell types, growth in osteogenic media resulted in decreased alamar blue staining compared to growth media (Fig. 2-6f). Treatment with 1α,25$(OH)_2D_3$ caused a further decrease only in Sh-Pdia3 cells.

2.4 Discussion

Our data show that Pdia3 mediates effects of 1α,25$(OH)_2D_3$ on osteoblasts, including rapid production of PGE_2 and activation of PKC. Importantly, the results demonstrate that Pdia3 dependent signaling results in changes in gene expression, via phosphorylation of transcription factors such as ERK1/2. Taking these observations together with our previous observations using growth plate chondrocytes (16,27,28) and osteoblasts (19,21), we propose a mechanism initiated at the plasma membrane and

culminating in downstream genomic regulation (Fig. 2-7). In this signaling pathway, 1α,25$(OH)_2D_3$ first binds with Pdia3 or a Pdia3-membrane receptor complex in caveolae, activating PLA_2. This results in arachidonic acid release; the arachidonic acid is processed further to PGE_2. In growth plate chondrocytes (1,16,18). PGE_2 binds its G-protein coupled receptor and activates PLC. Activated PLC acts on phosphatidylinositol, releasing inositol-trisphosphate (IP_3) and diacylglycerol (DAG). Increased intracellular Ca^{++} due to IP_3 works with DAG to translocate and activate PKC on the plasma membrane. This pathway also results in activation of ERK1/2 (22). The fact that key components of the signaling pathway are also present in osteoblasts (19,21) and that PKC and PLC were also reported to be rapidly activated by 1α,25$(OH)_2D_3$ in other cell types (29-32), suggests that the proposed pathway is likely to be conserved in 1α,25$(OH)_2D_3$-responsive cells.

Pdia3 has been reported to be present in endoplasmic reticulum, cytosol, nucleus, plasma membranes, extracellular matrix and matrix vesicles (33). Our results show that Pdia3 is present in the cytosol and plasma membranes of MC3T3-E1 osteoblasts as well. Part of the Pdia3 is in specialized compartments of the plasma membranes, co-localizing with lipid rafts by fluorescence microscopy. Moreover, western blot shows that Pdia3 is in the caveolar fraction of the plasma membrane based on the presence of caveolin-1 (34). We previously reported caveolae are required for rapid 1α,25$(OH)_2D_3$-dependent PKC signaling in chondrocytes, and caveolin-1 must be present based on studies using chondrocytes from Cav-1(-/-) mice (27). This suggests that caveolae provide a microenvironment that permits the interaction of Pdia3 with 1α,25$(OH)_2D_3$ together with other components of the signaling complex. Pdia3 was also present in plasma membrane fractions not associated with caveolin-1 and immunofluorescence demonstrated that not all Pdia3 was associated with lipid rafts. What role this Pdia3 may play with respect to 1α,25$(OH)_2D_3$, if any, is not clear.

In the present study, we were able to construct stably transfected cell lines that exhibited reduced or over expression of Pdia3. The changes in expression were confirmed by real-time PCR, confocal microscopy, and western blots. These changes in Pdia3 correlated with changes in cell response to 1α,25$(OH)_2D_3$, including activation of PKC, phosphorylation of ERK1/2, downstream regulation of gene expression and protein production, and ultimately, in von Kossa positive nodule formation. These results strongly implicate Pdia3 as a membrane receptor for 1α,25$(OH)_2D_3$. Moreover, we showed that by regulating expression of Pdia3, signaling could be either blocked or augmented. These data suggest that Pdia3 could be a determining factor, the abundance of which directly correlates with the magnitude of the membrane response.

Previous studies using antibodies to Pdia3 demonstrated a role for this protein in Ca^{++} ion uptake in chicken intestinal epithelium (35) and as a regulator of PKC signaling (36), but they did not demonstrate in a conclusive manner that Pdia3 is upstream of the earliest steps in the signaling pathway. Here we showed that the PLA_2 pathway was intact in the Sh-Pdia3 and Ov-Pdia3 cells. If Pdia3 had been a mediator downstream of PLA_2, either PLAA, the activator of PLA2, or arachidonic acid, the product of PLA2 action would stimulate a different response among the three-cell lines. However, we observed a similar effect of PLAA and arachidonic acid on PKC activation in all three-cell lines, indicating that Pdia3 functions in the very first step of this signaling cascade, potentially as the membrane receptor.

It has been unclear whether the Pdia3-dependent rapid membrane response to 1α,25$(OH)_2D_3$ also has a genomic function. By silencing and overexpressing Pdia3, we were able to assess the potential effect of rapid signaling on gene transcription in a new perspective. In growth plate chondrocytes, the rapid translocation and activation of PKC leads to the phosphorylation of ERK1/2 (22). ERK1/2 has been shown to regulate osteoblast differentiation in multiple signaling pathways (37-39). Therefore, it is very

likely for the rapid response to have a role in gene transcription through the activation of ERK1/2. In wild type cells, among the 12 bone related genes we studied, six were regulated by a 9min treatment with 1α,25$(OH)_2D_3$. Among the six genes, only OCN and OPN have been reported to have VDR response elements (VDRE) (40). All of the six genes have been previously reported to be regulated through a VDR-independent membrane pathway (24). Here we showed in Sh-Pdia3 cells, both rapid activation of ERK1/2 and regulation of these six genes were either completely blocked or significantly attenuated. Our result confirms the previous report and further, shows that this VDR-independent genomic effect is mediated by Pdia3.

It should be noted that three out of the six 1α,25$(OH)_2D_3$-regulated genes did not completely lose their response to 1α,25$(OH)_2D_3$ in Sh-Pdia3 cells. There are two possible explanations for this. First, in Sh-Pdia3 cells, thirty percent of Pdia3 was still on the plasma membrane to mediate the effect. Second, Pdia3 dependent rapid membrane signaling participates in these mechanisms by using kinase cascades to change activity of the transcription factor complex. Therefore, this kind of regulation may crosstalk with other pathways. For example, VDR could be phosphorylated and activated by PKC (41).

In wild type MC3T3-E1 cells, three genes were up-regulated in response to1α,25$(OH)_2D_3$: ALP is an early stage osteoblast differentiation marker (15); MMP-13 is an extracellular matrix remodeling proteinase (42); and OPN has been shown to be a mineralization inhibitor (43). Three genes were down-regulated. OCN is a late stage osteoblast differentiation marker (44) and OPG inhibits osteoclast differentiation (45). This suggests that the effect of pulse treatment with 1α,25$(OH)_2D_3$ promotes early osteoblast differentiation and extracellular matrix remodeling but prevents late stage osteoblast differentiation and mineralization. Others have shown that OCN is increased in response to 1α,25$(OH)_2D_3$ via VDR-mediated transcription (46), however, our study suggests that it is regulated via Pdia3 as well, and in the experimental design used for

this study, the Pdia3 pathway was dominant. Taken together, this suggests that Pdia3 and VDR act at different points in osteoblast differentiation and that the relative contributions of the mechanisms are dose-dependent as well as time-dependent.

If Pdia3 action modulates terminal differentiation of MC3T3-E1 cells, we would expect that 1α,25$(OH)_2D_3$ would cause an increase in mineralization in Sh-Pdia3 cells but a decrease in Ov-Pdia3 cells. Both of the transfected cell lines exhibited fewer von Kossa positive nodules when cultured in growth media than were seen in wild type cells, related at least in part to the reduced levels of viable cells in these cultures. In osteogenic media, however, we observed more von Kossa positive nodules in Sh-Pdia3 cultures and fewer nodules in Ov-Pdia3 cultures compared to wild type MC3T3-E1 cells and this was matched by corresponding differences in alizarin red positive nodules. Pulse treatment with 1α,25$(OH)_2D_3$ had no effect on nodule number in cultures of wild type or Ov-Pdia3 cells, whether determined as a function of calcium (alizarin red) or phosphate (von Kossa). In contrast, pulse treatment of the Sh-Pdia3 cultures with osteogenic media containing 1α,25$(OH)_2D_3$ reduced the number of von Kossa positive nodules without affecting the number of alizarin red positive nodules. von Kossa staining detects phosphate, which is produced by the action of alkaline phosphatase. Both wild type and Sh-Pdia3 cells exhibited increased ALP expression when pulse treated with 1α,25$(OH)_2D_3$, but only the Sh-Pdia3 cultures had increased von Kossa nodule formulation when grown in osteogenic media containing 1α,25$(OH)_2D_3$. These results support the hypothesis that Pdia3 acts in a dose-dependent manner and its actions vary with cell differentiation. The 1α,25$(OH)_2D_3$ content of the osteogenic media was determined by the content of the secosteroid in FBS, approximately 10^{-12}M (47). When differentiated osteoblasts were pulsed with exogenous 1α,25$(OH)_2D_3$, thereby increasing the concentration, the effect of the secosteroid was to reduce phosphate content, but without impacting Ca^{++}. This was more pronounced in the Sh-Pdia3 cultures, in part due

to the reduction in viable cells. In conclusion, our data suggest that in MC3T3-E1 cells, Pdia3 and its rapid membrane signaling decrease mineralization and by silencing Pdia3 mineralization could be largely augmented.

Considering the multiple cellular functions of Pdia3 when studying the consequence of silencing Pdia3, the effects of other Pdia3 dependent mechanisms must be considered. For example, Pdia3 is a chaperone protein that participates in the folding of N-glycosylated integral membrane proteins (12). Pdia3 also exists in the nucleus and binds with DNA, but the effect of this binding on transcription is still unclear (48). Thus, changing Pdia3 expression levels could result in changing various cellular processes and how much of these side effects contribute to our observation is not known. The observation that inhibitors targeting mediators of the rapid response successfully blocked 1α,25$(OH)_2D_3$-stimulated OPN protein, supports the idea that the observed effects in Sh-Pdia3 and Ov-Pdia3 are contributed by the specific role of Pdia3 in the 1α,25$(OH)_2D_3$ pathway, rather than side effects.

In conclusion, we mapped out a detailed mechanism of 1α,25$(OH)_2D_3$ stimulated rapid response in osteoblasts. The importance of this protein to the mechanism was shown by silencing and overexpressing Pdia3. The function of Pdia3 in the first step of our pathway was demonstrated. By establishing the role of Pdia3 in 1α,25$(OH)_2D_3$-dependent gene transcription, protein secretion and mineralization, we showed that the proposed Pdia3 signaling pathway has significant physiological relevance. This conclusion is supported by studies showing that mice with reduced levels of Pdia3 (Pdia3+/-) have a defective bone phenotype (49).

2.5 References

1. Boyan, B. D., Wang, L., Wong, K. L., Jo, H., and Schwartz, Z. (2006) *Steroids* **71**, 286-290
2. Zanello, L. P., and Norman, A. (2006) *Steroids* **71**, 291-297
3. Khanal, R. C., and Nemere, I. (2007) *Curr Med Chem* **14**, 1087-1093
4. Breen, E. C., van Wijnen, A. J., Lian, J. B., Stein, G. S., and Stein, J. L. (1994) *Proc Natl Acad Sci U S A* **91**, 12902-12906
5. Kraichely, D. M., and MacDonald, P. N. (1998) *Front Biosci* **3**, d821-833
6. Liu, R., Li, W., Karin, N. J., Bergh, J. J., Adler-Storthz, K., and Farach-Carson, M. C. (2000) *J Biol Chem* **275**, 8711-8718
7. Veldman, C. M., Schlapfer, I., and Schmid, C. (1997) *Bone* **21**, 41-47
8. Zanello, L. P., and Norman, A. W. (1997) *J Biol Chem* **272**, 22617-22622
9. Zanello, L. P., and Norman, A. W. (2004) *Proc Natl Acad Sci U S A* **101**, 1589-1594
10. Zanello, L. P., and Norman, A. W. (2004) *Steroids* **69**, 561-565
11. Nemere, I., Farach-Carson, M. C., Rohe, B., Sterling, T. M., Norman, A. W., Boyan, B. D., and Safford, S. E. (2004) *Proc Natl Acad Sci U S A* **101**, 7392-7397
12. Jessop, C. E., Chakravarthi, S., Garbi, N., Hammerling, G. J., Lovell, S., and Bulleid, N. J. (2007) *EMBO J* **26**, 28-40
13. Peaper, D. R., Wearsch, P. A., and Cresswell, P. (2005) *EMBO J* **24**, 3613-3623
14. Nemere, I., Dormanen, M. C., Hammond, M. W., Okamura, W. H., and Norman, A. W. (1994) *J Biol Chem* **269**, 23750-23756
15. Boyan, B. D., Bonewald, L. F., Sylvia, V. L., Nemere, I., Larsson, D., Norman, A. W., Rosser, J., Dean, D. D., and Schwartz, Z. (2002) *Steroids* **67**, 235-246
16. Schwartz, Z., Graham, E. J., Wang, L., Lossdorfer, S., Gay, I., Johnson-Pais, T. L., Carnes, D. L., Sylvia, V. L., and Boyan, B. D. (2005) *J Cell Physiol* **203**, 54-70
17. Schwartz, Z., Sylvia, V. L., Larsson, D., Nemere, I., Casasola, D., Dean, D. D., and Boyan, B. D. (2002) *J Biol Chem* **277**, 11828-11837
18. Schwartz, Z., Gilley, R. M., Sylvia, V. L., Dean, D. D., and Boyan, B. D. (1999) *Bone* **24**, 475-484
19. Baran, D. T. (1994) *J Cell Biochem* **56**, 303-306
20. Wali, R. K., Kong, J., Sitrin, M. D., Bissonnette, M., and Li, Y. C. (2003) *J Cell Biochem* **88**, 794-801
21. Matthews, L., Berry, A., Ohanian, V., Ohanian, J., Garside, H., and Ray, D. (2008) *Mol Endocrinol* **22**, 1320-1330
22. Schwartz, Z., Ehland, H., Sylvia, V. L., Larsson, D., Hardin, R. R., Bingham, V., Lopez, D., Dean, D. D., and Boyan, B. D. (2002) *Endocrinology* **143**, 2775-2786
23. Farach-Carson, M. C., Bergh, J. J., and Xu, Y. (2004) *Steroids* **69**, 543-547
24. Farach-Carson, M. C., and Xu, Y. (2002) *Steroids* **67**, 467-470
25. Huhtakangas, J. A., Olivera, C. J., Bishop, J. E., Zanello, L. P., and Norman, A. W. (2004) *Mol Endocrinol* **18**, 2660-2671
26. Sylvia, V. L., Schwartz, Z., Schuman, L., Morgan, R. T., Mackey, S., Gomez, R.,

and Boyan, B. D. (1993) *J Cell Physiol* **157**, 271-278
27. Yasuda, H., Shima, N., Nakagawa, N., Yamaguchi, K., Kinosaki, M., Mochizuki, S., Tomoyasu, A., Yano, K., Goto, M., Murakami, A., Tsuda, E., Morinaga, T., Higashio, K., Udagawa, N., Takahashi, N., and Suda, T. (1998) *Proc Natl Acad Sci U S A* **95**, 3597-3602
28. Larsson, B., and Nemere, I. (2003) *Endocrinology* **144**, 1726-1735
29. Yarram, S. J., Tasman, C., Gidley, J., Clare, M., Sandy, J. R., and Mansell, J. P. (2004) *Mol Cell Endocrinol* **220**, 9-20
30. Turano, C., Coppari, S., Altieri, F., and Ferraro, A. (2002) *J Cell Physiol* **193**, 154-163
31. Buitrago, C. G., Pardo, V. G., de Boland, A. R., and Boland, R. (2003) *J Biol Chem* **278**, 2199-2205
32. Boland, R., De Boland, A. R., Buitrago, C., Morelli, S., Santillan, G., Vazquez, G., Capiati, D., and Baldi, C. (2002) *Steroids* **67**, 477-482
33. Nemere, I., and Campbell, K. (2000) *Steroids* **65**, 451-457
34. Smart, E. J., Ying, Y. S., Mineo, C., and Anderson, R. G. (1995) *Proc Natl Acad Sci U S A* **92**, 10104-10108
35. Nemere, I., Schwartz, Z., Pedrozo, H., Sylvia, V. L., Dean, D. D., and Boyan, B. D. (1998) *J Bone Miner Res* **13**, 1353-1359
36. Boyan, B. D., Sylvia, V. L., McKinney, N., and Schwartz, Z. (2003) *J Cell Biochem* **90**, 1207-1223
37. Dai, Z., Li, Y., Quarles, L. D., Song, T., Pan, W., Zhou, H., and Xiao, Z. (2007) *Phytomedicine* **14**, 806-814
38. Jadlowiec, J., Koch, H., Zhang, X., Campbell, P. G., Seyedain, M., and Sfeir, C. (2004) *J Biol Chem* **279**, 53323-53330
39. Kanno, T., Takahashi, T., Tsujisawa, T., Ariyoshi, W., and Nishihara, T. (2007) *J Cell Biochem* **101**, 1266-1277
40. Haussler, M. R., Whitfield, G. K., Haussler, C. A., Hsieh, J. C., Thompson, P. D., Selznick, S. H., Dominguez, C. E., and Jurutka, P. W. (1998) *J Bone Miner Res* **13**, 325-349
41. Hsieh, J. C., Jurutka, P. W., Galligan, M. A., Terpening, C. M., Haussler, C. A., Samuels, D. S., Shimizu, Y., Shimizu, N., and Haussler, M. R. (1991) *Proc Natl Acad Sci U S A* **88**, 9315-9319
42. Jia, Z., and Nemere, I. (1999) *Steroids* **64**, 541-550
43. Ono, N., Nakashima, K., Rittling, S. R., Schipani, E., Hayata, T., Soma, K., Denhardt, D. T., Kronenberg, H. M., Ezura, Y., and Noda, M. (2008) *J Biol Chem* **283**, 19400-19409
44. Bronckers, A. L., Gay, S., Finkelman, R. D., and Butler, W. T. (1987) *Bone Miner* **2**, 361-373
45. Dormanen, M. C., Bishop, J. E., Hammond, M. W., Okamura, W. H., Nemere, I., and Norman, A. W. (1994) *Biochem Biophys Res Commun* **201**, 394-401
46. Lian, J. B., Coutts, M., and Canalis, E. (1985) *J Biol Chem* **260**, 8706-8710
47. Park, J. H., Lee, M. Y., and Han, H. J. (2009) *Int J Biochem Cell Biol* **41**, 659-665
48. Coppari, S., Altieri, F., Ferraro, A., Chichiarelli, S., Eufemi, M., and Turano, C.

(2002) *J Cell Biochem* **85**, 325-333
49. Wang, Y., Chen, J., Lee, C. S., Nizkorodov, A., Riemenschneider, K., Martin, D., Hyzy, S., Schwartz, Z., and Boyan, B. D. (2010) *J Steroid Biochem Mol Biol* **121**, 257-260

CHAPTER 3

Plasma membrane Pdia3 and VDR interact to elicit rapid responses to 1α,25(OH)2D3

Chapter 3 was submitted as [Chen J, Doroudi M, Cheung J, Grozier AL, Schwartz Z, Boyan BD (2012) Plasma membrane Pdia3 and VDR interact to elicit rapid responses to 1α,25(OH)2D3. Endocrinology.]

3.1 Introduction

Over the past two decades, the steroid hormone, 1α,25-dihydroxyvitamin D3 (1α,25$(OH)_2D_3$) has drawn increasing attention due to its functions in addition to maintaining calcium phosphate homeostasis. 1α,25$(OH)_2D_3$ directly regulates mineralization by osteoblasts (1), matrix production by chondrocytes (2) and contraction of cardiomyocytes (3). 1α,25$(OH)_2D_3$ and its analogues have shown beneficial effects in treating multiple sclerosis, diabetes and various types of cancer (4-8).

1α,25$(OH)_2D_3$ regulates its target cells through traditional vitamin D receptor (VDR) mediated genomic mechanisms as well as through membrane receptor-mediated rapid responses. This latter mechanism has been reported in many 1α,25$(OH)_2D_3$-responsive cells including myocytes, osteoblasts, chondrocytes, epithelial cells and cancer cells (1,9-12). The data suggest the actions of 1α,25$(OH)_2D_3$ are likely due to the overall effect of both genomic and rapid responses. However, compared to VDR-dependent gene expression, rapid responses to the secosteroid are less studied. The identity of the membrane receptor(s), downstream signaling pathways and downstream outcomes are not well understood.

Two candidates have been proposed as membrane receptors for 1α,25$(OH)_2D_3$: protein disulfide isomerase family A, member 3 (Pdia3, also known as ERp60, ERp57, Grp58, and 1,25-MARRS) and the traditional VDR. Pdia3 was initially isolated from the basal lateral membranes of chicken intestinal epithelial cells based on its saturable binding to 1α,25$(OH)_2D_3$ (13). Because antibodies to the N-terminal peptide of the protein blocked Ca++ and phosphate transport across the membrane in response to 1α,25$(OH)_2D_3$ (14) as well as rapid activation of protein kinase C (PKC) in chondrocytes and osteoblasts (15-17), the protein was termed 1α,25$(OH)_2D_3$ membrane associated rapid response to steroid (1,25-MARRS). 1,25-MARRS was subsequently shown to be identical to Pdia3 (14,18). More recently, our group found Pdia3 was located in the caveolae structure of plasma membrane where it physically interacted with scaffolding protein caveolin-1 (1,19).

Pdia3 is a chaperone protein (20) and global knockout is embryologically lethal (21), suggesting it plays many roles in addition to its function as a receptor for 1α,25$(OH)_2D_3$. Pdia3(+/-) heterozygote mice exhibit a bone abnormality with characteristics of vitamin D-deficient rickets heterozygote mice (22), and embryonic stem cells possess Pdia3 and respond to 1α,25$(OH)_2D_3$ with an increase in PKC (23), indicating that Pdia3 plays specific roles with respect to the secosteroid. Epithelial cells isolated from Pdia3-conditional knockout mice lost surface binding of 1α,25$(OH)_2D_3$ and 1α,25$(OH)_2D_3$ stimulated calcium uptake (24), supporting this hypothesis. Moreover, chondrocytes from VDR(-/-) mice have Pdia3 and exhibit rapid increases in PKC in response to 1α,25$(OH)_2D_3$ (25).

The traditional nuclear VDR is also present in caveolae in osteoblasts (26) and a functional VDR was shown to be necessary to initiate rapid Ca^{++} transport in a number of studies (27,28). An alternative 1α,25$(OH)_2D_3$ binding pocket was identified and was

hypothesized to be responsible for initiating rapid responses (29,30). Since both receptors were found to be present in caveolae and both were reported to be required for various rapid responses, the questions of whether they exist and interact within the same functional unit in caveolae and whether caveolin-1 is a component of that unit are raised. Knocking down caveolin-1 abolished Pdia3-dependent rapid PKC activation (31) and silencing caveolin-1 abolished VDR associated c-Src activation (9,32) in different cell models, indicating that caveolin-1 plays a key role in the interaction between the two receptors.

1α,25$(OH)_2D_3$ activates a number of rapid responses in its target cells. In chondrocytes and osteoblasts, 1α,25$(OH)_2D_3$ caused Pdia3-dependent activation of phospholipase A2 (PLA2) via phospholipase A2 activating protein (PLAA), resulting in release of arachidonic acid within seconds and subsequent production of prostaglandin E2 (PGE2) (18,19,33-35). In addition, phosphatidyl inositol-dependent phospholipase C, PKC and the extracellular signal-regulated kinases 1 and 2 (ERK1/2) were rapidly increased downstream of PLA2 activation (10,33,36). Also in osteoblasts, 1α,25$(OH)_2D_3$ has been reported to initiate a VDR-dependent rapid activation of the phosphatidylinositol 3-kinase (PI3K)/Akt pathway (37,38). Moreover, in skeletal muscle cells, c-Src was found to be rapidly activated by 1α,25$(OH)_2D_3$ via a VDR-dependent pathway (32,39,40).

Each of these enzymes initiates signaling pathways that result in changes in cell response. In chondrocytes, the 1α,25$(OH)_2D_3$ stimulated PLA2/PGE2 pathway promotes the production of cartilage matrix proteins (41). In osteoblasts and cancer cells, chemically induced apoptosis could be reduced by 1α,25$(OH)_2D_3$ initiated PI3K/Akt pathway (38,42). In muscle cells, rapid activation of c-Src to 1α,25$(OH)_2D_3$ resulted in the activation of MAPK (43), which was implicated in the regulation of muscle cell

proliferation (44).

The purpose of the present study was to assess the relative roles of Pdia3, VDR and caveolin-1 in one module and to examine the contributions of previously reported multiple signaling mediators in the context of their connections to the two different receptors and caveolin-1. Due to the differences in cell type, experimental methods, outcome measurements and different hypotheses favoring either Pdia3 or VDR, controversy remains. In this study, we silenced Pdia3, VDR and caveolin-1 separately in an osteoblast MC3T3-E1 model using the same method and systematically studied changes in PLA2/PGE2, PI3K/Akt and c-Src pathways and downstream cellular consequences, including proliferation, differentiation, and apoptosis. Interactions between Pdia3, VDR, caveolin-1 and the downstream mediators were determined with and without 1α,25$(OH)_2D_3$ treatment. The data demonstrate the importance of both receptors and their interactions in mediating rapid responses to 1α,25$(OH)_2D_3$, and subsequently in regulating osteoblast biology.

3.2 Materials and Methods

3.2.1 Pdia3/VDR/Caveolin1 Silencing

An MC3T3-E1 cell line with over 80% silencing of Pdia3 mRNA and protein (Sh-Pdia3) and another MC3T3-E1 cell line with over 90% silencing of caveolin-1 mRNA and protein (Sh-Cav1) were previously established (1,19), and confirmed to have retained reduced protein (Fig. 2-6 A,B). The same approach was used to develop MC3T3-E1 cells stably silenced for VDR (Sh-VDR). Briefly, VDR short hairpin RNA probes were designed to target the mouse VDR mRNA (NM_009504) and five different sequences were generated and incorporated into lentivirus particles (MISSION^{TM} shRNA,

Sigma-Aldrich, St. Louis, MO). MC3T3-E1 cells (CRL-2593, ATCC, Manassas, VA) were plated at a density of 20,000 cells/cm^2 in a 24-well plate in α-MEM supplemented with 10% fetal bovine serum (FBS) and 1% penicillin/streptomycin (P/S). After 24 hours, the medium was changed to α-MEM supplemented with 10% FBS, 1%P/S and 8μg/mL hexadimethrine bromide and transduced with lentivirus particles at a multiplicity of infection (MOI) of 7.5. Cells containing shRNAs or empty vectors were selected by culturing the cells for two weeks in medium containing 2.0μg/ml puromycin. Loss of VDR expression was quantified by real-time PCR. The clone with the highest silencing rate was chosen from the five different sh-RNA transfected clones. Reduction of VDR protein was verified by western blots (Fig. 2-6 A,B).

3.2.2 Cell Culture

WT, Sh-Pdia3, Sh-VDR and Sh-Cav1 MC3T3-E1 cells were plated at 20,000 cells/cm^2 in T75 flasks or 24 well plates with full media (α-MEM supplemented with 10% FBS 1%P/S with or without 2.0ug/ml puromycin). After 48 hours, full medium was changed to full medium containing 1% vitamin C to enable cross-linking of type I collagen in the extracellular matrix (45). [^{3}H]-thymidine incorporation and confocal microscope experiments were performed using pre-confluent cultures as described below. For all other experiments, cells were cultured for 10 days after plating and treated with full media containing either the 1α,25$(OH)_2D_3$ vehicle (ethanol) alone or with the appropriate dose of 1α,25$(OH)_2D_3$.

3.2.3 Gene Expression

Changes in alkaline phosphatase and osteopontin mRNA were used as indicators of the effect of 1α,25$(OH)_2D_3$ on osteoblast maturation. To study the dose-

dependent effects of 1α,25$(OH)_2D_3$, 10 days after plating, wild type MC3T3-E1 cells were treated with media containing vehicle (ethanol) or 10^{-9}, 10^{-8}, or 10^{-7} M of 1α,25$(OH)_2D_3$. To study the role of Pdia3, VDR and caveolin-1 in gene regulation, Sh-Pdia3, Sh-VDR and Sh-Cav1 cells were treated with vehicle or 10^{-7} M of 1α,25$(OH)_2D_3$. Fifteen minutes later, media were replaced with fresh media without 1α,25$(OH)_2D$ for another 8 hours. The transient treatment of 1α,25$(OH)_2D_3$ was designed to reduce genomic effects as previously described (1). RNA was extracted using TRIzol (Invitrogen, Carlsbad, CA) and reverse-transcribed into cDNA using the Omniscript RTkit (Qiagen, Valencia, CA). Real-time PCR was performed using SYBR Green SuperMix 170-8882 (Bio-Rad, Hercules, CA) for alkaline phosphatase (Alpl, forward primer: GTGGGCATTGTGACTACC; reverse primer: GGTGGCATCTCG TTATCC), osteopontin (Spp1, forward primer: AACTCTTCCAAGCAATTCC; reverse primer: TCTCAT CAGACTCATCCG) and glyceraldehyde 3-phosphate dehydrogenase (Gapdh, forward primer: TTCAACGGCACAGTCAAGG; reverse primer: TCTCGCTCCTGGAAGATGG). Oligonucleotide primers to the targeted genes were designed using Beacon Designer 7.0 software (PREMIER Biosoft International, Palo Alto, CA). Primers were synthesized by Eurofins MWG Operon (Huntsville, AL). Real-time PCR was performed using the Veriti 96 well Thermal Cycler (Applied Biosystems, Carlsbad, CA) with Step One software (Applied Biosystems). Data were normalized to the endogenous reference gene Gapdh.

3.2.4 Osteopontin levels and alkaline phosphatase activity

Changes in osteopontin secreted into the conditioned media and alkaline phosphatase specific activity of the cell layer were used as outcome measures of the

rapid signaling pathway and a verification of real-time PCR results. 10 days after plating, cells were treated with media containing vehicle (ethanol) or 10^{-9}, 10^{-8}, or 10^{-7} M $1\alpha,25(OH)_2D_3$ for 15 minutes. Media were replaced by fresh media and cells were cultured an additional 24 hours. Osteopontin in the conditioned medium was determined by ELISA using a mouse osteopontin ELISA kit (R&D Systems, Minneapolis, MN) and normalized by the total protein of the cell layer. The cell layers, which included cells and any matrix vesicles, were washed twice with cold phosphate buffered saline (PBS) and lysed in 0.05% Triton-100. Alkaline phosphatase specific activity was measured as the release of *p*-nitrophenol from *p*-nitrophenylphosphate at pH 10.2 as previously described (46) and normalized by the total protein of the cell layer.

3.2.5 [^{3}H]-Thymidine incorporation

[^{3}H]-Thymidine incorporation was used as an indicator of the effect of $1\alpha,25(OH)_2D_3$ on cell proliferation. Cells were plated at 20,000 cells/cm^2 in 24 well plates with full media. At 80% confluence, media were changed to media containing no FBS (α-MEM, 1%P/S) for 24 hours. This method avoids proliferation arrest caused by over-confluence (35). To study the dose response of $1\alpha,25(OH)_2D_3$, cells were treated with media containing vehicle (ethanol) or the appropriate dose of $1\alpha,25(OH)_2D_3$ for 15 minutes. Immediately after 15 minutes of treatment, the media were replaced by α-MEM containing 1%P/S and 1μCi/ml [^{3}H]-thymidine per well (1mCi/ml, PerkinElmer, Waltham, MA). Four hours later, the cell layer was harvested by washing with cold PBS and 5% trichloroacetic acid. Radioactivity in TCA-precipitable material was measured by liquid scintillation spectroscopy as previously described (2).

3.2.6 Annexin V staining

Annexin V staining was used as an outcome measurement for the effect of $1\alpha,25(OH)_2D_3$ on apoptosis. The protocol was adapted from a previous report (38). Briefly, cells were treated with media containing vehicle (ethanol), or the appropriate dose of $1\alpha,25(OH)_2D_3$ for 1 hour. Media were replaced with α-MEM containing 0.5%FBS, 1%P/S and 10^{-7}M staurosporine (Sigma-Aldrich) or vehicle to induce apoptosis. Cells were harvested after 24 hours by incubating with trypsin (Invitrogen) for 10 minutes and collected by centrifugation. Then, cells were incubated with FITC-conjugated annexin V for 15 minutes using a commercial kit (4830-250-K, R&D system), and fluorescence was detected using a BD LSR II flow cytometer (BD, Franklin Lakes, NJ).

3.2.7 Signaling by $1\alpha,25(OH)_2D_3$

To study the role of c-Src and PLA2 signaling in regulating $1\alpha,25(OH)_2D_3$ stimulated responses, experiments were performed as described above using specific inhibitors of each enzyme. 10 days after plating, wild type cells MC3T3-E1 cells were treated with vehicle (DMSO); the c-Src inhibitor PP2 (dissolved in DMSO, Sigma-Aldrich) or c-Src inhibitor-1 (dissolved in DMSO, Sigma-Aldrich); or the PLA2 inhibitor quinacrine (dissolved in H_2O, Sigma-Aldrich) or PLA2 inhibitor AACOCF3 (dissolved in DMSO, Sigma-Aldrich). All inhibitors were added to media at concentration of 10^{-7}, 10^{-6} and 10^{-5} M 30 minutes before and maintained during 15 minutes of $1\alpha,25(OH)_2D_3$ treatment for gene expression and [^{3}H]-thymidine incorporation, or during 1 hour of $1\alpha,25(OH)_2D_3$ treatment for annexin V staining.

In order to demonstrate activation of individual signaling pathways, 10 days after plating, wild type MC3T3-E1 cells were treated with vehicle (ethanol) or the appropriate

concentration of 10^{-9}, 10^{-8}, 10^{-7}M 1α,25$(OH)_2D_3$ (stock in ethanol). c-Src and Akt were assayed at 9 minutes based on reports showing 1α,25$(OH)_2D_3$ induced c-Src activation and Akt phosphorylation at this time (38,39). Cells were then washed twice with cold PBS and cell layers were harvested. Akt phosphorylation (p-Akt) at serine 473 was measured using commercial ELISA kit (DYC887, R&D Systems) and normalized by total protein. c-Src activity was measured in a separate set of cell layers using a fluorescence polarity-based kit (32-059, Millipore, Billerica, MA) and normalized by total protein in the cell layer. PGE2 was measured as an indirect product of PLA2 signaling. 10 days after plating, cells were treated with vehicle (ethanol), or 10^{-9}, 10^{-8}, or 10^{-7} M 1α,25$(OH)_2D_3$ for 30 minutes as previously described (1). The media were harvested and acidified by adding HCl to a final concentration of 0.1 M. PGE2 was measured using a commercial radioisotope-based kit (Perkin Elmer) and normalized by total protein of the cell layer. To study the role of Pdia3, VDR, and caveolin-1 in regulating rapid responses, wild type, Sh-Pdia3, Sh-VDR and Sh-Cav1 cells were treated with vehicle (ethanol) or 10^{-7}M 1α,25$(OH)_2D_3$ for either 9 minutes for c-Src activity or 30 minutes for PGE2 release. PGE2 in the conditioned media and c-Src activity in the cell layer were measured by the same method.

3.2.8 Whole cell lysates, plasma membrane and caveolae isolation

In order to study subcellular location of Pdia3, VDR, caveolin-1 and their mediators, a detergent-free method of plasma membrane and caveolae isolation was used as previously described (26). In short, 10 days after plating, cells were lysed in RIPA buffer (20mM Tris-HCl, 150mM NaCl, 5mM disodium EDTA, 1%NP-40). A separate set of cells were harvested by scraping in isolation buffer (0.25M sucrose, 1mM

EDTA, 20mM tricine, PH=7.8). Samples were homogenized using a tissue grinder for twenty strokes on ice. Homogenates were centrifuged at 20,000g for 10 minutes to pellet cell debris, including nucleus, mitochondria, and endoplasmic reticulum. The supernatant was collected, placed on top of 30% Percoll (GE Healthcare, Piscataway, NJ) in isolation buffer, and then centrifuged for 30 minutes at 84,000g. The plasma membranes formed a visible band and were collected by aspiration. A portion of the plasma membrane fraction was layered on a 10%-20% OptiPrep gradient (Sigma-Aldrich) and centrifuged at 52,000g for 90 minutes. The top layer was collected, overlaid with 5% OptiPrep, and centrifuged at 52,000g for another 90 minutes. Fractions were collected from the top to the bottom in thirteen fractions with 750ul for each fraction. The caveolae existed as an opaque band, which was collected in Fraction 3, based on the presence of caveolin-1 as described (Fig. 3-4 A). Fractions one to six are presented in the figures.

To study the protein levels in whole cell lysates and plasma membranes of WT, Sh-Pdia3, Sh-Cav1 and Sh-VDR cells, 10 days after plating, the whole cell lysates and plasma membrane fractions were isolated from these cell lines. To study the 1α,25$(OH)_2D_3$ stimulated change in the protein levels in the plasma membranes, 10 days after plating, WT, Sh-Pdia3, Sh-Cav1 and Sh-VDR cells were treated with or without 10^{-8}M of 1α,25$(OH)_2D_3$ for 15 minutes and the plasma membranes were isolated. Western blots were performed on the isolated samples to examine the protein levels as described later.

3.2.9 Co-Immunoprecipitation

To better understand the mechanism of how the Pdia3 and VDR activate

downstream mediators and whether the two receptors and the caveolin-1 interact with each other, a systemic co-immunoprecipitation experiment was performed. 10 days after plating, wild type cells were treated with or without 10^{-8}M of 1α,25$(OH)_2D_3$ for 15 minutes. The plasma membranes were isolated as described above. The protein concentration of the plasma membrane fractionations was adjusted to reach the final concentration of 1mg/ml. The samples were pre-cleared by adding protein A-agarose beads (IP06, Calbiochem, Gibbstown, NJ). To immunoprecipitate Pdia3, caveolin-1 and VDR: Pdia3 AB100 (custom made, Alpha Diagnostic International Inc, San Antonio, Texas), caveolin-1 (N-20, Santa Cruz Biotechnology, Santa Cruz, CA) and VDR (D-6, Santa Cruz), or IgG (NeoMarkers, Fermont, CA) were added to each sample group respectively at a concentration of 10µg per 500 µg total protein and incubated overnight. Then protein A-agarose (Calbiochem) beads were added for one hour and the beads were isolated by centrifuging at 13,000 rpm. The pellets were washed with PBS three times. Western blots were performed to detect proteins in the immunoprecipitated complexes as described below.

3.2.10 Western blots

Western blots were performed against Pdia3, VDR and caveolin-1 along with the signal mediators, P85 regulatory subunit of PI3K, c-Src, and PLAA in different cell fractions or the Pdia3, VDR or caveolin-1 immunoprecipitated samples. P85 was assayed because previous studies showed PI3K was rapidly activated by 1α,25$(OH)_2D_3$ and the regulatory subunit P85 has been immunoprecipitated with other steroid hormone receptors (47,48). c-Src was chosen because it was found to immunoprecipitate with VDR (39). PLAA was studied because it was shown to immunoprecipitate with Pdia3

and caveolin-1 (19). The samples were mixed with loading buffer, boiled and followed by gel electrophoresis using NuSep 4-20% LongLife Gels (NuSep, Lawrenceville, GA). Proteins were transferred to nitrocellulose membrane using an iBlot Dry Blotting System (Invitrogen). The membrane was subsequently blotted in 1% bovine serum albumin (BSA, Sigma-Aldrich) in PBS for 1 hour and incubated overnight with antibodies against glyceraldehyde 3-phosphate dehydrogenase (Gapdh, MAB374, Millipore) as the internal loading control for whole cell lysates, pan-cadherin (CDH, Abcam, Cambridge, MA) as the internal loading control for plasma membranes, TATA binding protein (Abcam) as a control for nuclear contamination (49), cytochrome c oxidase subunit IV (Abcam) for mitochondrial contamination (50), Pdia3 (Alplha Diagnostic International, Inc.), caveolin-1 (N-20, Santa Cruz Biotechnology), VDR (D-6, Santa Cruz Biotechnology), c-Src (B-12, Santa Cruz Biotechnology), PLAA (custom made, Strategic Diagnostics Inc., Newark, DE), and P85 (U5, Santa Cruz Biotechnology). After washing three times with PBS containing 0.05% Tween-20, the membrane was incubated with goat anti-rabbit or goat anti-mouse horse radish peroxidase conjugated secondary antibodies (Bio-Rad) in PBS containing 5% dry milk and 0.05% Tween-20 for one hour. After three washes, the membrane was developed using SuperSignal West Pico Chemiluminescent System (Thermo Fisher Scientific, Rockford, IL) and imaged with the VersaDoc imaging system (Bio-Rad). For co-immunoprecipitated samples, to lower the background, ONE-HOUR IP-Western kits were used (L00231 or L00232, GenScript, Piscataway, NJ).

3.2.11 Subcellular localization

Immunofluorescence was used to assess the subcellular location and co-localization of Pdia3, VDR and caveolin-1. Wild type MC3T3-E1 cells were plated at

10,000 cells/cm^2 on a glass chamber slide for 24 hours. To limit the extracellular matrix production, a short culture time of 24 hours was applied, as previously described (1). The cells were fixed in 4% paraformaldehyde for 20 minutes. Cells were then incubated with a 1:100 dilution of Hoechst 33342 (Invitrogen), Pdia3 primary antibody (Alplha Diagnostic International, Inc.), VDR primary antibody (D-6, Santa Cruz Biotechnology) or caveolin-1 primary (7C8, Santa Cruz Biotechnology) antibody in PBS containing 1% BSA (Sigma-Aldrich). After washing, cells were incubated with goat anti-rabbit Alexa 488 (Invitrogen) and goat anti-mouse Alexa 594 (Invitrogen) in PBS containing 1% BSA in PBS, fixed with GEL/MOUNT (Biomeda Corp, Foster City, CA), and imaged using a Zeiss LSM 510 confocal microscope (Carl Zeiss MicroImaging, Thornwood, NY). The pictures were taken at room temperature with 63X1.25 oil objective lens and 10X ocular lens. No digital enlargement was applied. To quantify the pixel distribution of Pdia3, VDR and caveolin-1, the intensity of the green signal of Pdia3 and red signal of caveolin-1 or VDR was calculated along a cross section, which is indicated as the red line in figure 2-4C, and plotted against the distance by Zeiss LSM Image software (Carl Zeiss MicroImaging) (Fig. 2-4D,E). To study changes in co-localization after 1α,25$(OH)_2D_3$ treatment, wild type MC3T3-E1 cells were plated at 10,000 cells/cm^2 on a glass chamber slide for 24 hours. Cell were treated with vehicle or 10^{-8} M of 1α,25$(OH)_2D_3$. The cells were fixed at 0, 5, 15, 30 and 90 minutes after treatment. The same method for fluorescence staining was performed. In order to quantify co-localization, 10 random cells from each condition were selected and the correlation factor R between the green signal of Pdia3 and the red signal of VDR or caveolin-1 was calculated by Zeiss LSM Image software (Carl Zeiss MicroImaging). The mean and standard error of the 10 cells are presented in the graph.

3.2.12 Statistical analysis

For quantitative data including realtime PCR (Alpl and Spp1), ELISAs (Akt, osteopontin), alkaline phosphatase activity, c-Src activity, [^{3}H]-thymidine Incorporation and Anneixn V staining, each data point represents the means ± SEM for six independent cell cultures. For fluorescence images, each data point represents the mean correlation value R ± SEM for ten randomly chosen cells. Each experiment was repeated two or more times to ensure the validity of the data. The data presented are from a single representative experiment. Significance was determined by one way analysis of variance and post hoc testing performed using Bonferroni's modification of Student's t- test for multiple comparisons. $P \leq 0.05$ was considered to be significant.

For the data on silenced cell strains, due to the difference in baseline levels, the data were presented as treatment over control. The value of each sample from the treated group was divided by the mean of the control group. Each data point represents the means ± SEM for six normalized values and the control was represented by a dashed line with a value equal to one. Due to the nature of non-normal distribution, significance was determined by Mann Whitney test. $P \leq 0.05$ was considered to be significant.

For Western blot intensity quantification in figure 2-5 and figure 2-6, each experiment was repeated 4 to 6 times with one blot per experiment. The values of experimental samples were divided by the value of control sample for each experiment. Each data point represents the mean± SEM of the 4 to 6 independent experiments with the control represented by a dashed line with value of one. Due to the non-normal distribution of the data and the paired control and experimental sample, significance was determined by Wilcoxon matched pair test. $P \leq 0.05$ was considered to be significant.

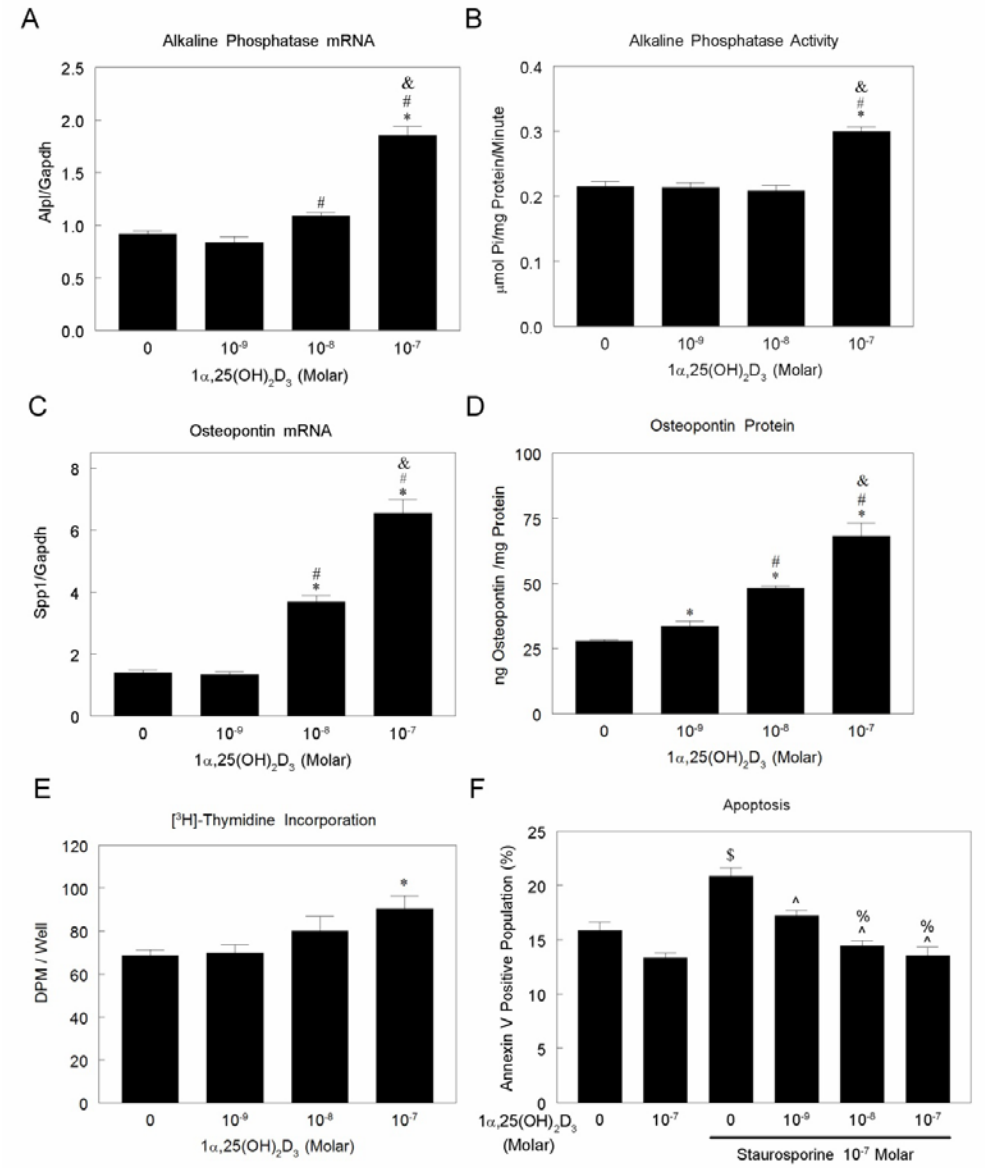

Figure 3-1. The effect of 1α,25(OH)$_2$D$_3$ on gene expression, protein production, [^{3}H]-thymidine incorporation and annexin V staining. (A, C): MC3T3-E1 cells were treated with vehicle (ethanol) or 10^{-9}, 10^{-8} or 10^{-7}M 1α,25(OH)$_2$D$_3$ for 15 minutes. Media were changed with full media and mRNA was harvested at 8 hours after treatment. mRNA for Alpl and Spp1 were normalized to Gapdh. (B, D): Osteopontin protein and alkaline phosphatase activity were measured at 24 hours after treatment and normalized to total protein. (E): After 15 minutes of treatment, [^{3}H]-thymidine was added to the medium and incorporation was measured 4 hours later. Data are presented as DPM/well. (F): MC3T3-E1 cells were treated with vehicle (ethanol) or with 10^{-9}, 10^{-8} or 10^{-7}M 1α,25(OH)$_2$D$_3$ for 1 hour followed by exposure to vehicle (DMSO) or 10^{-7} M staurosporine for 24 hours. Annexin V positive cells were determined as a percentage of total cells. *: p<0.05, 1α,25(OH)$_2$D$_3$ vs. control; #: p<0.05, 10^{-7}M and 10^{-8}M vs. 10^{-9}M, &: p<0.05, 10^{-7}M vs. 10^{-8}M. $: staurosporine vs. control. ^: P<0.05, 1α,25(OH)$_2$D$_3$ + staurosporine vs. staurosporine; %: 10^{-7}M and 10^{-8}M 1α,25(OH)$_2$D$_3$ + staurosporine vs. 10^{-9}M 1α,25(OH)$_2$D$_3$ + staurosporine.

3.3 Results

3.3.1 Transient 1α,25(OH)$_2$D$_3$ treatment modulates gene expression, protein production, [^{3}H]-thymidine incorporation and annexin V staining.

Alkaline phosphatase mRNAs (Alpl) were up-regulated by 15 minutes of 1α,25(OH)$_2$D$_3$ treatment (Fig. 3-1A). The increase in expression was dose-dependent and significant at 10^{-8} M and 10^{-7}M 1α,25(OH)$_2$D$_3$. A two-fold increase was achieved at 10^{-7} M of 1α,25(OH)$_2$D$_3$. The increase in mRNA was supported by an increase in alkaline phosphatase activity (Fig. 3-1B). 1α,25(OH)$_2$D$_3$ also stimulated a dose-dependent increase in osteopontin mRNA with a four-fold change at 10^{-7} M 1α,25(OH)$_2$D$_3$ (Fig. 3-1C) and a similar increase in osteopontin protein (Fig. 3-1D). 1α,25(OH)$_2$D$_3$ increased [^{3}H]-thymidine incorporation within 4 hours after 15 minutes of 1α,25(OH)$_2$D$_3$ treatment (Fig. 3-1E). In addition, 1α,25(OH)$_2$D$_3$ reduced staurosporine-induced apoptosis (Fig. 3-1F). Treatment of confluent MC3T3-E1 cells with staurosporine for 24 hours significantly increased the annexin V positive population from 15% in resting stage to 22%. Priming cells with 1α,25(OH)$_2$D$_3$ for 1 hour dose dependently decreased the annexin V positive population. At 10^{-7} M 1α,25(OH)$_2$D$_3$, the annexin V positive population was reduced to 13%.

3.3.2 The rapid membrane response to 1α,25(OH)$_2$D$_3$ activates production of signaling molecules through Pdia3, VDR and caveolin-1.

Treatment with 1α,25(OH)$_2$D$_3$ for 30 minutes caused a dose dependent increase in PGE2 in the conditioned media (Fig. 3-2A). A four-fold increase was observed at the highest dose. Treatment with 10^{-7} M 1α,25(OH)$_2$D$_3$ for 9 minutes increased c-Src activity by 50% compared to control cultures (Fig. 3-2B). In contrast to c-Src, the amount of phosphorylated Akt was not different after 9 minutes of 1α,25(OH)$_2$D$_3$ treatment (Fig.

3C).

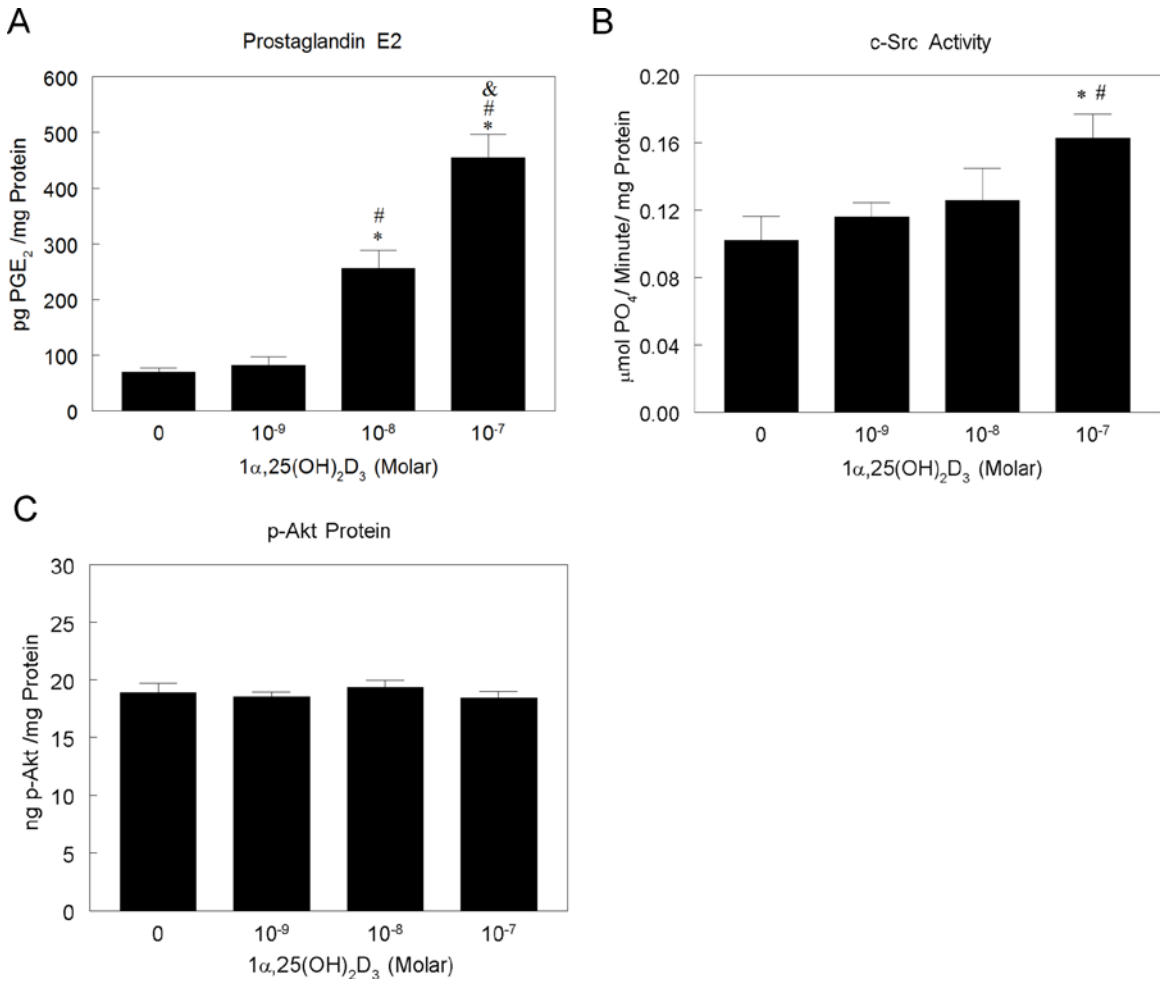

Figure 3-2. The effect of 1α,25$(OH)_2D_3$ on PGE2 production, c-Src activity and Akt phosphorylation in MC3T3-E1 cells. (A): MC3T3-E1 cells were treated with vehicle (ethanol) or with 10^{-9}, 10^{-8} or 10^{-7}M 1α,25$(OH)_2D_3$ for 30 minutes. Conditioned media were collected and PGE2 was measured and normalized to total protein in the cell layer. (B): MC3T3-E1 cells were treated with vehicle (ethanol) or with 10^{-9}, 10^{-8} or 10^{-7}M 1α,25$(OH)_2D_3$ for 9 minutes. c-Src activity was measured and normalized to total protein. (C): After 9 minutes of treatment, S473-phosphorylated Akt was measured and normalized to total protein. *: $p<0.05$, 1α,25$(OH)_2D_3$ treatments vs. control; #: $p<0.05$, 10^{-7}M and 10^{-8}M vs. 10^{-9}M, &: $p<0.05$, 10^{-7}M vs. 10^{-8}M.

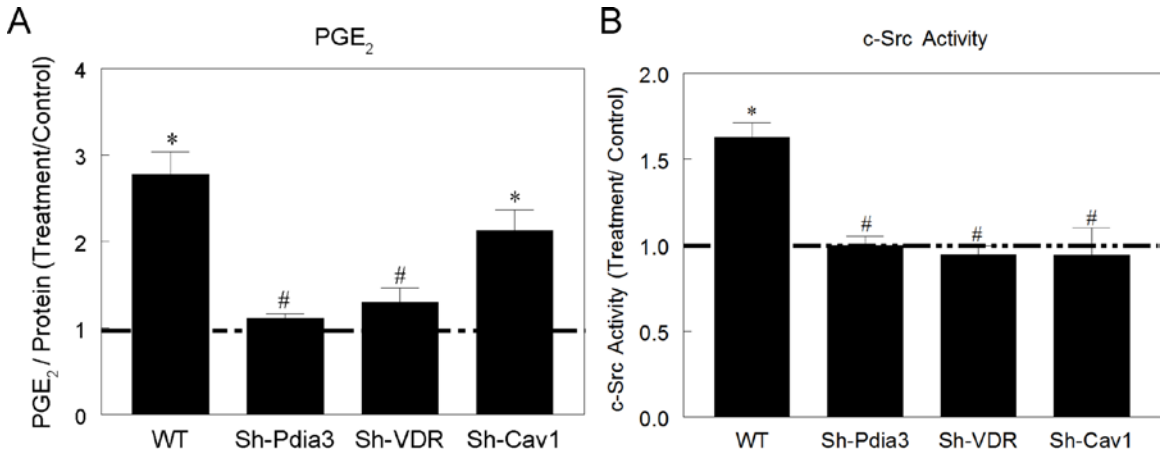

Figure 3-3. The role of Pdia3, VDR and caveolin-1 in 1α,25$(OH)_2D_3$-stimulated PGE2 production and c-Src activity in MC3T3-E1 cells. (A): Wild type, Sh-Pdia3, Sh-VDR and Sh-Cav1 MC3T3-E1 cells were treated with vehicle (ethanol) or 10^{-7}M 1α,25$(OH)_2D_3$ for 30 minutes. Conditioned media were collected and PGE2 was measured and normalized to the total protein of the cell layer. (B): Wild type, Sh-Pdia3, Sh-VDR and Sh-Cav1 MC3T3-E1 cells were treated with vehicle (ethanol) or 10^{-7}M 1α,25$(OH)_2D_3$ for 9 minutes. c-Src activity was measured and normalized to total protein. Treatment over control ratios were calculated for each parameter. The dashed line represents the value for the control cultures, which was set to 1. *:$p<0.05$, 1α,25$(OH)_2D_3$ treatment vs. control; #: $p<0.05$, Sh-Pdia3, Sh-VDR, Sh-Cav1 vs. wild type.

1α,25$(OH)_2D_3$ stimulated release of PGE2 was completely blocked in Sh-Pdia3 and Sh-VDR cells while in Sh-Cav1 cells, it was reduced but still greater than in wild type cells (Fig. 3-3A). Whereas c-Src activation was increased 50% in wild type cells, 1α,25$(OH)_2D_3$ had no effect in Sh-Pdia3, Sh-VDR or Sh-Cav1 cells (Fig. 3-3B), indicating Pdia3, VDR and caveolin-1 are all required for rapid activation c-Src and release of PGE2.

3.3.3 Subcellular location of Pdia3 and VDR is differentially regulated by 1α,25$(OH)_2D_3$.

Pdia3, VDR and caveolin-1 were present in whole cell lysates and isolated plasma membranes (Fig. 3-4A). Western blots against nuclear TATA binding protein (TBP) and mitochondria COXIV protein showed no nuclear or mitochondrial contamination in the plasma membrane fraction. Caveolin-1 was present in fraction 3 of the plasma membrane, indicating the enrichment of caveolae in this fraction. Interestingly, Pdia3 was detected in fraction 3, but not VDR (Fig. 3-4A). The regulatory subunit of PI3K, P85, was detected in the whole cell lysate and plasma membrane but not in fraction 3; whereas c-Src and PLAA were present in the whole cell lysate, plasma membranes and fraction 3 (Fig. 3-4B).

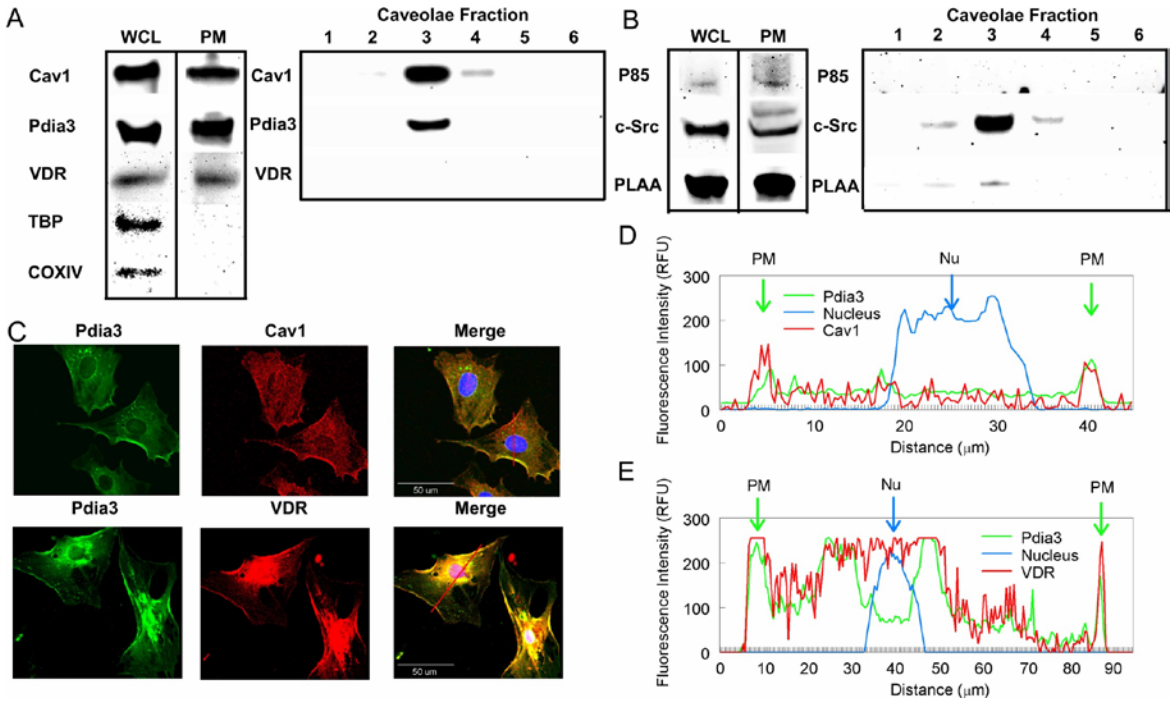

Figure 3-4. The subcellular location of Pdia3, VDR and caveolin-1 in MC3T3-E1 cells. (A,B): Western blots against Cav-1, Pdia3, VDR, P85, c-Src and PLAA were performed on whole cell lysates, isolated plasma membranes and caveolae. Caveolae were prepared by subfractionation of the isolated plasma membranes, yielding thirteen fractions. Fractions one to six are shown; caveolae were present in fraction 3. TATA box binding protein and COXIV were used to detect contamination with nuclei or mitochondria. (C): Confocal image of permeabilized MC3T3-E1 cells. Green: Pdia3; Red: Cav1 (upper panel) / VDR (lower panel); Yellow: merge of Pdia3 and Cav1 or VDR. (D): The histogram of co-localization along a line across the cell (the red lines in C). Green: Pdia3; Red: Cav1 (upper panel) / VDR (lower panel); Blue: nucleus. Green arrows show the overlap of peaks between Pdia3 and caveolin-1 or VDR on the boundaries of cells. Blue arrows indicate the nucleus.

Confocal microscopy showed that Pdia3 was distributed over the surface and was also enriched in the perinuclear area. Pdia3 was excluded from nucleus in most of the cells. VDR was also distributed over the cell surface and perinuclear area, similarly to Pdia3, and it also presented in nucleus. Caveolin-1 was evenly distributed over the cell surface without enrichment around the nucleus. When the confocal images were merged, the yellow merged signal was particularly enriched on the cell boundary, indicating Pdia3 co-localized with caveolin-1 and VDR on the plasma membrane. Strong co-localization between Pdia3 and VDR was also observed in the perinuclear area (Fig. 3-4C). Two cross sections were taken of the Pdia3/Caveolin-1 image and Pdia3/VDR image and pixel intensity histograms were graphed along the cross sections. Pdia3, VDR and caveolin-1 all showed peaks at the cell boundaries. Moreover, the Pdia3 peaks overlapped with caveolin-1 and VDR peaks, indicating Pdia3 co-localized with caveolin-1 and VDR on the plasma membrane (Fig. 3-4D,E).

Co-localization of Pdia3 and caveolin-1 decreased in a time dependent manner and was reduced by 50% at 90 minutes (Fig. 3-5A). In cultures treated with 1α,25$(OH)_2D_3$ co-localization of Pdia3 and caveolin-1 was reduced at 15 and 30 minutes compared to the vehicle-only control cultures indicating that the hormone stimulated dissociation. 1α,25$(OH)_2D_3$ decreased co-localization of Pdia3 and VDR within 5 minutes and the dissociation was significant through the entire treatment time (Fig. 3-5B).

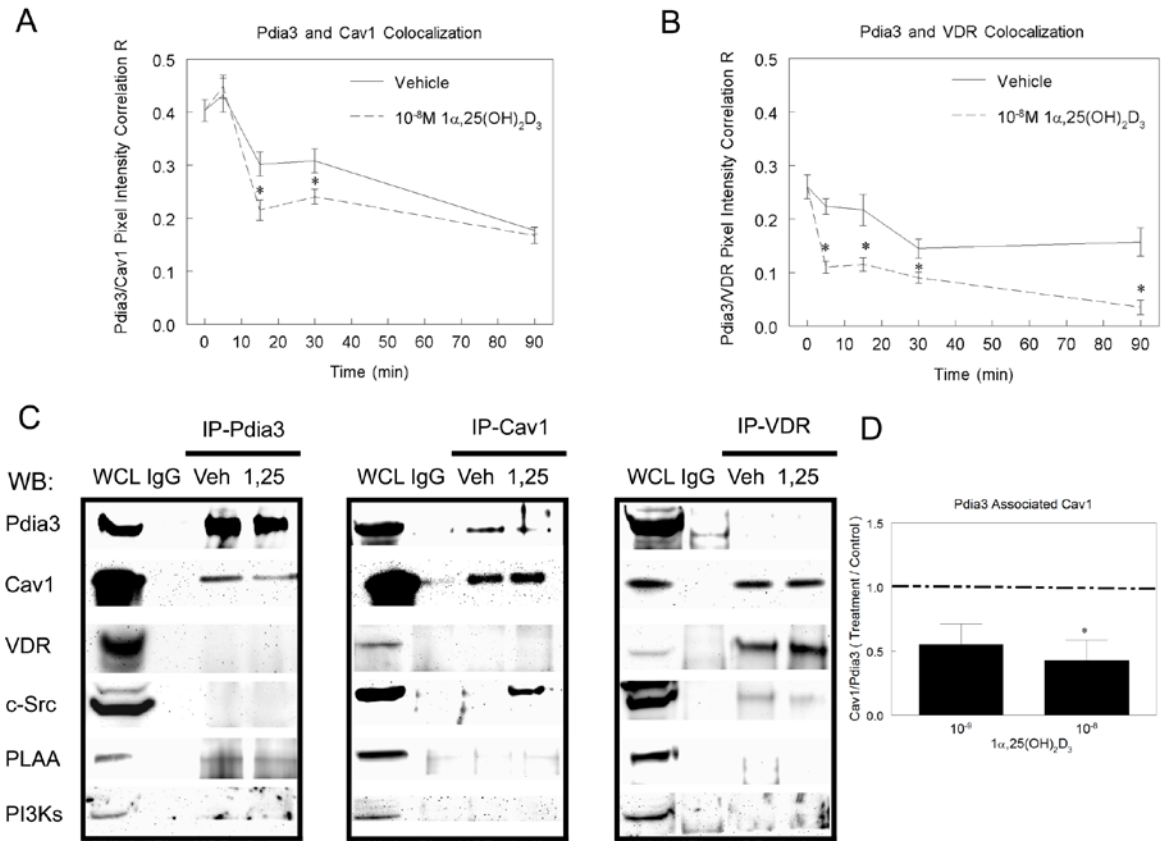

Figure 3-5. The effect of 1α,25(OH)$_2$D$_3$ on membrane association of Pdia3, VDR and caveolin-1 in MC3T3-E1 cells. Western blots using antibodies against Gapdh, Pdia3, VDR and caveolin-1 in the whole cell lysate (A) and plasma membrane (C) of wild type, Sh-Pdia3, Sh-VDR and Sh-Cav1 MC3T3-E1 cells. (B): Pixel quantification of figure A. (D): Pixel quantification of figure C. The targeted protein intensity was first normalized by the intensity of Gapdh for whole cell lysates or pan-cadherin (CDH) for plasma membranes and then divided by the wild type value. The dashed line represents wild type, which equals 1. * p<0.05, Sh-Pdia3, Sh-VDR, Sh-Cav1 vs. wild type. (E): MC3T3-E1 cells were treated with or without 10^{-8} M 1α,25(OH)$_2$D$_3$ for 15 minutes and the plasma membranes were isolated and blotted against pan-cadherin (internal loading control), VDR, Pdia3 and caveolin-1. (F): The pixel quantification result of figure E. The targeted protein intensities were first normalized by the intensity of pan-cadherin from the same group and then values of 1α,25(OH)$_2$D$_3$ treated groups were divided by the value of the vehicle treated groups. The line represents vehicle, which equals to 1. *: p<0.05, treatment vs. control.

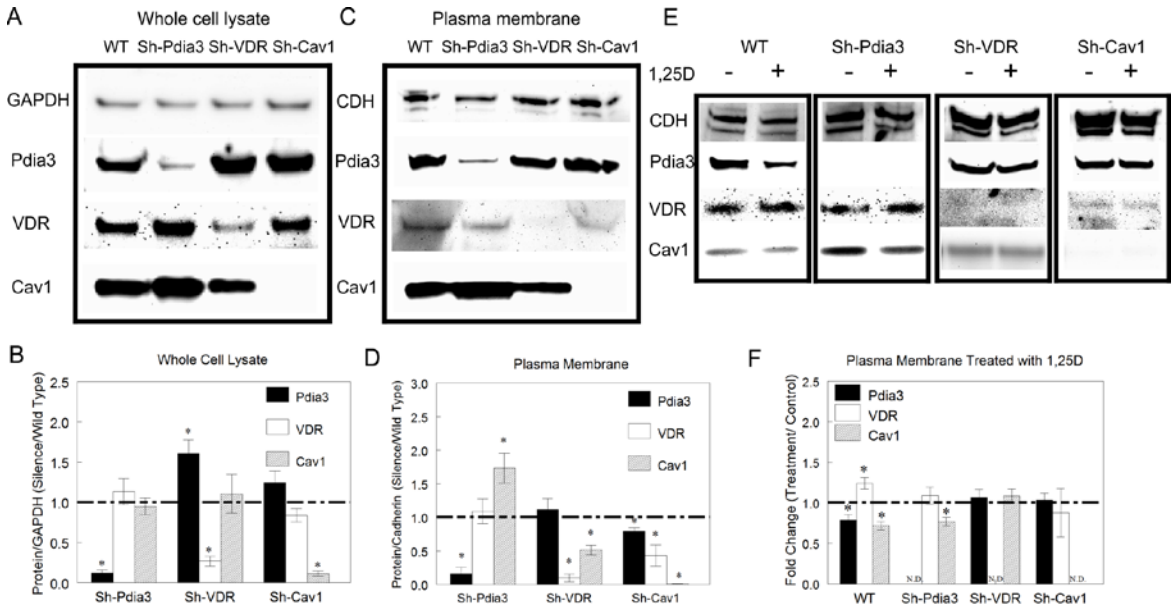

Figure 3-6. The effect of 1α,25$(OH)_2D_3$ on membrane association of Pdia3, VDR and caveolin-1 in MC3T3-E1 cells. Western blots using antibodies against Gapdh, Pdia3, VDR and caveolin-1 in the whole cell lysate (A) and plasma membrane (C) of wild type, Sh-Pdia3, Sh-VDR and Sh-Cav1 MC3T3-E1 cells. (B): Pixel quantification of figure A. (D): Pixel quantification of figure C. The targeted protein intensity was first normalized by the intensity of Gapdh for whole cell lysates or pan-cadherin (CDH) for plasma membranes and then divided by the wild type value. The dashed line represents wild type, which equals 1. * $p<0.05$, Sh-Pdia3, Sh-VDR, Sh-Cav1 vs. wild type. (E): MC3T3-E1 cells were treated with or without 10^{-8} M 1α,25$(OH)_2D_3$ for 15 minutes and the plasma membranes were isolated and blotted against pan-cadherin (internal loading control), VDR, Pdia3 and caveolin-1. (F): The pixel quantification result of figure E. The targeted protein intensities were first normalized by the intensity of pan-cadherin from the same group and then values of 1α,25$(OH)_2D_3$ treated groups were divided by the value of the vehicle treated groups. The line represents vehicle, which equals to 1. *: $p<0.05$, treatment vs. control.

3.3.4 Pdia3 and VDR separately formed two 1α,25$(OH)_2D_3$ responsive complexes on the plasma membrane.

We were successfully able to immunoprecipitate Pdia3, caveolin-1 and VDR (Fig. 3-5C). Immunoprecipitates of plasma membranes using antibodies to Pdia3 (IP-Pdia3) were negative for VDR, c-Src and P85 but positive for PLAA and caveolin-1 (Fig. 3-5C, left panel). Treatment with 1α,25$(OH)_2D_3$ for 15 minutes had no effect on PLAA but reduced caveolin-1. Treatment/control ratios for 4 different plasma membrane preparations showed that treatment of the cells with 10^{-9} or 10^{-8} M 1α,25$(OH)_2D_3$ induced a 50% to 60% decrease in Pdia3 associated caveolin-1 (Fig. 3-5D). Western blots of plasma membranes immunoprecipitated with antibodies to caveolin-1 (IP-Cav1) demonstrated a decrease in caveolin-1 associated Pdia3 after addition of 1α,25$(OH)_2D_3$ (Fig. 3-5C, middle panel). Caveolin-1 also interacted with c-Src but only after 1α,25$(OH)_2D_3$ treatment. VDR, PLAA and PI3K did not show an interaction with caveolin-1. Immunoprecipitation of VDR demonstrated interaction with c-Src with or without 1α,25$(OH)_2D_3$ treatment (IP-VDR) (Fig. 3-5C, right panel). An interaction was also detected between VDR and caveolin-1, which was not seen in IP-Cav1 immunoprecipitates. These data indicate Pdia3 forms a complex with caveolin-1 and PLAA while VDR forms a complex with c-Src and possibly caveolin-1.

3.3.5 The membrane presence and transport of Pdia3, VDR and caveolin-1 are interdependent.

Western blots of whole cell lysates from MC3T3-E1 cells silenced for Pdia3 (Sh-Pdia3), VDR (Sh-VDR) or caveolin-1 (Sh-Cav1) showed a specific decrease in the band intensities of the targeted proteins compared to wild type cells (Fig. 3-6A). Specific

reduction of Pdia3 and Cav-1 did not affect the levels of VDR; however when VDR was reduced, Pdia3 was upregulated (Fig. 3-5B). Plasma membranes also exhibited specific loss of the targeted protein in each of the silenced cell lines (Fig. 3-5C). In addition, Sh-Pdia3 cells exhibited increased plasma membrane caveolin-1; Sh-VDR cells had reduced caveolin-1; and Sh-Cav1 cells had reduced Pdia3 and reduced VDR (Fig. 3-5D).

The plasma membrane distribution of Pdia3, VDR and caveolin-1 was 1α,25$(OH)_2D_3$ dependent (Fig. 3-6E,F). When wild type MC3T3-E1 cells were treated for 15 minutes with 1α,25$(OH)_2D_3$, Pdia3 decreased 20%, VDR increased 20%, and caveolin-1 decreased 30%. The effect of 1α,25$(OH)_2D_3$ treatment depended on the relative presence of each protein. Lack of Pdia3 blocked the stimulatory effect of 1α,25$(OH)_2D_3$ on VDR but had no effect on caveolin-1. Silencing VDR blocked the 1α,25$(OH)_2D_3$ dependent reduction in Pdia3 and caveolin-1. Silencing caveolin-1 blocked the reduction in Pdia3 and the increase in VDR caused by 1α,25$(OH)_2D_3$ treatment.

3.3.6 The effect of 1α,25$(OH)_2D_3$ on Alpl expression and alkaline phosphatase activity, [^{3}H]-thymidine incorporation, and annexin V staining is mediated by Pdia3, VDR and caveolin-1.

1α,25$(OH)_2D_3$ treatment increased Alpl expression by 100% in wild type cells (Fig. 3-7A). This effect was lost in Sh-VDR and Sh-Pdia3 cells and was attenuated in Sh-Cav1 cells. Alkaline phosphatase specific activity was affected in a similar manner (Fig. A-3). Surprisingly, the highest dose of the c-Src inhibitor PP2 augmented Alpl expression (Fig. 3-7B), whereas the highest dose of the PLA2 inhibitor quinacrine

attenuated it (Fig. 3-7C). To confirm the unexpected stimulatory effect of the c-Src inhibitor-PP2, the experiment was repeated using another c-Src inhibitor, c-Src inhibitor-1, and a similar augmented expression was observed, also at the highest dose (Fig. A-4).

1α,25$(OH)_2D_3$ treatment induced a 40% increase in [^{3}H]-thymidine incorporation in wild type cells (Fig. 3-7D). Silencing Pdia3 or VDR blocked this effect. Lack of caveolin-1 resulted in an inhibition of [^{3}H]-thymidine incorporation in response to 1α,25$(OH)_2D_3$. Both PP2 and quinacrine blocked 1α,25$(OH)_2D_3$–dependent [^{3}H]-thymidine incorporation at all doses tested (Fig. 3-7E,F).

Treatment of wild type MC3T3-E1 cells for one hour with 1α,25$(OH)_2D_3$ caused a 25% reduction in staurosporine induced annexin V staining (Fig. 3-7G). The rapid decrease in annexin V was attenuated in Sh-Pdia3 cells and was blocked in cells lacking VDR or caveolin-1. Neither PP-2 nor the PLA2 inhibitor AACOCF3 altered the inhibitory effect of 1α,25$(OH)_2D_3$ on apoptosis in the wild type cells.

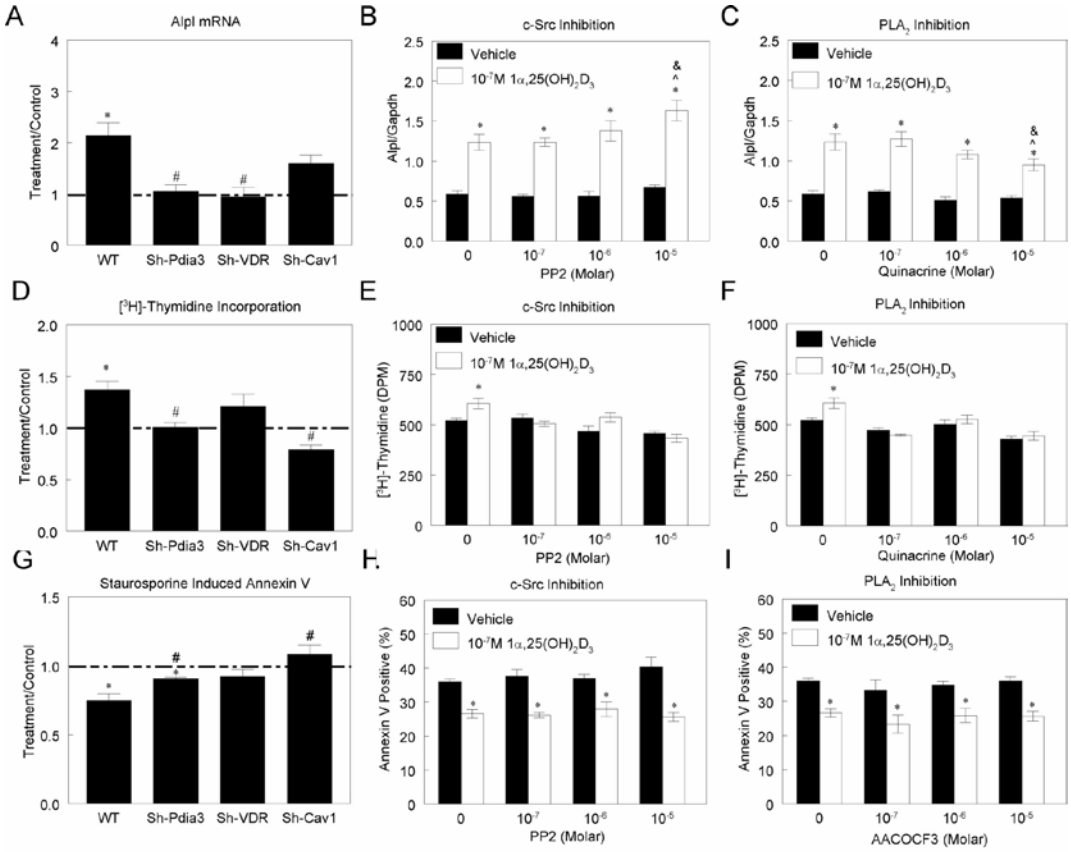

Figure 3-7. The role of Pdia3, VDR and caveolin-1 and their associated signaling mediators on 1α,25(OH)$_2$D$_3$-stimulated Alpl expression, [^{3}H]-thymidine incorporation and reduction of annexin V staining. For Alpl expression, (A): cells were treated with vehicle (ethanol) or 10^{-7}M 1α,25(OH)$_2$D$_3$ for 15 minutes. mRNA was harvested at 8 hours. For the inhibitor study, cells were treated with vehicle (DMSO) or with 10^{-7}, 10^{-6} or 10^{-5} M c-Src inhibitor-PP2 (B) and the PLA2 inhibitor quinacrine (C) (dissolved in H_2O) for 30 minutes before, and maintained during, 15 minutes of 1α,25(OH)$_2$D$_3$ treatment. mRNA was harvested at 8 hours. Alpl mRNA was normalized to Gapdh and treatment/control ratios were calculated. For [^{3}H]-thymidine incorporation, (D): cells were treated with vehicle (ethanol) or 10^{-7}M 1α,25(OH)$_2$D$_3$ for 15 minutes. [^{3}H]-Thymidine was added to the medium and its incorporation was measured 4 hours later; data are presented as DPM/well. Treatment/control ratios were calculated. For the inhibitor study, wild type cells were treated with vehicle (DMSO), or with 10^{-7}, 10^{-6} or 10^{-5} M c-Src inhibitor-PP2 (E) and the PLA2 inhibitor quinacrine (F) (dissolved in H_2O) 30 minutes before, and maintained during, 15 minutes of 1α,25(OH)$_2$D$_3$ treatment. [^{3}H]-Thymidine incorporation was measured 4 hours later and is presented as DPM/well. For the annexin V study (G): cells were treated with vehicle (ethanol) or 10^{-7}M 1α,25(OH)$_2$D$_3$ for 1 hour followed by exposure to 10^{-7} M staurosporine for 24 hours. For the inhibitor study, wild type cells were treated with vehicle (DMSO) or with 10^{-7}, 10^{-6} or 10^{-5} M c-Src inhibitor-PP2 (H) or the PLA2 inhibitor AACOCF3 (I) (dissolved in H_2O) 30 minutes before and maintained during 1 hour of 1α,25(OH)$_2$D$_3$ treatment followed by exposure to vehicle (DMSO) or 10^{-7} M of staurosporine for 24 hours. Annexin V positive cells were calculated as a percentage of total cells and treatment over control values were calculated. *: $p<0.05$, 1α,25(OH)$_2$D$_3$ vs. control; #: $p<0.05$, Sh-Pdia3, Sh-VDR and Sh-Cav1 vs. WT; ^: $p<0.05$, inhibitor vs. control, &: $p<0.05$, 10^{-5}M and 10^{-6}M vs. 10^{-7}M of inhibitors.

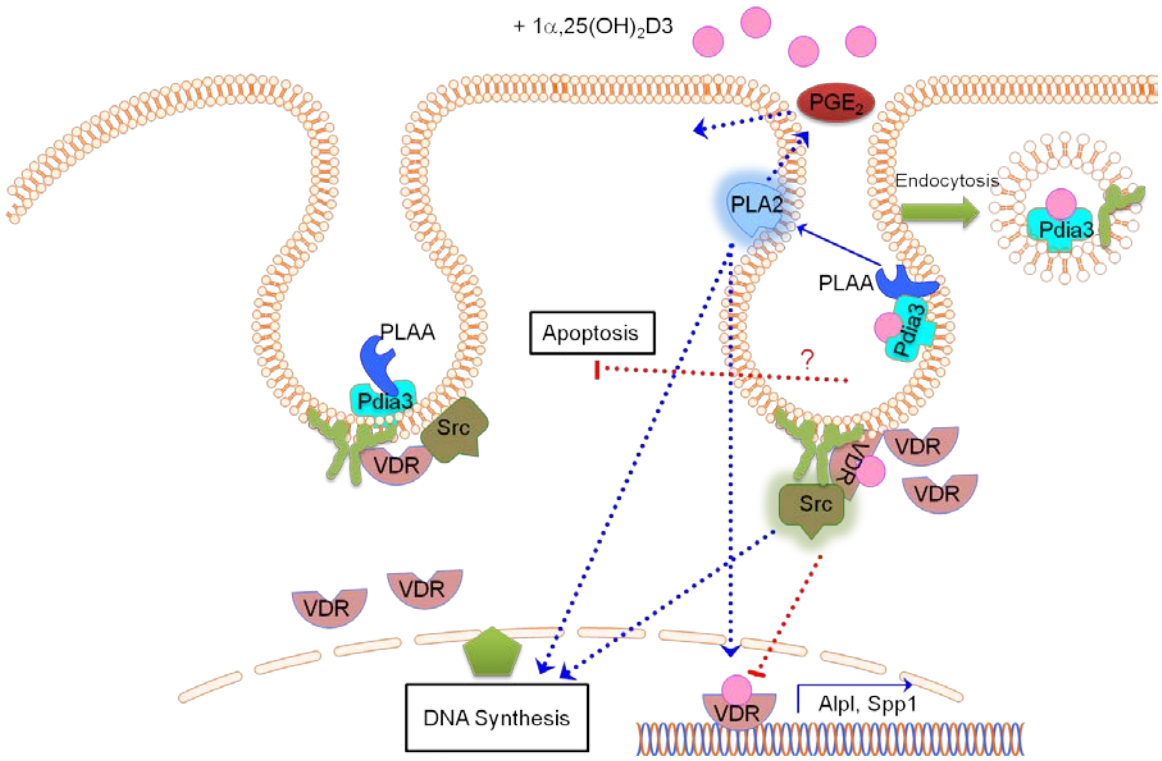

Figure 3-8. Cartoon showing the proposed signaling pathway for 1α,25$(OH)_2D_3$ stimulated rapid responses in osteoblasts. In the absence of 1α,25$(OH)_2D_3$, Pdia3 forms a complex with caveolin-1 and PLAA at the membrane whereas VDR forms a complex with caveolin-1 and c-Src in the peri-membrane cytoplasm. 1α,25$(OH)_2D_3$ binds with VDR, which activates VDR-associated c-Src. c-Src attaches and phosphorylates caveolin-1, causing the release of the Pdia3/PLAA complex from caveolin-1. The released Pdia3/PLAA complex activates PLA2 and eventually triggers the release of PGE2. After activation, Pdia3 and caveolin-1 are endocytosed while VDR is further recruited to the plasma membrane. The activated pathways subsequently affect downstream cellular biology. The Pdia3 associated PLA2 pathway promotes Alpl gene expression while VDR associated c-Src pathway inhibits it. Both pathways contribute to DNA synthesis; but neither is involved in annexin reduction.

3.4 Discussion

This study demonstrates in one model system the importance of both receptors and caveolin-1 in mediating the rapid responses of $1\alpha,25(OH)_2D_3$. It provides mechanistic information by showing that Pdia3 and VDR form two separate complexes with caveolin-1 and downstream mediators, and these complexes respond to $1\alpha,25(OH)_2D_3$ treatment by changing protein-protein interaction and plasma membrane translocation. Moreover, events at the signaling level were correlated with the downstream biology by showing the importance of the receptor complexes and signaling mediators in regulating $1\alpha,25(OH)_2D_3$ induced changes in gene expression, DNA synthesis and apoptosis. The signaling pathway based on the results of this study is illustrated in figure 3-8 and discussed in detail below.

Our results indicate that Pdia3 and VDR are co-localized on the plasma membrane, but the question of whether they are co-localized in caveolae is more complex. We and others have reported that the two receptors are present in caveolae based on Western blots of plasma membrane fractions using antibodies to each receptor and to caveolin-1(1,19,26). However, in the present study Pdia3, but not VDR, was presented in the caveolae-enriched plasma membrane fraction 3. Similarly, we showed that Pdia3 is present in chondrocyte caveolae via confocal imaging of intact cells and by Western blots of isolated membranes (31). These experiments were also inconsistent in their identification of VDR. Our immunoprecipitation data also showed that VDR interacted with caveolin-1 and in Sh-Cav1 cells, there was a 60% reduction of membrane associated VDR. Taking these observations together, we propose that VDR exists in caveolae as a peripheral membrane protein through attachment to caveolin-1, but its connection is via weak protein-protein interactions that are disrupted during vigorous caveolae fractionation. In contrast, Pdia3 has a putative myristate site through

which Pdia3 may be able to anchor in the caveolae and survive the harsh caveolae isolation procedure (51). Therefore the spatial proximity strongly suggests the two receptors exist in one functional unit in caveolae (Fig. 3-8).

Our immunoprecipitation study indicates that Pdia3 forms a complex with caveolin-1 and PLAA, while VDR forms a complex with c-Src. Interaction between caveolin-1 and VDR was observed in IP-VDR Western blots, but not in IP-Cav1 blots. As suggested above, this may be due to low levels of VDR in the plasma membrane compared to Pdia3 and caveolin-1. Given the large number of proteins attached to caveolin-1, any VDR may have been below the limits of detection when using antibodies to caveolin-1 for immunoprecipitation. In contrast, by using anti-VDR antibodies, we enriched the population for proteins associated with VDR and thus were able to find its abundant linker protein, caveolin-1.

Pdia3 did not directly form a complex with VDR in the plasma membrane, although both receptors interacted with caveolin-1. Others have reported that Pdia3 interacts with VDR in non-nuclear extracts of fibroblasts (52). It may be possible the Pdia3/VDR direct interaction exists in other cell fractions besides plasma membrane.

The results of this study also reveal how these receptor complexes dynamically respond to 1α,25$(OH)_2D_3$ treatment. Upon addition of exogenous 1α,25$(OH)_2D_3$, confocal data showed that Pdia3 moved away from caveolin-1 and VDR compared to control cells. Immunoprecipitation results further confirmed that the interaction between Pdia3 and caveolin-1 decreased. The time-dependent dissociation of Pdia3 and caveolin-1 observed in control cells may have been due to low concentrations of 1α,25$(OH)_2D_3$ in the fetal bovine serum used in the medium (53).

In contrast to the dissociation of Pdia3 and caveolin-1, the interaction between c-

Src and caveolin-1 increased after 1α,25$(OH)_2D_3$ treatment. Others have shown that c-Src phosphorylates caveolin-1 in response to 17β-estradiol, resulting in caveolin-1's release of ERα, which then activates its downstream mediator (54). We believe that a similar mechanism exists in our pathway, where 1α,25$(OH)_2D_3$ binding to VDR activates its associated c-Src. c-Src phosphorylates caveolin-1, which causes caveolin-1 to release Pdia3. The dissociated Pdia3 together with its interacting protein PLAA triggers activation of its downstream PLA2/PGE2 signaling pathways. At the same time, the VDR associated c-Src could also initiate its own downstream signaling pathway. These interactions and responses to 1α,25$(OH)_2D_3$ are illustrated in Figure 3-8.

Our data show that the two receptor complexes not only respond to 1α,25$(OH)_2D_3$ treatment by changing protein interaction but also by changing subcellular location. 1α,25$(OH)_2D_3$ rapidly decreased Pdia3 and caveolin-1 and rapidly increased VDR on the plasma membrane. The increase of VDR on the plasma membrane has also been reported in human hepatocytes and skeleton muscle cells treated with 1α,25$(OH)_2D_3$ (9,55). We postulate this may be a mechanism used by cells to enhance the rapid response. A similar dislocation of Pdia3 from the basal lateral membrane has been described in chicken intestine cells after 1α,25$(OH)_2D_3$ treatment (56), potentially participating in gene transcription. However, in our study, we did not find clear increase of Pdia3 in the nucleus by confocal microscopy within 90 minutes of 1α,25$(OH)_2D_3$ treatment. Others have shown that 1α,25$(OH)_2D_3$-stimulated translocation of Pdia3 into the nucleus could be cell type specific (57). Pdia3-mediated signaling results in ERK1/2 MAP kinase activation (1,10,15), which can also modulate gene transcription. Thus, rather than participating directly in transcriptional activity in the nucleus, Pdia3 lost from the membrane may enter the endocytic pathway together with decreased caveolin-1, as has been found for other plasma membrane receptor mediated signaling pathways (58).

The membrane recruitment of VDR and endocytosis of Pdia3/caveolin-1 after 1α,25$(OH)_2D_3$ treatment are also illustrated in the diagram (Fig. 3-8).

1α,25$(OH)_2D_3$ activated c-Src within 9 minutes, as has been shown for other steroid hormone receptors, indicating c-Src's conserved role in mediating steroid hormone rapid responses (39,55,59). We also showed that 1α,25$(OH)_2D_3$ stimulated PGE2 release within 30 minutes. In chondrocytes, 1α,25$(OH)_2D_3$ first activates PLA2 via Pdia3 dependent activation of PLAA, triggering the release of arachidonic acid within seconds and the arachidonic acid is processed via cyclooxygenase-1 to PGE2 (1,18,34,35).

1α,25$(OH)_2D_3$ can rapidly activate PI3K and Akt phosphorylation as well (38) and PI3K has also been reported to be co-immunoprecipitated with estrogen, androgen, and glucocorticoid receptors (47,48,54,60). However, in our MC3T3-E1 cells, neither Akt phosphorylation nor PI3K association was detected, suggesting that the PI3K pathway does not mediate the rapid response to 1α,25$(OH)_2D_3$. More importantly, we showed that silencing Pdia3 could block VDR-dependent c-Src activation and silencing VDR could also block the activation of Pdia3-dependent PGE2 release. This experiment, along with our co-immunoprecipitation and confocal results, further confirms that the Pdia3/VDR/caveolin-1 complex is not only spatially and physically connected, but also functionally connected as one unit to activate the downstream signaling molecules.

We previously used Sh-Pdia3 cells to demonstrate the role of Pdia3 in mediating 1α,25$(OH)_2D_3$ stimulated Alpl expression (1). However, since Alpl has a putative VDRE (61) and VDR is also important for rapid membrane responses, it was not clear to what extent VDR contributes to this regulation. Here, we used Sh-Pdia3, Sh-VDR and Sh-Cav1 cells to further compare the contribution of the two membrane receptors and

caveolin-1 in regulating Alpl expression. Our data show both receptors as well as caveolin-1 contribute to the increase in Alpl. Our data further show that the VDR/c-Src pathway inhibits Alpl expression while the Pdia3/PLA2 pathway stimulates it. One possibility is that the AP-1 site in the VDRE of Alpl plays a role, based on the observation that Pdia3-dependent signaling activates ERK1/2 MAP kinase (1).

c-Jun and c-Fos bind the AP-1 site in VDRE blocking VDR dependent Alpl expression; thus proliferating osteoblasts have high c-Jun and c-Fos and low Alpl (61). c-Src and v-Src promote cell proliferation through activation of c-Jun and c-Fos (62-64), suggesting that by inhibiting c-Src we amplified 1α,25$(OH)_2D_3$-induced Alpl by reducing the inhibitory effect of c-Jun and c-Fos. These data suggest the possibility that the two receptors and their separate signaling pathways provide a way for cells to tailor gene expression in response to the same 1α,25$(OH)_2D_3$ stimulation via regulating the levels of the receptors or their associated mediators. Moreover, involvement of multiple signaling pathways also offers more possibilities for interacting with other pathways and other hormones. Our results support a two point regulation of Alpl expression both through the transcription factor VDR in the nucleus and via signaling from the receptor complex on plasma membrane (Fig. 3-8).

1α,25$(OH)_2D_3$ is generally known for its ability to inhibit proliferation through VDR mediated genomic effects (65,66). In our previous work where we treated chondrocytes for 24 hours, we also observed an inhibitory effect on proliferation (2). Because our goal in the present study was to investigate the contribution of the rapid membrane response to proliferation, we measured [^{3}H]-thymidine incorporation at 4 hours and observed a stimulatory effect of 1α,25$(OH)_2D_3$ on DNA synthesis. 1α,25$(OH)_2D_3$ has been reported to change gene expression within 4 hours (67), supporting our observation, while traditional VDR-dependent mechanism are likely to be involved, our results implicate

mechanisms involving rapid membrane associated signaling cascades. Moreover, both receptors play a role. Silencing any component of the plasma membrane receptor complex reduced the increase in [^{3}H]-thymidine incorporation. In addition, inhibitors against PLA2 or c-Src also blocked this increase. This result is particularly interesting, because we showed the rapid membrane effect of 1α,25$(OH)_2D_3$ may boost proliferation shortly after treatment, before the inhibitory genomic effect takes place.

The hypothesis that the rapid response to 1α,25$(OH)_2D_3$ promotes proliferation is supported by the observation that treating MC3T3-E1 cells for one hour with the seco-steroid could block apoptosis induced by a 24 hour treatment with staurosporine, similar to previous observations (38). Due to the extended treatment time, this result alone could not rule out a role of VDR-mediated genomic effects, but the evidence that silencing either Pdia3 or caveolin-1 could significantly attenuate this regulation strongly supports a major role for rapid signaling. In other work examining the anti-apoptotic effect of 1α,25$(OH)_2D_3$, PI3K and Akt were identified as major mediators (37,38,68). However, we found that the PI3K/Akt pathway was not activated in our cell model and the inhibitors against PLA2 and c-Src did not change the rescue effect of 1α,25$(OH)_2D_3$, suggesting possible involvement of other pathways. Pdia3 has been shown to play a role in the photo-protective effect of 1α,25$(OH)_2D_3$ on UV-induced DNA damage (52) supporting our results.

In conclusion, this study investigated the relative roles of two membrane receptors for 1α,25$(OH)_2D_3$ -Pdia3 and VDR, and the scaffolding protein caveolin-1 in one system. The results show that each receptor separately forms complexes with caveolin-1 and activating its own downstream mediators-PLAA and c-Src respectively. The complexes respond to 1α,25$(OH)_2D_3$ by translocation and changes in protein-protein interaction. Moreover, the complexes interact in such a way that loss of either receptor

or caveolin-1 reduces the dynamic response to 1α,25$(OH)_2D_3$. Biological responses to transient 1α,25$(OH)_2D_3$ treatment, including Alpl expression and activity, [^{3}H]-thymidine incorporation and annexin V, are mediated through the membrane receptor complex involving VDR, Pdia3 and caveolin-1. The Pdia3 associated PLA2 pathway and VDR associated c-Src pathway regulate Alpl gene expression in an opposite manner; both contribute to DNA synthesis; but neither are involved in annexin reduction. This study provides important new approaches to evaluate the role of 1α,25$(OH)_2D_3$ in the variety of 1α,25$(OH)_2D_3$ responsive cells.

3.5 References

1. Chen, J., Olivares-Navarrete, R., Wang, Y., Herman, T. R., Boyan, B. D., and Schwartz, Z. (2010) *J Biol Chem* **285**, 37041-37050
2. Schwartz, Z., Schlader, D. L., Ramirez, V., Kennedy, M. B., and Boyan, B. D. (1989) *J Bone Miner Res* **4**, 199-207
3. Tishkoff, D. X., Nibbelink, K. A., Holmberg, K. H., Dandu, L., and Simpson, R. U. (2008) *Endocrinology* **149**, 558-564
4. Becklund, B. R., Hansen, D. W., Jr., and Deluca, H. F. (2009) *Proc Natl Acad Sci U S A* **106**, 5276-5281
5. Mathieu, C., Waer, M., Casteels, K., Laureys, J., and Bouillon, R. (1995) *Endocrinology* **136**, 866-872
6. Yudoh, K., Matsuno, H., and Kimura, T. (1999) *The Journal of laboratory and clinical medicine* **133**, 120-128
7. Lee, H. J., Paul, S., Atalla, N., Thomas, P. E., Lin, X., Yang, I., Buckley, B., Lu, G., Zheng, X., Lou, Y. R., Conney, A. H., Maehr, H., Adorini, L., Uskokovic, M., and Suh, N. (2008) *Cancer Prev Res (Phila)* **1**, 476-484
8. Wali, R. K., Bissonnette, M., Khare, S., Hart, J., Sitrin, M. D., and Brasitus, T. A. (1995) *Cancer Res* **55**, 3050-3054
9. Buitrago, C., and Boland, R. (2010) *J Steroid Biochem Mol Biol* **121**, 169-175
10. Schwartz, Z., Ehland, H., Sylvia, V. L., Larsson, D., Hardin, R. R., Bingham, V., Lopez, D., Dean, D. D., and Boyan, B. D. (2002) *Endocrinology* **143**, 2775-2786
11. Dixon, K. M., Norman, A. W., Sequeira, V. B., Mohan, R., Rybchyn, M. S., Reeve, V. E., Halliday, G. M., and Mason, R. S. (2011) *Cancer Prev Res (Phila)*
12. Tunsophon, S., and Nemere, I. (2010) *Steroids* **75**, 307-313
13. Nemere, I., Dormanen, M. C., Hammond, M. W., Okamura, W. H., and Norman, A. W. (1994) *J Biol Chem* **269**, 23750-23756
14. Nemere, I., Farach-Carson, M. C., Rohe, B., Sterling, T. M., Norman, A. W., Boyan, B. D., and Safford, S. E. (2004) *Proc Natl Acad Sci U S A* **101**, 7392-7397
15. Nemere, I., Schwartz, Z., Pedrozo, H., Sylvia, V. L., Dean, D. D., and Boyan, B. D. (1998) *J Bone Miner Res* **13**, 1353-1359
16. Boyan, B. D., Bonewald, L. F., Sylvia, V. L., Nemere, I., Larsson, D., Norman, A. W., Rosser, J., Dean, D. D., and Schwartz, Z. (2002) *Steroids* **67**, 235-246
17. Pedrozo, H. A., Schwartz, Z., Rimes, S., Sylvia, V. L., Nemere, I., Posner, G. H., Dean, D. D., and Boyan, B. D. (1999) *J Bone Miner Res* **14**, 856-867
18. Boyan, B. D., Wang, L., Wong, K. L., Jo, H., and Schwartz, Z. (2006) *Steroids* **71**, 286-290
19. Doroudi, M., Schwartz, Z., and Boyan, B. D. (2012) *J Steroid Biochem Mol Biol*
20. Oliver, J. D., van der Wal, F. J., Bulleid, N. J., and High, S. (1997) *Science* **275**, 86-88
21. Garbi, N., Tanaka, S., Momburg, F., and Hammerling, G. J. (2006) *Nat Immunol* **7**, 93-102
22. Wang, Y., Chen, J., Lee, C. S., Nizkorodov, A., Riemenschneider, K., Martin, D., Hyzy, S., Schwartz, Z., and Boyan, B. D. (2010) *J Steroid Biochem Mol Biol* **121**, 257-260
23. Olivares-Navarrete, R., Sutha, K., Hyzy, S. L., Hutton, D. L., Schwartz, Z., McDevitt, T., and Boyan, B. D. (2012) *Stem Cells Dev*
24. Nemere, I., Garbi, N., Hammerling, G. J., and Khanal, R. C. (2010) *J Biol Chem* **285**, 31859-31866
25. Boyan, B. D., Sylvia, V. L., McKinney, N., and Schwartz, Z. (2003) *J Cell*

Biochem **90**, 1207-1223
26. Huhtakangas, J. A., Olivera, C. J., Bishop, J. E., Zanello, L. P., and Norman, A. W. (2004) *Mol Endocrinol* **18**, 2660-2671
27. Zanello, L. P., and Norman, A. W. (2004) *Proc Natl Acad Sci U S A* **101**, 1589-1594
28. Van Cromphaut, S. J., Dewerchin, M., Hoenderop, J. G., Stockmans, I., Van Herck, E., Kato, S., Bindels, R. J., Collen, D., Carmeliet, P., Bouillon, R., and Carmeliet, G. (2001) *Proc Natl Acad Sci U S A* **98**, 13324-13329
29. Mizwicki, M. T., Keidel, D., Bula, C. M., Bishop, J. E., Zanello, L. P., Wurtz, J. M., Moras, D., and Norman, A. W. (2004) *Proc Natl Acad Sci U S A* **101**, 12876-12881
30. Norman, A. W. (2006) *Endocrinology* **147**, 5542-5548
31. Boyan, B. D., Wong, K. L., Wang, L., Yao, H., Guldberg, R. E., Drab, M., Jo, H., and Schwartz, Z. (2006) *J Bone Miner Res* **21**, 1637-1647
32. Boland, R., De Boland, A. R., Buitrago, C., Morelli, S., Santillan, G., Vazquez, G., Capiati, D., and Baldi, C. (2002) *Steroids* **67**, 477-482
33. Boyan, B. D., Sylvia, V. L., Dean, D. D., Pedrozo, H., Del Toro, F., Nemere, I., Posner, G. H., and Schwartz, Z. (1999) *Steroids* **64**, 129-136
34. Schwartz, Z., Gilley, R. M., Sylvia, V. L., Dean, D. D., and Boyan, B. D. (1999) *Bone* **24**, 475-484
35. Schwartz, Z., Graham, E. J., Wang, L., Lossdorfer, S., Gay, I., Johnson-Pais, T. L., Carnes, D. L., Sylvia, V. L., and Boyan, B. D. (2005) *J Cell Physiol* **203**, 54-70
36. Schwartz, Z., Sylvia, V. L., Luna, M. H., DeVeau, P., Whetstone, R., Dean, D. D., and Boyan, B. D. (2001) *Steroids* **66**, 683-694
37. Vertino, A. M., Bula, C. M., Chen, J. R., Almeida, M., Han, L., Bellido, T., Kousteni, S., Norman, A. W., and Manolagas, S. C. (2005) *J Biol Chem* **280**, 14130-14137
38. Zhang, X., and Zanello, L. P. (2008) *J Bone Miner Res* **23**, 1238-1248
39. Buitrago, C., Vazquez, G., De Boland, A. R., and Boland, R. L. (2000) *J Cell Biochem* **79**, 274-281
40. Buitrago, C., Vazquez, G., De Boland, A. R., and Boland, R. (2001) *Biochem Biophys Res Commun* **289**, 1150-1156
41. Boyan, B. D., Posner, G. H., Greising, D. M., White, M. C., Sylvia, V. L., Dean, D. D., and Schwartz, Z. (1997) *J Cell Biochem* **66**, 457-470
42. Ma, Y., Yu, W. D., Kong, R. X., Trump, D. L., and Johnson, C. S. (2006) *Cancer Res* **66**, 8131-8138
43. Buitrago, C. G., Pardo, V. G., de Boland, A. R., and Boland, R. (2003) *J Biol Chem* **278**, 2199-2205
44. Morelli, S., Buitrago, C., Vazquez, G., De Boland, A. R., and Boland, R. (2000) *J Biol Chem* **275**, 36021-36028
45. Franceschi, R. T., Iyer, B. S., and Cui, Y. (1994) *J Bone Miner Res* **9**, 843-854
46. Martin, J. Y., Schwartz, Z., Hummert, T. W., Schraub, D. M., Simpson, J., Lankford, J., Jr., Dean, D. D., Cochran, D. L., and Boyan, B. D. (1995) *J Biomed Mater Res* **29**, 389-401
47. Mannella, P., and Brinton, R. D. (2006) *J Neurosci* **26**, 9439-9447
48. Yu, J., Akishita, M., Eto, M., Ogawa, S., Son, B. K., Kato, S., Ouchi, Y., and Okabe, T. (2010) *Endocrinology* **151**, 1822-1828
49. Rahl, P. B., Lin, C. Y., Seila, A. C., Flynn, R. A., McCuine, S., Burge, C. B., Sharp, P. A., and Young, R. A. (2010) *Cell* **141**, 432-445
50. Chaudhri, R. A., Olivares-Navarrete, R., Cuenca, N., Hadadi, A., Boyan, B. D., and Schwartz, Z. (2012) *J Biol Chem* **287**, 7169-7181

51. Khanal, R. C., and Nemere, I. (2007) *Curr Med Chem* **14**, 1087-1093
52. Sequeira, V. B., Rybchyn, M. S., Tongkao-On, W., Gordon-Thomson, C., Malloy, P. J., Nemere, I., Norman, A. W., Reeve, V. E., Halliday, G. M., Feldman, D., and Mason, R. S. (2012) *Mol Endocrinol*
53. Schwartz, Z., Brooks, B., Swain, L., Del Toro, F., Norman, A., and Boyan, B. (1992) *Endocrinology* **130**, 2495-2504
54. Sud, N., Wiseman, D. A., and Black, S. M. (2010) *Mol Endocrinol* **24**, 1637-1649
55. Han, S., Li, T., Ellis, E., Strom, S., and Chiang, J. Y. (2010) *Mol Endocrinol* **24**, 1151-1164
56. Nemere, I., Ray, R., and McManus, W. (2000) *Am J Physiol Endocrinol Metab* **278**, E1104-1114
57. Wu, W., Beilhartz, G., Roy, Y., Richard, C. L., Curtin, M., Brown, L., Cadieux, D., Coppolino, M., Farach-Carson, M. C., Nemere, I., and Meckling, K. A. (2010) *Exp Cell Res* **316**, 1101-1108
58. Lobie, P. E., Sadir, R., Graichen, R., Mertani, H. C., and Morel, G. (1999) *Exp Cell Res* **246**, 47-55
59. Migliaccio, A., Di Domenico, M., Castoria, G., Nanayakkara, M., Lombardi, M., de Falco, A., Bilancio, A., Varricchio, L., Ciociola, A., and Auricchio, F. (2005) *Cancer Res* **65**, 10585-10593
60. Leis, H., Page, A., Ramirez, A., Bravo, A., Segrelles, C., Paramio, J., Barettino, D., Jorcano, J. L., and Perez, P. (2004) *Mol Endocrinol* **18**, 303-311
61. Owen, T. A., Bortell, R., Yocum, S. A., Smock, S. L., Zhang, M., Abate, C., Shalhoub, V., Aronin, N., Wright, K. L., van Wijnen, A. J., and et al. (1990) *Proc Natl Acad Sci U S A* **87**, 9990-9994
62. Catling, A. D., Wyke, J. A., and Frame, M. C. (1993) *Oncogene* **8**, 1875-1886
63. Murakami, M., Sonobe, M. H., Ui, M., Kabuyama, Y., Watanabe, H., Wada, T., Handa, H., and Iba, H. (1997) *Oncogene* **14**, 2435-2444
64. Jehn, B., Costello, E., Marti, A., Keon, N., Deane, R., Li, F., Friis, R. R., Burri, P. H., Martin, F., and Jaggi, R. (1992) *Mol Cell Biol* **12**, 3890-3902
65. Akutsu, N., Lin, R., Bastien, Y., Bestawros, A., Enepekides, D. J., Black, M. J., and White, J. H. (2001) *Mol Endocrinol* **15**, 1127-1139
66. Towsend, K., Trevino, V., Falciani, F., Stewart, P. M., Hewison, M., and Campbell, M. J. (2006) *Oncology* **71**, 111-123
67. Karmali, R., Bhalla, A. K., Farrow, S. M., Williams, M. M., Lal, S., Lydyard, P. M., and O'Riordan, J. L. (1989) *J Mol Endocrinol* **3**, 43-48
68. Xiaoyu, Z., Payal, B., Melissa, O., and Zanello, L. P. (2007) *J Steroid Biochem Mol Biol* **103**, 457-461

CHAPTER 4

Chaperone properties of Pdia3 participate in rapid plasma membrane associated actions of 1α,25-dihydroxyvitamin D3

Chapter 4 was submitted as [Chen J, Lobachev KS, Grindel BJ, Farach-Carson MC, Olivares-Navarrete R, Doroudi M, Boyan BD, Schwartz Z (2012) Chaperone properties of Pdia3 participate in rapid plasma membrane associated actions of 1α,25-dihydroxyvitamin D3. Molecular Endocrinology]

4.1 Introduction

Over the past two decades, the steroid hormone, 1α,25-dihydroxyvitamin D_3 (1α,25$(OH)_2D_3$) has drawn increasing attention due to its newly discovered functions outside of maintaining calcium/phosphate homeostasis. These include regulation of mineralization by osteoblasts (1), matrix production and remodeling by chondrocytes (2) and contraction of cardiomyocytes (3). In pathological conditions, 1α,25$(OH)_2D_3$ and its analogues have beneficial effects in treatment of multiple sclerosis, diabetes and various types of cancer (4-8). While many of the effects of 1α,25$(OH)_2D_3$ occur through classic nuclear vitamin D receptor (VDR) mediated gene expression, receptor-mediated activation of membrane associated signaling pathways also plays an important role.

A number of rapid responses have been reported in 1α,25$(OH)_2D_3$-responsive cells. In chondrocytes and osteoblasts, 1α,25$(OH)_2D_3$ activates phospholipase A2 (PLA2) via phospholipase A2 activating protein (PLAA), resulting in release of arachidonic acid within seconds and subsequent production of prostaglandin E2 (PGE2) (9-13). In addition, phosphatidyl inositol-dependent phospholipase C, protein kinase C (PKC) and the extracellular signal-regulated kinases 1 and 2 (ERK1/2) are rapidly

increased downstream of PLA2 activation (9,14,15). Moreover, in skeletal muscle cells, c-Src was found to be rapidly activated by 1α,25$(OH)_2D_3$ (16-18) and rapid movement of Ca^{2+} across cell membranes was shown in a number of cells to follow 1α,25$(OH)_2D_3$ addition (19,20).

Protein disulfide isomerase family A, member 3 (Pdia3, also called ERp57, ERp60, Grp58, and 1,25-MARRS) has been proposed to mediate many of these rapid responses to 1α,25$(OH)_2D_3$. Pdia3 was initially isolated from the basal lateral membranes of chicken intestinal epithelial cells based on its saturable binding to 1α,25$(OH)_2D_3$ (21). Antibodies to the N-terminal peptide of the protein block Ca^{2+} and phosphate transport across the membrane in response to 1α,25$(OH)_2D_3$ (22) and interfere with rapid activation of PKCα in chondrocytes and osteoblasts (23-25). Similarly, epithelial cells isolated from Pdia3-conditional knockout mice lack surface binding of 1α,25$(OH)_2D_3$ and 1α,25$(OH)_2D_3$-stimulated calcium uptake (19). The stimulatory effect of 1α,25$(OH)_2D_3$ is stereospecific, indicating a receptor-mediated mechanism (26). Moreover, mice lacking a functional VDR possess Pdia3 and cells isolated from these mice respond to 1α,25$(OH)_2D_3$ with an increase in PKC activity (27). Recently, we showed that embryonic stem cells possess Pdia3 and respond to 1α,25$(OH)_2D_3$ with an increase in PKC activity (28).

These observations support the hypothesis that Pdia3 is a receptor for the secosteroid. Pdia3 can be located in caveolae where it physically interacts with the scaffolding protein caveolin-1 and with PLAA (1,29). Disruption of caveolae with beta-cyclodextrin prevents 1α,25$(OH)_2D_3$-dependent PKC activation (13,30). In addition, cells from mice lacking functional caveolin-1 ($Cav1^{-/-}$) fail to increase enzyme activity in response to the secosteroid (30), demonstrating the importance of this specialized plasma membrane domain to the function of the receptor. While these data demonstrate

the role of Pdia3 in the rapid response to 1α,25$(OH)_2D_3$, global knockout of Pdia3 is embryologically lethal (31), suggesting it also plays additional critical roles along with its function as a receptor for 1α,25$(OH)_2D_3$.

Outside the field of vitamin D, Pdia3 can act as a chaperone protein in the endoplasmic reticulum (ER) where it promotes formation of disulfide bonds in its N-glycosylated protein substrate through interaction with the ER lectin chaperones, calreticulin and calnexin (32-34). Pdia3 is also intensively studied for its role in assisting the formation of the major histocompatibility complex (MHC) class I peptide-loading complex, which is essential for formation of the final antigen conformation and export from the ER to the cell surface (31,35,36). How these chaperone properties might impact Pdia3's role as a membrane receptor for 1α,25$(OH)_2D_3$ is not known. However, a number of studies suggest that Pdia3 does act in the assembly of proteins involved in membrane signaling by the hormone. In addition to the association of calreticulin and calnexin with Pdia3 as a chaperone protein (32-34), calreticulin was also shown to participate in the action of 1α,25$(OH)_2D_3$ (37). PLAA and caveolin-1 can be immunoprecipitated with Pdia3 in MC3T3-E1 pre-osteoblasts (29), and c-Src was found to be immunoprecipitated with VDR and to be involved in rapid responses to 1α,25(OH)2D3 in muscle cells (16).

Previous mutagenesis studies have found certain amino acids are important to the chaperone function of Pdia3. Pdia3 is composed of four thioredoxin-like domains a, a′, b, and b′ with two catalytic CGHC motifs in the a and a′ domains (38). Amino acid C406 is located in the a′ domain and functions as one of the two catalytic sites; mutating C406 (C406S) significantly decreases oxidoreductase activity and chaperone function (36,39,40). The cliff between b and b′ interacts with the proline-rich P-domain of calnexin and calreticulin (38,41,42). This interaction is required for the proper folding of the

substrate and is completely blocked by mutating arginine 282 to alanine (R282A) (38). Another important amino acid at this interface is K214, which when mutated (K214A), reduces the interaction by eight fold (38). Interestingly, calreticulin has been shown to interact with the ligand-VDR complex in ROS 2.8 osteoblastic cells (37).

Pdia3 has broad subcellular distribution. It has been found in the ER, plasma membrane, extracellular matrix, cytoplasm, and nucleus (1,40,43,44). This is partially attributable to its compromised and inefficient ER retention signal. Pdia3 has a C-terminal QEDL retention signal, rather than the classic KDEL retention signal. As a result, Pdia3 can escape from ER retrieval, go through the constitutive secretary pathway, and eventually be secreted into the extracellular matrix (40); or as is the case in cartilage, Pdia3 is released into the matrix as a component of extracellular matrix vesicles (23). We have shown that 1α,25$(OH)_2D_3$ directly activates Pdia3-dependent PKC and PLA2 in isolated plasma membranes (23,29,33,45), indicating that the apparatus needed is present, but whether Pdia3 can function as a mediator of 1α,25$(OH)_2D_3$ rapid actions in other subcellular compartments is less clear.

The mechanism of how Pdia3 associates with the plasma membrane is not known. The protein has myristoylation sites, which may participate in its retention as a plasma membrane associated protein during membrane biosynthesis. The recent observation that steroid hormone receptors associate with the plasma membrane via palmitoylation (46-48), suggests the possibility that Pdia3 uses this mechanism as well. However, no palmitoylation sites have been identified in Pdia3, but its function may require other components that use this membrane-association strategy.

The purpose of this study was to determine if the same amino acids that are critical for the chaperone function of Pdia3 in the endoplasmic reticulum are also critical

for its function in mediating rapid signaling by 1α,25$(OH)_2D_3$ at the plasma membrane. While there are considerable data indicating that Pdia3 is present in caveolae and that caveolae are required for its receptor function, it is not known if some of its 1α,25$(OH)_2D_3$-dependent effects occur in other cellular compartments, including the endoplasmic reticulum, where it works as a chaperone. To address the first question, we used site-directed mutagenesis of three important amino acids: C406, K214 and R282, which are required for the chaperone role of Pdia3, to dissect these individual functions. To answer the second question, we changed the original QEDL ER-retention signal to either a classic KDEL signal to trap Pdia3 in ER or removed QEDL completely to prevent ER retrieval and allow Pdia3 to move to other cellular locations including the plasma membrane. We also inhibited palmitoylation to investigate if it is also important to the plasma membrane association of Pdia3 and its function in rapid responses.

4.2 Materials and Methods

4.2.1 Plasmid Construction

4.2.1.1 Chaperone Function

To study whether the amino acids involved in Pdia3's chaperone function in the ER are also important to its receptor function, we mutated lysine 214 to alanine (K214A), arginine 282 to alanine (R282A) and cystine 406 to serine (C406S) on a native mouse Pdia3 overexpression vector ($Pdia3_{Ovr}$, OriGene, Rockville, MD) (Fig. 4-1A) using a QuikChange II XL Site-Directed Mutagenesis Kit (Agilent Technologies, Santa Clara, CA). In the kit, a polymerase chain reaction was used to generate the mutation. Briefly, the original plasmid was denatured and annealed with the mutagenic primers containing the desired mutation. Then the primers were extended by pfuUltra DNA polymerase followed by Dpn I enzyme digestion to break down the parental methylated and hemi-

methylated DNA. The mutated plasmid was further transformed into XL10-Gold ultra-competent cells for nick repair. Plasmids were isolated and purified with EndoFree plasmid maxi kit (Qiagen, Valencia, CA) for sequencing (Eurofins MWG Operon, Huntsville, AL) or later transfection. The whole open reading frames of $Pdia3_{Ovr}$, K214A, R282A and C406S were sequenced to ensure no random mutations had occurred (data not shown). Sequence results showed that the desired site-directed mutations were achieved in all constructs (Fig. 4-1B).

4.2.1.2 Endoplasmic Reticulum v. Plasma Membrane Location

To study the effect of subcellular location of Pdia3 on rapid responses, we used a $Pdia3_{[+KDEL]}$ construct generated as described previously (44). Briefly, the DNA plasmid was based on a mammalian expression vector from Clontech (Mountain View, CA). This plasmid contains the full length human Pdia3 gene with a deletion of the ER retention signal QEDL on the C-terminal. This Pdia3 was fused with green fluorescent protein (GFP) containing an A206K mutation on the C-terminal followed by a classic ER retention signal KDEL (Fig. 4-2A). In order to delete KDEL, the last amino acid codon of GFP on the C-terminal was mutated to a stop codon ($Pdia3_{[-KDEL]}$) using the same strategy described above for the site directed mutagenesis of the chaperone catalytic sites. Plasmids containing $Pdia3_{[+KDEL]}$ or $Pdia3_{[-KDEL]}$ were prepared as above. The entire open reading frame was sequenced; no random mutations were observed (Fig. 4-2B). Sequences of the primers used in site-directed mutagenesis are available upon request.

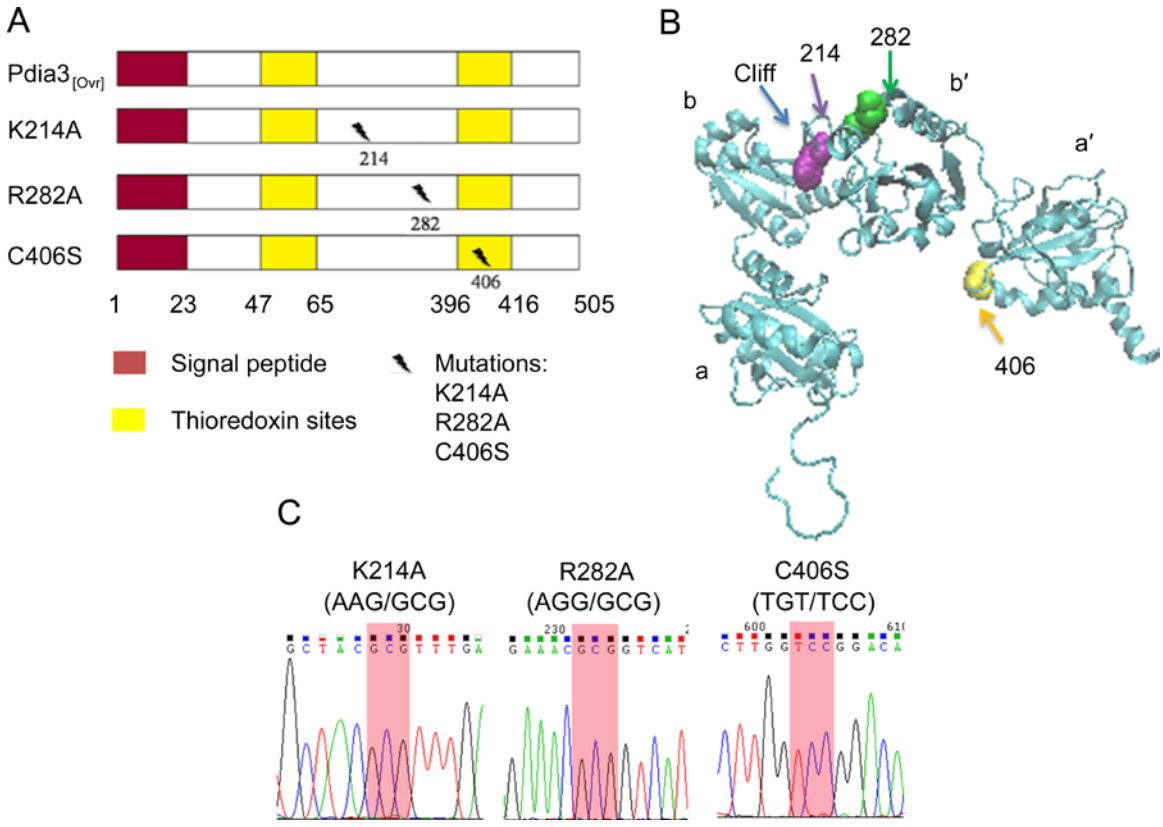

Figure 4-1. Diagram showing strategy for site-directed mutagenesis. (A): Four different plasmid constructs. (B): 3D structure of Pdia3 showing the location of the three mutated amino acids. Purple: K214; green: R282; yellow: C406. Blue: the cliff between b and b′ domain. (C): Sequencing result of mutated 214, 282 and 406. For 214, AAG (lysine) was mutated to GCG (alanine); for 282, AGG (arginine) was mutated to GCG (alanine); for 406; TGT (cystine) was mutated to TCC (serine).

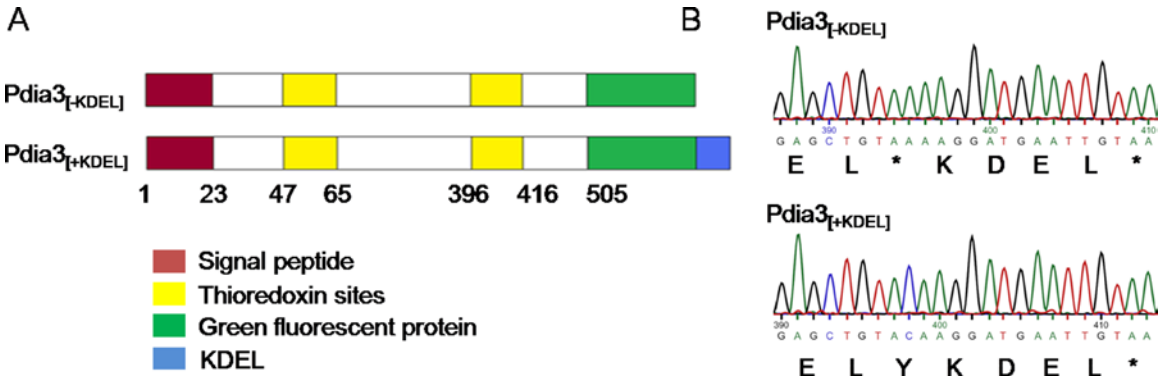

Figure 4-2. Diagram showing strategy for changing ER retention signal. (A): Pdia3$_{[-KDEL]}$ and Pdia3$_{[+KDEL]}$ constructs. (B): The sequencing result of the deletion of ER retention signal KDEL. Lower panel is the sequence result of Pdia3$_{[+KDEL]}$ showing that the KDEL retention signal is present on the c-terminal of green fluorescence protein. Upper panel is the sequence result of Pdia3$_{[-KDEL]}$ showing that the last amino acid (nucleotides TAC) of green fluorescent protein was mutated to a stop codon (TAA).

4.2.2 Transfection and Overexpression

The respective Pdia3 native or mutant proteins were overexpressed in wild type (WT) mouse MC3T3-E1 pre-osteoblast-like cells (CRL-2593, ATCC, Manassas, VA). As a result, normal Pdia3 was also present. Unfortunately, we were not able to generate MC3T3-E1 cells that were both silenced for Pdia3 and were viable after transfection with any of the overexpression plasmids. The MC3T3-E1 cells were plated at a density of 20,000 cells/cm^2 in 6-well plates and cultured in α-MEM supplied with 10% (v/v) fetal bovine serum (FBS). After 24 hours, 500µl of Opti-MEM (Invitrogen, Carlsbad, CA) containing 5µl lipofectamine LTX (Invitrogen), 2.5µl plus reagent (Invitrogen) and 2.5µg plasmids were added into each well. After 48 hours, cells were cultured in selection medium (α-MEM containing 10% FBS, 1% (v/v) penicillin/streptomycin (P/S) and 550 µg/ml G418 (Cellgro, Manassas, VA)) for two weeks. A stable transfected cell line for each clone of plasmid was chosen.

Successful overexpression of $Pdia3_{[+KDEL]}$ and $Pdia3_{[-KDEL]}$ ($Pdia3_{[\pm KDEL]}$) was determined by realtime PCR measurement of Pdia3GFP fused mRNA in $Pdia3_{[+KDEL]}$ and $Pdia3_{[-KDEL]}$ cells. Ten days after plating, cell layers were dissolved in TRIzol (Invitrogen) and mRNA extracted and reverse-transcribed into cDNA using the high-capacity cDNA reverse transcription kit (Applied Biosystems, Carlsbad, CA) according to the manufacturer's directions. Real-time PCR was performed using SYBR Green Master Mix (Applied Biosystems) for Pdia3GFP and glyceraldehyde 3-phosphate dehydrogenase (*Gapdh*) encoding transcripts. Oligonucleotide primers were designed using Beacon Designer 7.0 software. For Pdia3GFP transcripts, the forward primer (ACCATATACTTCTCTCCAGCCAAC) targeted the C terminal of human Pdia3 (NM_005313.4) and the reverse primer (TCCTCGCCCTTGCTCACC) targeted the N terminal of GFP (FM177581.1). The primers were designed using Beacon Designer 7.0

software (PREMIER Biosoft International, Palo Alto, CA) and synthesized by Eurofins MWG Operon (Huntsville, AL). Real-time PCR was performed using the Veriti 96 well Thermal Cycler (Applied Biosystems, Carlsbad, CA) with Step One software (Applied Biosystems). Data were normalized to the endogenous reference gene *Gapdh*.

4.2.3 Cell Culture

All cell lines were plated at 10,000 cells/cm^2 in T75 or 24-well plates with full medium (α-MEM containing 10% FBS, and 1% P/S) with or without 550 μg/ml G418 to select for successfully transfected cells. After 48 hours, full medium was changed to full medium containing 1% (w/v) vitamin C to enable cross-linking of type I collagen in the extracellular matrix (49). Other than for experiments involving confocal microscopy, all cells were cultured for 10 days after plating and treated with full medium containing either the ethanol vehicle alone or with the appropriate dose of 1α,25$(OH)_2D_3$.

4.2.4 Effect of Mutant Pdia3 Overexpression

4.2.4.1 Plasma Membrane Isolation

In order to study the changes in plasma membrane association of Pdia3 and of proteins potentially involved in its mechanism of action, a detergent-free method of plasma membrane isolation was used as described previously (50). Ten days after plating, cell layers were scraped in isolation buffer (0.25M sucrose, 1mM EDTA, 20mM tricine, pH 7.8). Samples were homogenized using a tissue grinder for twenty strokes. Homogenates were centrifuged at 20,000g for 10 minutes to pellet cell debris including nuclei, mitochondria, and ER. The supernatant was collected, placed on top of 30% (v/v) Percoll (GE Healthcare, Piscataway, NJ) in isolation buffer, and then centrifuged for 30 minutes at 84,000g. The plasma membranes formed a visible band and were collected by aspiration. The levels of each protein of interest in the plasma membrane fraction

were examined by western blots.

4.2.4.2 Western Blots

Western blots were performed using whole cell lysates and isolated plasma membranes to examine the protein level of Pdia3, caveolin-1, Pdia3-interacting proteins calreticulin and calnexin, and the signaling mediators c-Src and PLAA. The samples were mixed with loading buffer, boiled and followed by gel electrohoresis using NuSep 4-20% LongLife Gels (NuSep, Lawrenceville, GA). Proteins were transferred to nitrocellulose membrane by iBlot Dry Blotting System (Invitrogen). The membrane was subsequently blotted in 1% (w/v) bovine serum albumin (Sigma-Aldrich, St. Louis, MO) in PBS with primary antibodies against Pdia3 (Alpha Diagnostic International, Inc.), Gapdh (MAB374, Millipore, Billerica, MA), calreticulin (TO-5, Santa Cruz Biotechnology), calnexin (A-9, Santa Cruz Biotechnology), caveolin-1 (N-20, Santa Cruz Biotechnology), c-Src (B-12, Santa Cruz Biotechnology), and PLAA (custom antibody, Strategic Diagnostics, Inc., Newark, DE). After washing with PBS containing 0.05% (v/v) Tween-20, the membrane was incubated with goat anti-rabbit, goat anti-mouse or donkey anti-goat horseradish peroxidase conjugated secondary antibodies (Bio-Rad, Hercules, CA) in PBS containing 5% (w/v) dry milk and 0.05% Tween-20. After washes, the membrane was developed using SuperSignal West Pico Chemiluminescent System (Thermo Fisher Scientific, Rockford, IL) and imaged with the VersaDoc imaging system (Bio-Rad, Hercules, CA).

In order to compare the effect of each Pdia3 mutation on association of proteins with the plasma membrane, we quantified the data by normalizing the intensity of targeted proteins to the corresponding Pdia3 intensity and the ratio in the mutant-overexpressing cells was further divided by the ratio for cells overexpressing the wild type Pdia3 ($Pdia3_{Ovr}$).

4.2.5 Subcellular Location of Pdia3

To determine if the presence of the ER-retention signal KDEL altered the amount of Pdia3 in the plasma membrane, plasma membranes were isolated from wild type, $Pdia3_{[+KDEL]}$ and $Pdia3_{[-KDEL]}$ cells as described before. A Synergy H4 multi-mode plate reader (Biotek, Winooski, VT) was used to detect the green fluorescence in the samples. The relative fluorescence units were further normalized by total protein levels of the isolated membranes.

To visualize the difference in subcellular location, confocal fluorescence microscopy was performed to detect the green fluorescence signal of the Pdia3GFP fused protein. Pdia3 was previously shown to colocalize with lipid rafts in the plasma membrane (1), wild type, $Pdia3_{[+KDEL]}$ and $Pdia3_{[-KDEL]}$ cells were cultured in chamber slides for 24 hours and stained with Vybrant® Alexa Fluor® 594 Lipid Raft Labeling Kit (Invitrogen). Cells were further stained with Hoechst 33342 (Invitrogen) to label the nucleus. After washing, the cells were fixed with FLURO-GEL mounting medium (Electron Microscopy Sciences, Hatfield, PA) and visualized using a Zeiss LSM 510 confocal microscope (Carl Zeiss MicroImaging, Thornwood, NY). Images were obtained at room temperature with 40X1.3 objective lens and 10X ocular lens. No digital enlargement was applied. To quantify the pixel distribution of Pdia3, the intensities of the green Pdia3 signal and the red lipid raft signal were calculated along a cross section, and plotted against the distance by Zeiss LSM Image software (Carl Zeiss MicroImaging).

4.2.6 Signaling by $1\alpha,25(OH)_2D_3$

To study the effect of genetically modifying Pdia3 on $1\alpha,25(OH)_2D_3$ induced rapid responses, 10 days after plating, all cell lines were treated with vehicle (ethanol) or 10^{-7}

M 1α,25$(OH)_2D_3$. To measure PKC activity, treatment was stopped at 15 minutes and cell layers were washed twice with PBS and lysed in RIPA buffer (20mM Tris-HCl, 150mM NaCl, 5mM disodium EDTA, 1% (v/v) NP-40). PKC activity was measured using a commercial kit (RPN77, GE Healthcare, Piscataway, NJ) and normalized by total protein of the cell layer.

Our lab has previously shown the effect of 1α,25$(OH)_2D_3$ on PKC is via a PLA_2-dependent pathway (11). PGE2 as an indirect product of PLA2 action has been used as an outcome measurement of rapid responses (1). To measure PGE2 release into the media, after 30 minutes of treatment, the conditioned media were collected and acidified by adding hydrochloride to a final concentration of 0.1M. PGE2 in the conditioned media was measured using a commercial PGE2 radioimmunoassay kit (Perkin Elmer, Waltham, MA) and normalized by total DNA of the cell layer.

4.2.7 Palmitoylation

To determine if palmitoylation is required for the membrane association of Pdia3 or its function in mediating 1α,25$(OH)_2D_3$ dependent PKC activation, we depleted the palmitoylated protein from the plasma membrane by pretreating the cells with tunicamycin prior to treatment with 1α,25$(OH)_2D_3$ (51). Tunicamycin inhibits the N-linked glycosylation of proteins and has been demonstrated to inhibit palmitoylation of membrane associated receptors (46,51). Ten days after plating, wild type MC3T3-E1 cells were treated with vehicle (DMSO) or 1μg/ml tunicamycin for 48 hours. To detect the changes in plasma membrane association of Pdia3, at the end of 48 hours, plasma membrane isolation was performed followed by western blots against pan-cadherin (CDH, Abcam, Cambridge, MA), caveolin-1 and Pdia3 as described previously. To study the effect of tunicamycin on 1α,25$(OH)_2D_3$ induced rapid responses, at the end of 48

hours, cells were treated with vehicle (ethanol) or 10^{-7}M 1α,25$(OH)_2D_3$ for 15 minutes and the PKC activity was measured as described previously.

4.2.8 Statistical Analysis

Each experiment was repeated at least once to ensure the validity of the data. The data presented are from a single representative experiment. Each data point represents the means ± standard error for six independent cell cultures. Significance was determined by one-way analysis of variance and post hoc testing performed using Bonferroni's modification of Student's t-test for multiple comparisons. P≤0.05 was considered significant.

For experiments using separation of functional alleles, because 5 different cell lines were compared, treatment/control ratios were calculated to show the effect of 1α,25$(OH)_2D_3$. The value for each sample in the treated group was divided by the mean of the control group. Each data point represents the means ± standard error for six normalized values and a dashed line with value of 1 represents the control. Due to the non-normal distribution, significance was determined using the Mann Whitney test. P≤0.05 was considered significant.

For quantification of western blots, the values of experimental samples were divided by the value of control sample for each experiment. Four independent experiments were performed. Each data point represents the mean ± standard error of mean (SEM) of the 4 independent experiments with the control represented by a dashed line with value of one. Because the data are both non-normal distributed and paired, significance was determined by Wilcoxon matched pair test between the mutants and the $Pdia3_{Ovr}$ control and Wilcoxon rank-sum test between mutants; P ≤0.05 was considered to be significant.

4.3 Results

4.3.1 Overexpression of Pdia3 mutants changed the plasma membrane presence of signaling molecules.

Western blots showed that all cells containing the overexpression plasmid, including the wild type control plasmid $Pdia3_{Ovr}$, and the mutant proteins K214A, R282A and C406S had a darker immunoreactive Pdia3 band compared to wild type cells without a plasmid (Fig. A-4). Bands for the internal loading control Gapdh were comparable among cell lines. Plasma membranes isolated from the overexpressing cell lines also had more immunoreactive Pdia3 compared to wild type plasma membranes (Fig. 4-3A). Calreticulin was also increased in the plasma membranes isolated from the $Pdia3_{Ovr}$ cells and to an even greater extent in plasma membranes isolated from each of the mutant cell lines. PLAA was reduced in $Pdia3_{Ovr}$ and K214A cell membranes compared to plasma membranes from non-transfected cells, whereas there appeared to be more immunoreactive PLAA in plasma membranes from R282A cells. Similarly, c-Src band intensity was increased in the R282A membranes but it was reduced in the $Pdia3_{Ovr}$ membranes. Caveolin-1 band intensity was comparable in all plasma membranes. Immunoreactive calnexin bands were not seen in any of the plasma membranes examined.

Normalizing individual protein bands to their corresponding Pdia3 and then comparing the ratio to that of the $Pdia3_{Ovr}$ plasma membranes demonstrated that mutations in the chaperone interaction sites altered the presence of proteins in the plasma membrane fraction. The ratio between calreticulin and Pdia3 was unchanged in any of the mutants (Fig. 4-3B), but R282A cells exhibited increased caveolin-1 per Pdia3 than K214A cells (Fig. 4-3C), greater PLAA per Pdia3 than K214A cells (Fig. 4-3D) and

greater Src/Pdia3 than either K214A or C406S cells (Fig. 4-3E). In contrast, no differences were observed in western blots of the whole cell lysates for any of these proteins (data no shown). These data suggest that by changing specific amino acids in Pdia3 we could change the plasma membrane association of downstream signaling molecules.

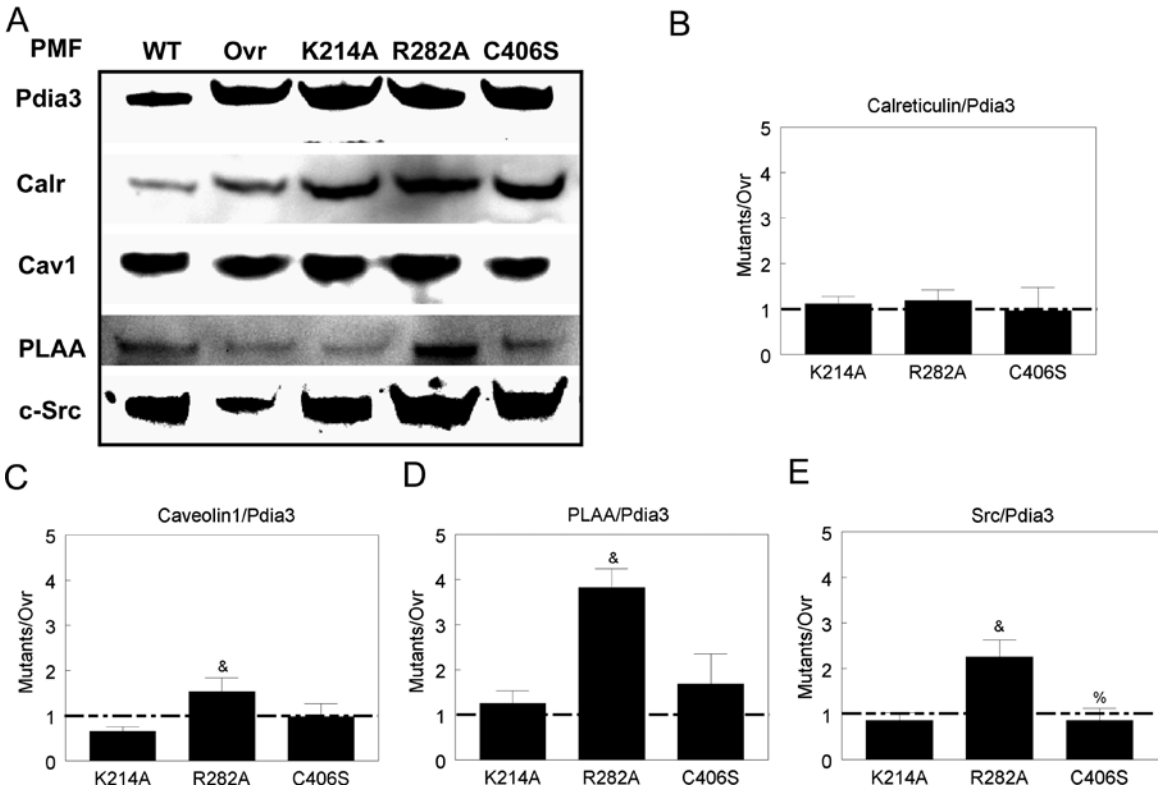

Figure 4-3. Effect of overexpressing site directed mutants of Pdia3 on plasma membrane association of signaling molecules. Ten days after plating, wild type, $Pdia3_{Ovr}$, K214A, R282A, and C406S MC3T3-E1 cells were harvested for plasma membrane isolation. (A): Western blots of Pdia3, calreticulin, caveolin-1, PLAA, and c-Src in plasma membranes. (B to E): Image quantification of (A). The pixel intensity of the targeted proteins was first normalized by its corresponding Pdia3 intensity, then the ratio in the mutant cells was further divided by the value in $Pdia3_{Ovr}$ blots. & $P<0.05$, R282A and C406S vs. K214A; % $P<0.05$, C406S vs. R282A.

4.3.2 Mutating Pdia3 alters 1α,25$(OH)_2D_3$-stimulated rapid responses.

1α,25$(OH)_2D_3$ stimulated PKC specific activity in wild type MC3T3-E1 cells, causing a 30% increase after 15 minutes (Fig. 4-4A). The effect of 1α,25$(OH)_2D_3$ was greater in $Pdia3_{Ovr}$ cells overexpressing the native Pdia3. The stimulatory effect of the secosteroid was abolished in cells overexpressing Pdia3 with the K214A or C406S mutation. The effect of 1α,25$(OH)_2D_3$ on PKC in cells overexpressing the R282A mutation was comparable to that of wild type cells.

PGE2 release was affected in a similar manner (Fig. 4-4B). 1α,25$(OH)_2D_3$ increased PGE2 in the conditioned media at 30 minutes in wild type cells and this response was enhanced in cells transfected with the normal $Pdia3_{Ovr}$ plasmid. Mutating C406S blocked PGE2 release whereas mutating R282A or K214A resulted in PGE2 release comparable to that of wild type cells, preventing the increase observed in the $Pdia3_{Ovr}$ cells.

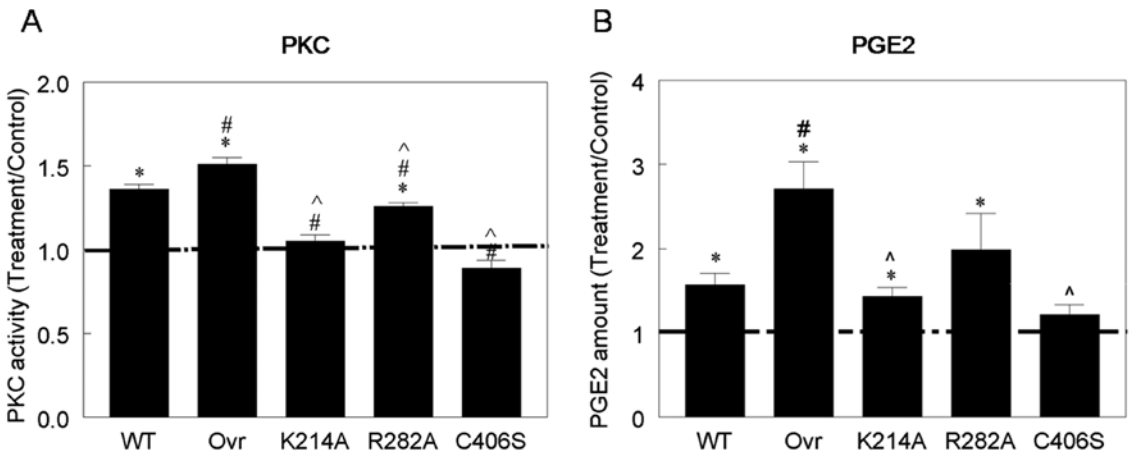

Figure 4-4. The effect of overexpressing site directed mutants of Pdia3 on rapid responses to 1α,25$(OH)_2D_3$. 10 days after plating, wild type, $Pdia3_{Ovr}$, K214A, R282A, and C406S MC3T3-E1 cells were treated with or without 10^{-7} M 1α,25$(OH)_2D_3$. (A): PKC activity was measured at 15 minutes. (B): PGE2 in conditioned media was measured at 30 minutes. PKC activity was normalized to total protein and PGE2 was normalized to total DNA. Data were normalized to the vehicle treated group (dashed line=1). * $P<0.05$, 1α,25$(OH)_2D_3$ vs. control; # $P<0.05$, mutations vs. WT; ^ $P<0.05$, mutations vs. $Pdia3_{Ovr}$.

4.3.3 The subcellular location of Pdia3 was sensitive to the presence of the retention signal.

Realtime PCR of the fused Pdia3GFP mRNA showed a similar amount of overexpression in both $Pdia3_{[+KDEL]}$ cells and $Pdia3_{[-KDEL]}$ cells (Fig. 4-5A). $Pdia3_{[+KDEL]}$ cells had greater green fluorescence intensity in the isolated plasma membranes than wild type cells and the fluorescence signal was markedly greater in $Pdia3_{[-KDEL]}$ cells (Fig. 4-5B). Confocal microscope images of wild type cells exhibited lipid raft staining diffusely throughout the cell surface and no green signal was observed in the background (Fig. 4-5C). The GFP signal of $Pdia3_{[+KDEL]}$ was present in the peri-nuclear region and nucleus but little fluorescence was observed in the cytoplasm and plasma membrane. In contrast, the GFP signal of $Pdia3_{[-KDEL]}$ was observed in the perinuclear region, nucleus, cytoplasm, and plasma membrane as indicated by the white arrows. The histogram of pixel intensity across the cell confirmed these observations. The green $Pdia3_{[+KDEL]}$ signal peaked near the blue nuclear signal (Fig. 4-5D) whereas the red plasma membrane signal distributed evenly across the cell. In contrast, $Pdia3_{[-KDEL]}$ fluorescence intensity was high in the plasma membrane and nuclear regions while fluctuating at a low level in cytosol (Fig. 4-5E). These data suggest that the ER retention signal is an important switch to control the presence of Pdia3 on the plasma membrane.

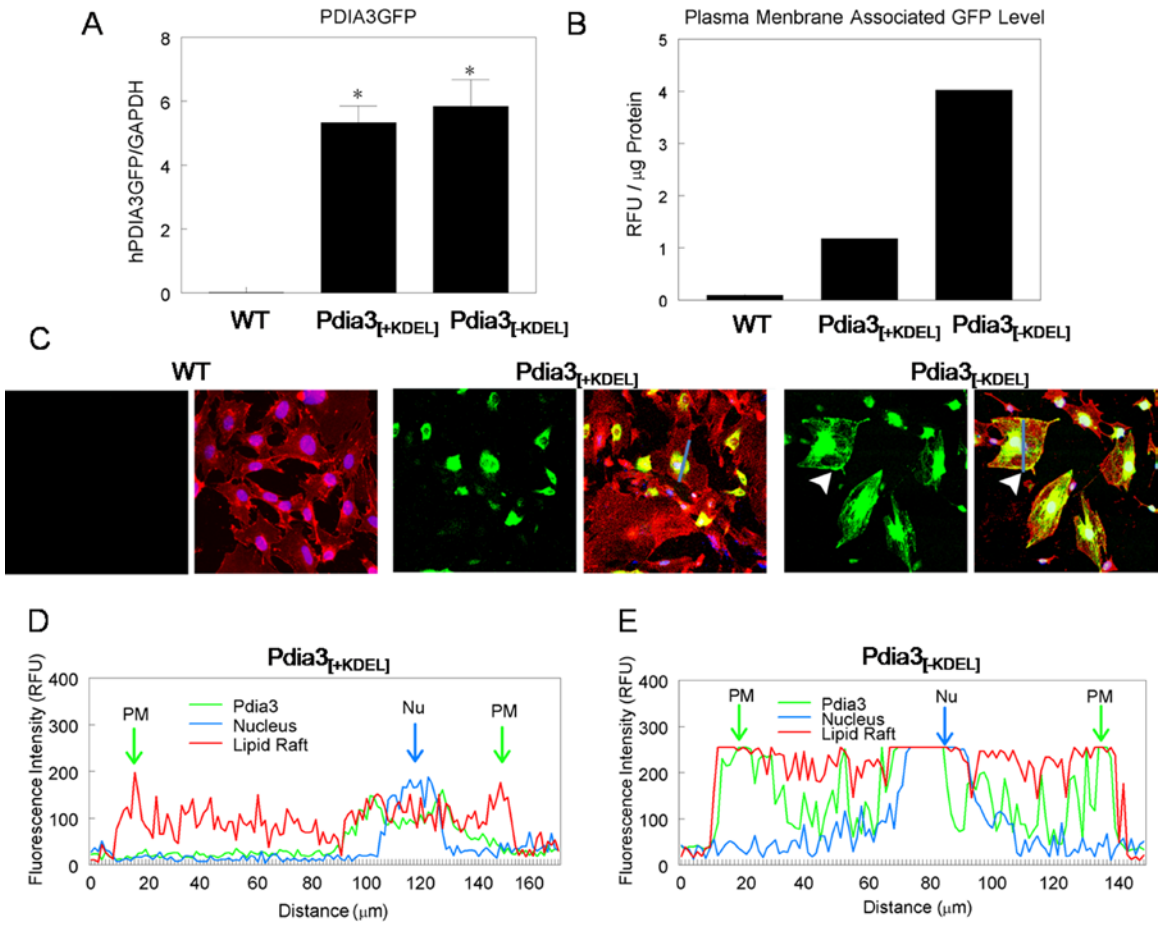

Figure 4-5. Subcellular location of Pdia3$_{[+KDEL]}$ and Pdia3$_{[-KDEL]}$ proteins. (A): mRNA for Pdia3GFP in wild type, Pdia3$_{[+KDEL]}$ and Pdia3$_{[-KDEL]}$ cells. The realtime PCR was performed with forward primer targeting on Pdia3 and reverse primer targeting on GFP. (B): Green fluorescence intensity in the plasma membranes of wild type, Pdia3$_{[+KDEL]}$ and Pdia3$_{[-KDEL]}$ cells. Cells were harvested for plasma membrane isolation. The green fluorescence intensity in the plasma membranes was measured by microplate reader and normalized by total protein. (C): Confocal microscopy image of wild type, Pdia3$_{[+KDEL]}$, and Pdia3$_{[-KDEL]}$ cells. At 80% confluence, lipid raft staining (red) and Hoechst staining (blue) of the nucleus were performed. Green fluorescence (green) of Pdia3GFP fused protein was detected. Yellow represents the merged signal of Pdia3 and lipid rafts. White arrows show green merges with red on the cell boundary. (D, E): Fluorescence intensity histogram of confocal microscopy image. Pixel intensity was calculated along the blue lines indicated Pdia3$_{[+KDEL]}$ and Pdia3$_{[-KDEL]}$ images. Green: Pdia3; Blue: nucleus; Red: lipid raft. *: $p<.05$ Pdia3$_{[\pm KDEL]}$ vs. WT.

4.3.4 Rapid responses to 1α,25$(OH)_2D_3$ are sensitive to the presence of the ER retention signal.

The presence of KDEL did not alter the level of PKC activity in MC3T3-E1 cells in comparison to wild type cultures, which contained endogenous Pdia3 (Fig. 4-6A). However, removal of the ER retention signal resulted in a 100% increase in PKC compared to the wild type cells. Despite this increase in enzyme activity due to overexpression of $Pdia3_{[-KDEL]}$ in these cells, the stimulatory effect of 1α,25$(OH)_2D_3$ was unchanged. In contrast, PGE2 release was not affected by the presence or absence of the KDEL motif (Fig. 4-6B). 1α,25$(OH)_2D_3$ increased PGE2 by 50% in the conditioned media of wild type cells but overexpression of either $Pdia3_{[+KDEL]}$ or $Pdia3_{[-KDEL]}$ augmented the increase to more than 100%.

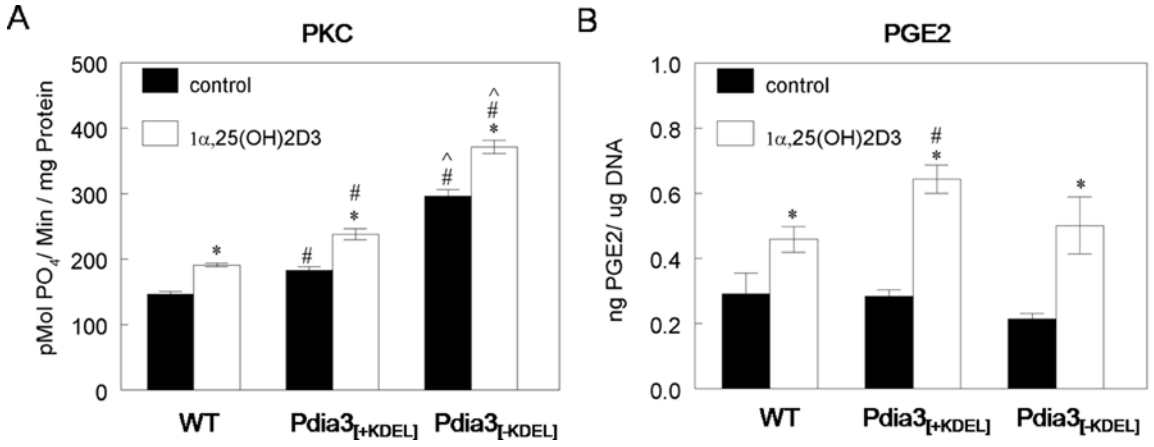

Figure 4-6. The effect of changing subcellular location of Pdia3 on rapid responses to 1α,25(OH)$_2$D$_3$. Cells were treated with vehicle or 10^{-7}M 1α,25(OH)$_2$D$_3$. PKC activity was measured at 15 minutes (A). PGE2 in conditioned media was measured at 30 minutes (B). PKC was normalized to total protein and PGE2 was normalized to DNA. Then the 1α,25(OH)$_2$D$_3$ treated group was normalized to the vehicle treated group. The dashed line with value of 1 represents vehicle treated group. *: p<.05 vehicle vs. treatment; #: p<.05 Pdia3$_{[\pm KDEL]}$ vs. WT.

4.3.5 Pdia3 mediated rapid increase in PKC activity in response to 1α,25$(OH)_2D_3$ does not require palmitoylation.

Treatment with tunicamycin decreased the plasma membrane association of N-glycosylated pan-cadherin and S-palmitoylated caveolin-1 but did not affect Pdia3 (Fig. 4-7A). Pan-cadherin was reduced by 90% and caveolin-1 was reduced by 25% (Fig. 4-7B). In contrast, Pdia3 was slightly increased. Moreover, the rapid 30% increase in PKC activity in response to 1α,25$(OH)_2D_3$ was not affected in the tunicamycin treated cells (Fig. 4-7C).

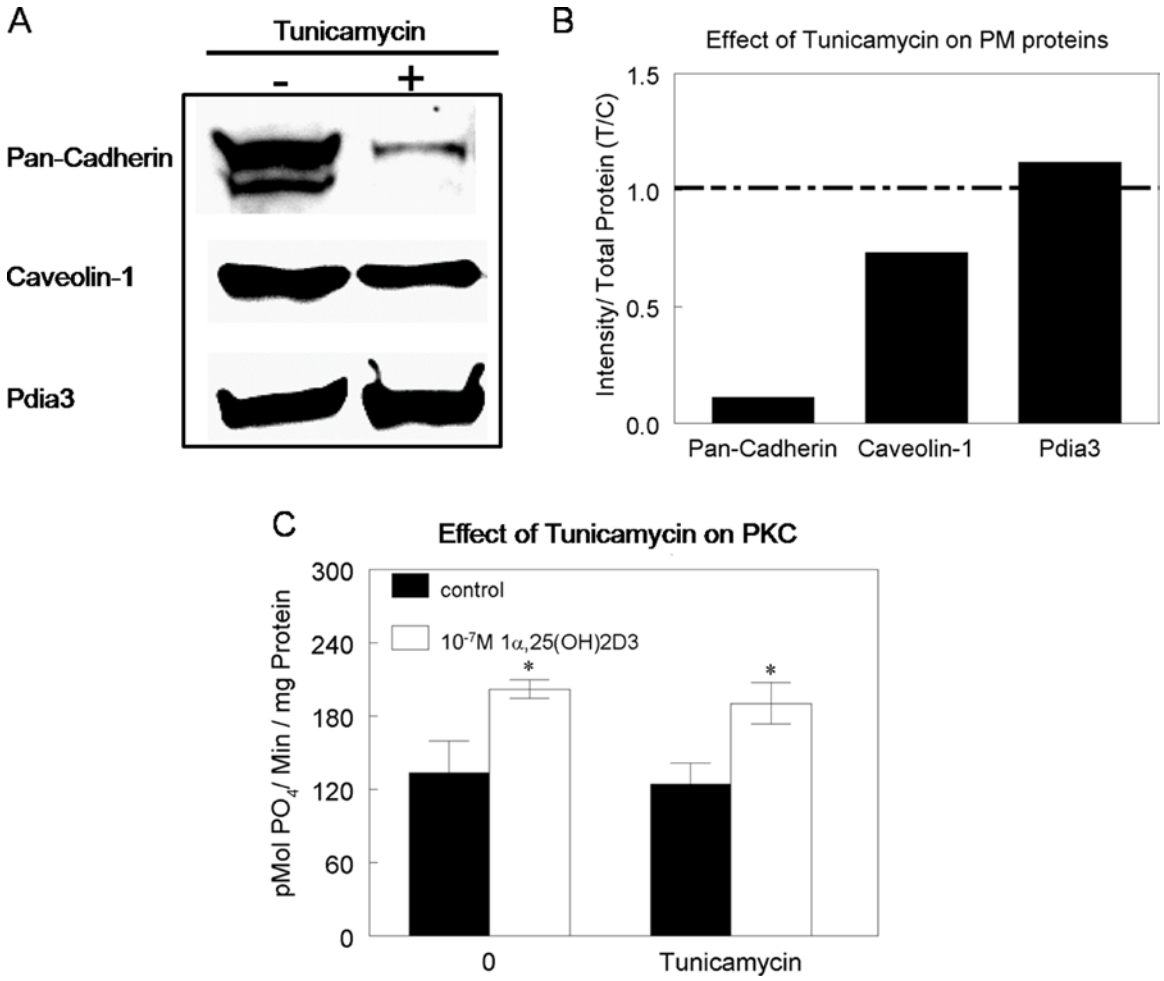

Figure 4-7. The effect of tunicamycin on the membrane association of Pdia3 and rapid responses to 1α,25$(OH)_2D_3$. (A): Western blots of pan-cadherin, caveolin-1 and Pdia3 in isolated plasma membranes. Wild type MC3T3-E1 cells were treated with vehicle (DMSO) or 1μg/ml tunicamycin for 48 hours. Plasma membrane isolation and western blots were performed. (B): the pixel intensity quantification of the Western blot image. The pixel intensity was calculated from the Western blot image, normalized by the total protein loaded into the gel electrophoresis, and then normalized by the values for the vehicle only treated group (dashed line=1). (C): the effect of tunicamycin on 1α,25$(OH)_2D_3$ stimulated PKC activity. Cells were treated with vehicle (DMSO) or 1μg/ml tunicamycin for 48 hours. Media were replaced by media containing vehicle or 10^{-7}M 1α,25$(OH)_2D_3$. PKC activity was measured at 15 minutes and normalized to total protein. * $P<0.05$, 1α,25$(OH)_2D_3$ vs. control.

4.4 Discussion

This study shows that the chaperone scaffolding property of Pdia3 plays an important role in mediating the rapid effects of 1α,25$(OH)_2D_3$ on two signal transduction pathways, PKC and PLA2, in MC3T3-E1 pre-osteoblasts. Site directed mutations of three amino acids involved in Pdia3's chaperone function impacted the presence of downstream mediators associated with the plasma membrane, the activity of PKC in response to 1α,25$(OH)_2D_3$ and the release of PGE2 into the conditioned medium. The subcellular location of Pdia3 was influenced by the presence of the ER retention signal KDEL. Interestingly, baseline PKC activity was sensitive to the retention signal, but the net increase in enzyme activity due to 1α,25$(OH)_2D_3$ was not impacted by this variable. In contrast, PLA2 activity was unaffected by the retention of Pdia3 in the ER or its elevated levels in the cytoplasm in the absence of KDEL, but the stimulatory effect of the seco-steroid was increased in cells overexpressing Pdia3 with or without ER retention signal. Finally, our results show that the association of Pdia3 with the plasma membrane does not require palmitoylation, nor does the rapid activation of PKC by 1α,25$(OH)_2D_3$.

Our results support the hypothesis that Pdia3 serves a scaffolding function in assembling proteins involved in the mechanism of 1α,25$(OH)_2D_3$ action at the plasma membrane and that the same sites that are required for its role as a chaperone in the ER are required for its role in mediating 1α,25$(OH)_2D_3$ signaling. Overexpression of native Pdia3 increased the presence of calreticulin in the plasma membrane compared to wild type MC3T3-E1 cells, as was noted by others studying the interaction of Pdia3 and calreticulin in cancer cells (52). Calreticulin was also increased in the plasma membranes from cells overexpressing all three mutant Pdia3 transcripts, but there was no change in its ratio to Pdia3 regardless of the mutation. This indicates that the amino acids required for the interaction mechanism between Pdia3 and calreticulin in the ER

are not important to their interaction at the plasma membrane. Calreticulin can mediate calcium signaling and interact with PKC (53,54), both of which are also important in rapid responses to 1α,25$(OH)_2D_3$ (33,55). Hruska and colleagues (37) reported that calreticulin was involved in intracellular transport of 1α,25$(OH)_2D_3$-VDR in ROS 17/2.8 osteoblastic cells, but whether this is the case in the MC3T3-E1 cells was not addressed in the present study.

The ratios of Pdia3 to caveolin-1, PLAA and c-Src varied amongst the cell lines suggesting that specific sites were responsible for assembling each protein. We previously reported that Pdia3 forms a complex with PLAA and caveolin-1 (29) and c-Src also interacts with caveolin-1 in rapid response to 1α,25$(OH)_2D_3$ (56). In the present study we found that by changing single amino acids in Pdia3 we could alter the complex formation. There was more caveolin-1, PLAA and c-Src per Pdia3 in R282A cells compared to $Pdia3_{ovr}$, K214A or C406S cells.

These data support the hypothesis that changes in the chaperone sites can alter formation of the complex required for 1α,25$(OH)_2D_3$ signaling at the plasma membrane and suggest that the protein assembly in R282A cells may be more active than in the other cell line examined. Indeed, R282A cells were the only mutant cell line that responded to 1α,25$(OH)_2D_3$ treatment by increasing both PKC activity and PGE2 release. However, the effect of 1α,25$(OH)_2D_3$ in the R282A cells was comparable to wild type cells, indicating that the mutation blocked the effect of overexpression seen in $Pdia3_{Ovr}$ cells but did not impact the native Pdia3 function. In contrast, K214A and C406S cells had levels of caveolin-1, c-Src and PLAA similar to the $Pdia3_{Ovr}$ cells. K214A cells exhibited no change in PKC and increased PGE2 to levels comparable to wild type cells. PKC activity was reduced in C406S cells compared to wild type and there was no effect of 1α,25$(OH)_2D_3$ on PGE2 activity. Thus, even single amino acid changes

to Pdia3 to the same sites that mediate its role as a chaperone protein in the ER, can have profound consequences for its scaffolding function at the plasma membrane, particularly with respect to 1α,25$(OH)_2D_3$ signaling.

K214A and R282A are both located at the b and b′ cliff of Pdia3. This region interacts with calreticulin and calnexin, and when mutated, the interaction between Pdia3 and calreticulin or calnexin is abolished (38). In our study, calreticulin was present in the plasma membrane of all cell lines whereas calnexin was not. This suggests that Pdia3 recruits only calreticulin to the plasma membrane. However, in the mutant K214A cells, association between Pdia3 and calreticulin did not support downstream signaling even of native Pdia3. This indicates that there is a specific conformational arrangement that mediates the subsequent recruitment of other components of the signaling complex, and that there may be novel interactions through the same b and b′ cliff of Pdia3 to other proteins than the well-established interaction with calreticulin, which are important to rapid responses. Moreover, the R282A mutation prevented the stimulatory effect of 1α,25$(OH)_2D_3$ on PKC and PGE2 seen in $Pdia3_{Ovr}$ cells, indicating that calreticulin may not be important for mediating the action of the secosteroid on these two signaling pathway, but instead the role of calreticulin may be as a chaperone for 1α,25$(OH)_2D_3$-VDR after activation of the membrane receptor complex (37).

Amino acid C406 is the second cystine in CGHC catalytic motif of the thioredoxin-like a′ domain of Pdia3 and is important for the isomerase activity of Pdia3. Our mutagenesis data show C406 is also important to rapid response to 1α,25$(OH)_2D_3$. Pdia3 forms transient disulfide bonds with all of its N-glycosylated protein substrates, many of which are plasma membrane proteins (57), and forms stable disulfide bonds with some of its ER partners (35). Mutation of C406 in our study resulted in loss of downstream signaling in response to 1α,25$(OH)_2D_3$ compared to wild type and $Pdia3_{Ovr}$

cells but it did not alter the relationship between Pdia3 and caveolin-1, PLAA or c-Src. This suggests that C406 is responsible for catalyzing formation of disulfide bonds with other proteins required for PKC activation and PGE2 production.

Our data showed the C-terminal ER retention signal is important to the subcellular location of Pdia3. $Pdia3_{[-KDEL]}$ was present in the cytoplasm as well as the plasma membrane, indicating transport in the form of membrane vesicles. $Pdia3_{[-KDEL]}$ and $Pdia3_{[+KDEL]}$ were both present in the nucleus as well. Some of our previous work has suggested the inefficient N-terminal signal peptide of Pdia3 will cause a portion of Pdia3 to escape the ER into the cytosol and later translocate into the nucleus via the nuclear location sequence (44), which could explain our observation. The significance of nuclear Pdia3 is not yet known but PDI family members have been speculated that it can alter the redox state of transcription factors such as NFκB and AP1 and alter their binding with DNA (58,59).

Our results show that palmitoylation is not required for plasma membrane localization of Pdia3 nor for its ability to mediate rapid actions of $1\alpha,25(OH)_2D_3$. The glycosylation and palmitoylation inhibitor tunicamycin reduced the membrane association of cadherin and caveolin-1, but did not affect Pdia3. It is likely that Pdia3 associates with the plasma membrane during its formation. Myristate is another lipid that can increase plasma membrane affinity and sequence analysis shows that Pdia3 possesses myristoylation sites (60). In contrast to reversible palmitoylation, through which ER receptor increases membrane affinity upon estradiol treatment (48), myristoylation is irreversible. Cadherin is N-glycosylated (61) and caveolin-1 is palmitoylated (62), explaining their reduced association with the membrane. Caveolin-1 is important to the function of Pdia3 and 75% of the plasma membrane protein was still present after tunicamycin treatment.

Surprisingly, we found that the stimulating effect of 1α,25$(OH)_2D_3$ on PKC activity was comparable among wild type, Pdia3$_{[+KDEL]}$ and Pdia3$_{[-KDEL]}$ cells. Instead, there was a marked increase in baseline PKC activity in Pdia3$_{[-KDEL]}$ cells compared to wild type control cultures. One possibility is that the effect of 1α,25(OH)2D3 was maximized in all cultures and did not depend on the increased amount of enzyme but on other factors. The fact that our Pdia3$_{[+KDEL]}$ cells were transfected, cultured, and treated in the same way as Pdia3$_{[-KDEL]}$ cells, but had baseline PKC activity similar to wild type cells, supports the role of plasma membrane associated Pdia3 in mediating PKC activity. It is also possible that only native Pdia3 was responsive to 1α,25$(OH)_2D_3$ whereas the increased PKC activity present in Pdia3$_{[+KDEL]}$ and Pdia3$_{[-KDEL]}$ cultures simply represented increased Pdia3GFP, which was not sensitive to the secosteroid. Support for this is the fact Pdia3$_{Ovr}$ cells, where we overexpressed native mouse Pdia3, not only had elevated baseline PKC activity but also an augmented fold increase in PKC after 1α,25$(OH)_2D_3$ treatment compared to wild type cells. The Pdia3GFP construct used the human Pdia3 sequence, which has 93% identity with mouse Pdia3 at the amino acid level. Whether this accounts for its insensitivity to 1α,25$(OH)_2D_3$ is not known.

Both Pdia3$_{[+KDEL]}$ and Pdia3$_{[-KDEL]}$ responded to 1α,25$(OH)_2D_3$ with an increase in PGE2 production. In chondrocytes, 1α,25$(OH)_2D_3$ activates PLA2 through a Pdia3-dependent pathway resulting in arachidonic acid release, which is further processed to PGE2 through cyclooxygenase-1 (COX-I) (9-11,13). Cox-1 is found predominantly in endoplasm reticulum and peri-nuclear region (63) and cytosolic PLA2 translocates to the peri-nuclear region after activation (64). Overexpressed Pdia3$_{[+KDEL]}$ and Pdia3$_{[-KDEL]}$ were present in this region as well, providing spatial proximity to c-PLA2 and COX-1, the data may suggest a role for ER-associated Pdia3 in mediating the production of PGE2. Antibodies to Pdia3 block the stimulatory effect of 1α,25$(OH)_2D_3$ on PKC supporting its

plasma membrane location (23,24), but it is not known if anti-Pdia3 antibody could block 1α,25$(OH)_2D_3$ -stimulated PGE2 release. We measured PGE2 production at 30 mins, whereas PKC activation occurs as quickly as 3 minutes (65) and arachidonic acid release as early as 15 seconds in chondrocytes (66) . It is possible there is a secondary role of Pdia3 in mediating the PGE2 pathway in the peri-nuclear region downstream of its initial action on PLA2 and PKC. Alternatively, Pdia3 may mediate effects in PGE2 production in the ER itself. A novel estrogen receptor GPR30 was found to be present in ER where it binds estradiol and initiates rapid responses (67).

In conclusion, this study shows that amino acids K214 and R282 in the calreticulin interaction site and C406 in catalytic site are important to Pdia3 dependent rapid responses to 1α,25$(OH)_2D_3$. Moreover, K214, R282 and C406 are important for the membrane association of caveolin-1, c-Src and PLAA. Deletion of the ER retention signal can increase plasma membrane associated Pdia3 but its effects on rapid responses are complex implying additional levels of regulation occur. Palmitoylation is not required for the plasma membrane association of Pdia3 and rapid increases in PKC and PLA2 signaling by 1α,25$(OH)_2D_3$.

4.5 References

1. Chen, J., Olivares-Navarrete, R., Wang, Y., Herman, T. R., Boyan, B. D., and Schwartz, Z. (2010) *J Biol Chem* **285**, 37041-37050
2. Schwartz, Z., Schlader, D. L., Ramirez, V., Kennedy, M. B., and Boyan, B. D. (1989) *J Bone Miner Res* **4**, 199-207
3. Tishkoff, D. X., Nibbelink, K. A., Holmberg, K. H., Dandu, L., and Simpson, R. U. (2008) *Endocrinology* **149**, 558-564
4. Becklund, B. R., Hansen, D. W., Jr., and Deluca, H. F. (2009) *Proc Natl Acad Sci U S A* **106**, 5276-5281
5. Mathieu, C., Waer, M., Casteels, K., Laureys, J., and Bouillon, R. (1995) *Endocrinology* **136**, 866-872
6. Yudoh, K., Matsuno, H., and Kimura, T. (1999) *The Journal of laboratory and clinical medicine* **133**, 120-128
7. Lee, H. J., Paul, S., Atalla, N., Thomas, P. E., Lin, X., Yang, I., Buckley, B., Lu, G., Zheng, X., Lou, Y. R., Conney, A. H., Maehr, H., Adorini, L., Uskokovic, M., and Suh, N. (2008) *Cancer Prev Res (Phila)* **1**, 476-484
8. Wali, R. K., Bissonnette, M., Khare, S., Hart, J., Sitrin, M. D., and Brasitus, T. A. (1995) *Cancer Res* **55**, 3050-3054
9. Boyan, B. D., Sylvia, V. L., Dean, D. D., Pedrozo, H., Del Toro, F., Nemere, I., Posner, G. H., and Schwartz, Z. (1999) *Steroids* **64**, 129-136
10. Schwartz, Z., Gilley, R. M., Sylvia, V. L., Dean, D. D., and Boyan, B. D. (1999) *Bone* **24**, 475-484
11. Schwartz, Z., Graham, E. J., Wang, L., Lossdorfer, S., Gay, I., Johnson-Pais, T. L., Carnes, D. L., Sylvia, V. L., and Boyan, B. D. (2005) *J Cell Physiol* **203**, 54-70
12. Doroudi, M., Schwartz, Z., and Boyan, B. D. (2012) *J Steroid Biochem Mol Biol* **132**, 48-56
13. Boyan, B. D., Wang, L., Wong, K. L., Jo, H., and Schwartz, Z. (2006) *Steroids* **71**, 286-290
14. Schwartz, Z., Sylvia, V. L., Luna, M. H., DeVeau, P., Whetstone, R., Dean, D. D., and Boyan, B. D. (2001) *Steroids* **66**, 683-694
15. Schwartz, Z., Ehland, H., Sylvia, V. L., Larsson, D., Hardin, R. R., Bingham, V., Lopez, D., Dean, D. D., and Boyan, B. D. (2002) *Endocrinology* **143**, 2775-2786
16. Buitrago, C., Vazquez, G., De Boland, A. R., and Boland, R. L. (2000) *J Cell Biochem* **79**, 274-281
17. Boland, R., De Boland, A. R., Buitrago, C., Morelli, S., Santillan, G., Vazquez, G., Capiati, D., and Baldi, C. (2002) *Steroids* **67**, 477-482
18. Buitrago, C., Vazquez, G., De Boland, A. R., and Boland, R. (2001) *Biochem Biophys Res Commun* **289**, 1150-1156
19. Nemere, I., Garbi, N., Hammerling, G. J., and Khanal, R. C. (2010) *J Biol Chem* **285**, 31859-31866
20. Van Cromphaut, S. J., Dewerchin, M., Hoenderop, J. G., Stockmans, I., Van Herck, E., Kato, S., Bindels, R. J., Collen, D., Carmeliet, P., Bouillon, R., and Carmeliet, G. (2001) *Proc Natl Acad Sci U S A* **98**, 13324-13329

21. Nemere, I., Dormanen, M. C., Hammond, M. W., Okamura, W. H., and Norman, A. W. (1994) *J Biol Chem* **269**, 23750-23756
22. Nemere, I., Farach-Carson, M. C., Rohe, B., Sterling, T. M., Norman, A. W., Boyan, B. D., and Safford, S. E. (2004) *Proc Natl Acad Sci U S A* **101**, 7392-7397
23. Nemere, I., Schwartz, Z., Pedrozo, H., Sylvia, V. L., Dean, D. D., and Boyan, B. D. (1998) *J Bone Miner Res* **13**, 1353-1359
24. Boyan, B. D., Bonewald, L. F., Sylvia, V. L., Nemere, I., Larsson, D., Norman, A. W., Rosser, J., Dean, D. D., and Schwartz, Z. (2002) *Steroids* **67**, 235-246
25. Pedrozo, H. A., Schwartz, Z., Rimes, S., Sylvia, V. L., Nemere, I., Posner, G. H., Dean, D. D., and Boyan, B. D. (1999) *J Bone Miner Res* **14**, 856-867
26. Schwartz, Z., Shaked, D., Hardin, R. R., Gruwell, S., Dean, D. D., Sylvia, V. L., and Boyan, B. D. (2003) *Steroids* **68**, 423-437
27. Boyan, B. D., Sylvia, V. L., McKinney, N., and Schwartz, Z. (2003) *J Cell Biochem* **90**, 1207-1223
28. Olivares-Navarrete, R., Sutha, K., Hyzy, S. L., Hutton, D. L., Schwartz, Z., McDevitt, T., and Boyan, B. D. (2012) *Stem Cells Dev*
29. Doroudi, M., Schwartz, Z., and Boyan, B. D. (2012) *J Steroid Biochem Mol Biol*
30. Boyan, B. D., Wong, K. L., Wang, L., Yao, H., Guldberg, R. E., Drab, M., Jo, H., and Schwartz, Z. (2006) *J Bone Miner Res* **21**, 1637-1647
31. Garbi, N., Tanaka, S., Momburg, F., and Hammerling, G. J. (2006) *Nat Immunol* **7**, 93-102
32. Costa, J. L., Eijk, P. P., van de Wiel, M. A., ten Berge, D., Schmitt, F., Narvaez, C. J., Welsh, J., and Ylstra, B. (2009) *BMC genomics* **10**, 499
33. Sylvia, V. L., Schwartz, Z., Ellis, E. B., Helm, S. H., Gomez, R., Dean, D. D., and Boyan, B. D. (1996) *J Cell Physiol* **167**, 380-393
34. Lindquist, J. A., Jensen, O. N., Mann, M., and Hammerling, G. J. (1998) *EMBO J* **17**, 2186-2195
35. Peaper, D. R., Wearsch, P. A., and Cresswell, P. (2005) *EMBO J* **24**, 3613-3623
36. Peaper, D. R., and Cresswell, P. (2008) *Proc Natl Acad Sci U S A* **105**, 10477-10482
37. Kim, Y. S., MacDonald, P. N., Dedhar, S., and Hruska, K. A. (1996) *Endocrinology* **137**, 3649-3658
38. Kozlov, G., Maattanen, P., Schrag, J. D., Pollock, S., Cygler, M., Nagar, B., Thomas, D. Y., and Gehring, K. (2006) *Structure* **14**, 1331-1339
39. Beynon-Jones, S. M., Antoniou, A. N., and Powis, S. J. (2006) *FEBS letters* **580**, 1897-1902
40. Hirano, N., Shibasaki, F., Sakai, R., Tanaka, T., Nishida, J., Yazaki, Y., Takenawa, T., and Hirai, H. (1995) *European journal of biochemistry / FEBS* **234**, 336-342
41. Frickel, E. M., Riek, R., Jelesarov, I., Helenius, A., Wuthrich, K., and Ellgaard, L. (2002) *Proc Natl Acad Sci U S A* **99**, 1954-1959
42. Leach, M. R., Cohen-Doyle, M. F., Thomas, D. Y., and Williams, D. B. (2002) *J Biol Chem* **277**, 29686-29697

43. Wu, W., Beilhartz, G., Roy, Y., Richard, C. L., Curtin, M., Brown, L., Cadieux, D., Coppolino, M., Farach-Carson, M. C., Nemere, I., and Meckling, K. A. (2010) *Exp Cell Res* **316**, 1101-1108
44. Grindel, B. J., Rohe, B., Safford, S. E., Bennett, J. J., and Farach-Carson, M. C. (2011) *J Cell Biochem*
45. Schwartz, Z., Schlader, D. L., Swain, L. D., and Boyan, B. D. (1988) *Endocrinology* **123**, 2878-2884
46. Acconcia, F., Ascenzi, P., Bocedi, A., Spisni, E., Tomasi, V., Trentalance, A., Visca, P., and Marino, M. (2005) *Molecular biology of the cell* **16**, 231-237
47. Marino, M., and Ascenzi, P. (2006) *IUBMB Life* **58**, 716-719
48. Li, L., Haynes, M. P., and Bender, J. R. (2003) *Proc Natl Acad Sci U S A* **100**, 4807-4812
49. Franceschi, R. T., Iyer, B. S., and Cui, Y. (1994) *J Bone Miner Res* **9**, 843-854
50. Huhtakangas, J. A., Olivera, C. J., Bishop, J. E., Zanello, L. P., and Norman, A. W. (2004) *Mol Endocrinol* **18**, 2660-2671
51. Fan, G., Goldsmith, P. K., Collins, R., Dunn, C. K., Krapcho, K. J., Rogers, K. V., and Spiegel, A. M. (1997) *Endocrinology* **138**, 1916-1922
52. Obeid, M. (2008) *J Immunol* **181**, 2533-2543
53. Coppolino, M. G., Woodside, M. J., Demaurex, N., Grinstein, S., St-Arnaud, R., and Dedhar, S. (1997) *Nature* **386**, 843-847
54. Rendon-Huerta, E., Mendoza-Hernandez, G., and Robles-Flores, M. (1999) *The Biochemical journal* **344 Pt 2**, 469-475
55. Liu, R., Li, W., Karin, N. J., Bergh, J. J., Adler-Storthz, K., and Farach-Carson, M. C. (2000) *J Biol Chem* **275**, 8711-8718
56. Buitrago, C., and Boland, R. (2010) *J Steroid Biochem Mol Biol* **121**, 169-175
57. Elliott, J. G., Oliver, J. D., and High, S. (1997) *J Biol Chem* **272**, 13849-13855
58. Clive, D. R., and Greene, J. J. (1996) *Cell biochemistry and function* **14**, 49-55
59. Grillo, C., D'Ambrosio, C., Scaloni, A., Maceroni, M., Merluzzi, S., Turano, C., and Altieri, F. (2006) *Free radical biology & medicine* **41**, 1113-1123
60. Khanal, R. C., and Nemere, I. (2007) *Curr Med Chem* **14**, 1087-1093
61. Langer, M. D., Guo, H., Shashikanth, N., Pierce, J. M., and Leckband, D. E. (2012) *Journal of cell science*
62. Uittenbogaard, A., and Smart, E. J. (2000) *J Biol Chem* **275**, 25595-25599
63. Rollins, T. E., and Smith, W. L. (1980) *J Biol Chem* **255**, 4872-4875
64. Muthalif, M. M., Benter, I. F., Uddin, M. R., and Malik, K. U. (1996) *J Biol Chem* **271**, 30149-30157
65. Sylvia, V. L., Schwartz, Z., Schuman, L., Morgan, R. T., Mackey, S., Gomez, R., and Boyan, B. D. (1993) *J Cell Physiol* **157**, 271-278
66. Swain, L. D., Schwartz, Z., and Boyan, B. D. (1992) *Biochimica et biophysica acta* **1136**, 45-51
67. Revankar, C. M., Cimino, D. F., Sklar, L. A., Arterburn, J. B., and Prossnitz, E. R. (2005) *Science* **307**, 1625-1630

CHAPTER 5

Mineralization of three dimensional osteoblast cultures is enhanced by interaction of 1α,25-dihydroxyvitamin D3 and BMP2 via two specific vitamin D receptors

Chapter 5 was submitted as [Chen J, Dosier CR, Park JH, De S, Guldberg RE, Boyan BD, Schwartz Z (2012) Mineralization of three dimensional osteoblast cultures is enhanced by interaction of 1α,25-dihydroxyvitamin D3 and BMP2 via two specific vitamin D receptors. Journal of Tissue Engineering and Regenerative Medicine]

5.1 Introduction

The vitamin D metabolite 1α,25-dihydroxyvitamin D3 [1α,25(OH)2D3] is known for its role in maintaining calcium and phosphate homeostasis. Mineralization of growth plate cartilage and bone is reduced in 1α,25(OH)2D3 deficiency, leading to skeletal deformities associated with rickets (1,2). In addition to its systemic effects on mineral ion homeostasis, 1α,25(OH)2D3 has effects on development of these tissues (3,4), indicating that skeletal cells possess receptors for this secosteroid. Two receptors for 1,25(OH)2D3 have been identified in osteoblasts: the canonical nuclear vitamin D receptor (VDR) (5,6) and a plasma membrane receptor, protein disulfide isomerase family A, member 3 (Pdia3) (7,8). Both VDR and Pdia3 contribute to rapid membrane-associated signaling (7,9,10) leading to altered gene expression, in addition to the traditional role of the VDR (11,12).

The role that 1α,25(OH)2D3 plays in mineralization is complex. Mice lacking a functional VDR exhibit rickets (13,14), which can be healed by restoring serum Ca^{++} content through diet (15). Although mineralization of the growth plate and bone matrix is

restored, growth plate anomalies remain (3,4), indicating that VDR-dependent signaling is involved in more aspects of skeletal development than mineral ion transport. Moreover, $VDR^{-/-}$ mice possess Pdia3 and osteoblasts from $VDR^{-/-}$ mice retain Pdia3-dependent rapid responses to 1α,25(OH)2D3 (16). Global knockout of Pdia3 is embryologically lethal, but $Pdia3^{+/-}$ heterozygous mice exhibit a bone phenotype (17). Thus, both receptors play important roles in bone development, but their independent contributions to osteoblast differentiation and mineralization have not been compared in one model system.

In culture, 1α,25(OH)2D3 has been shown to both increase (18-20) and decrease (21-23) calcium phosphate deposition, suggesting that the effects of 1α,25(OH)2D3 may depend on culture conditions, cell source, or cell maturation stage. In addition to 1α,25(OH)2D3, cell culture models examining osteoblast differentiation frequently include factors to stimulate osteoblast differentiation, such as dexamethasone and β-glycerophosphate (24) as well as bone morphogenetic protein-2 (BMP2) (25). These media additives can alter the effects of 1α,25(OH)2D3 in different ways. For example, addition of transforming growth factor β1 (TGF-β1) to osteoblast cultures modulates the effect of 1α,25(OH)2D3 on osteoblast differentiation, increasing alkaline phosphatase activity but inhibiting osteocalcin production (26). While these studies demonstrate that osteoblast differentiation in two dimensional (2D) cultures is mediated by multiple interacting factors, few studies have been done to investigate the interaction between 1α,25(OH)2D3 and BMP2 signaling pathways, either in 2D or in 3D systems.

To better understand the roles of Pdia3 and VDR in mediating the interaction of 1α,25(OH)2D3 and BMP2 in the regulation of osteoblast differentiation, we took advantage of a 3D cell culture model in which we were able to examine the ability of osteoblasts stably silenced for Pdia3 or VDR to support calcium phosphate deposition.

In this model, MC3T3-E1 cells were cultured in poly ε-caprolactone (PCL)/collagen scaffolds. The PCL provided a consistent porosity, and the collagen facilitated cell adhesion and retention within the scaffold (27). We first investigated the interaction of 1α,25(OH)2D3 and BMP2 through the expression of osteoblast markers in 2D cultures and then studied the roles of Pdia3 and VDR in mediating this interaction. Finally, we studied the roles of Pdia3 and VDR in mediating 1α,25(OH)2D3 and BMP2 stimulated calcification by osteoblasts in the 3D model.

5.2 Materials and methods

5.2.1 Pdia3/VDR Silencing

An MC3T3-E1 cell line with over 80% silencing of Pdia3 mRNA and protein (Sh-Pdia3) was previously established (7). The same approach was used to develop MC3T3-E1 cells stably silenced for VDR (Sh-VDR). Briefly, VDR short hairpin RNA probes were designed to target the mouse VDR mRNA (NM_009504) and five different sequences were generated and incorporated into lentivirus particles (MISSION^{TM} shRNA, Sigma-Aldrich, St. Louis, MO). MC3T3-E1 cells (CRL-2593, ATCC, Manassas, VA) were plated at a density of 20,000 cells/cm^2 in a 24-well plate in α-MEM supplemented with 10% fetal bovine serum (FBS) and 1% penicillin/streptomycin (P/S). After 24 hours, the medium was changed to α-MEM supplemented with 10% FBS, 1%P/S and 8μg/mL hexadimethrine bromide and transduced with lentivirus particles at a multiplicity of infection (MOI) of 7.5. Cells containing shRNAs or empty vectors were selected by culturing the cells for two weeks in medium containing 2.0μg/ml puromycin. Loss of VDR expression was quantified by real-time PCR. The clone with the highest silencing rate was chosen from the five different shRNA transfected clones. The selected Sh-VDR cell

line exhibited a 90% reduction in VDR mRNA and a comparable reduction in VDR protein (data not shown).

5.2.2 Two Dimensional Cell Culture

Wild type (WT), Sh-Pdia3, and Sh-VDR MC3T3-E1 cells were plated at 20,000 cells/cm^2 in T75 flasks with full medium (α-MEM supplemented with 10% FBS, 1%P/S, with or without 2.0μg/ml puromycin). After 48 hours, full medium was changed to full medium containing 1% vitamin C to enable cross-linking of type I collagen in the extracellular matrix.

Ten days after plating, wild type, Sh-Pdia3 and Sh-VDR MC3T3-E1 cells were treated with vehicle or 10^{-8} M 1α,25(OH)2D3 (Biomol, Plymouth Meeting, PA) for 15 minutes to activate Pdia3-dependent signaling via protein kinase C (PKC) and ERK1/2 mitogen activated protein kinase (MAPK) (7). Alternatively, the medium was replaced by fresh medium with or without 50 ng/ml recombinant human BMP2 (B3555, Sigma-Aldrich, St. Louis, MO). This resulted in cultures treated with medium containing no additives (I); cultures treated with medium containing 1α,25(OH)2D3, followed by medium without BMP2 (II); cultures treated with medium alone for 15 minutes, followed by medium containing BMP2 (III); and cultures treated with medium containing 1α,25(OH)2D3 for 15 minutes followed by medium containing BMP2 (IV). Cell layers were lysed with TRizol (Invitrogen, Carlsbad, CA) 12 hours later to harvest RNA.

5.2.2.1 Gene Expression

RNA was reverse-transcribed into cDNA using the high capacity cDNA reverse transcription kit (Applied Biosystems, Carlsbad, CA) according to the manufacturer's directions. In order to determine if there was cross-talk at the expression level amongst

Pdia3, VDR and BMP2, mRNAs for Pdia3 (Pdia3) and VDR (Vdr), as well as BMP2 (Bmp2) and the BMP2 inhibitor Noggin (Nog) were measured in wild type, Sh-Pdia3 and Sh-VDR cells. mRNAs for alkaline phosphatase (Alpl), osteocalcin (Bglap), and osteopontin (Spp1) were measured as indicators of osteoblast differentiation. In addition, others have shown BMP2 directly up regulates Distal-less homeobox5 expression mRNA (Dlx5) and indirectly up regulates Runt-related transcription factor 2 mRNA (Runx2) (28,29). Therefore, these two transcription factors, which are also associated with osteoblastic differentiation, were measured.

Oligonucleotide primers to the targeted genes were designed using Beacon Designer 7.0 software (PREMIER Biosoft International, Palo Alto, CA). A homology blast search was performed within the mammalian genome to exclude the possibility of sequence similarity. Primers were synthesized by Eurofins MWG Operon (Huntsville, AL) and are shown in Table 5-1. Real-time PCR was performed using SYBR Green SuperMix, the Veriti 96 well Thermal Cycler, and Step One software (Applied Biosystems). Data were normalized to the endogenous reference gene glyceraldehyde 3-phosphate dehydrogenase (Gapdh).

Table 5-1 Oligonucleotide primers for real time PCR of mRNAs for Pdia3, VDR (Vdr), BMP2 (Bmp2), Noggin (Nog), alkaline phosphatase (Alpl), osteocalcin (Bglap), osteopontin (Spp1), Dlx5, Runx2, and GAPDH.

Gene	Forward Primer	Reverse Primer
Pdia3	CGA TGT GTT GGA ACT GAC G	TTC ATA CTC AGG GGC AAG C
Vdr	AGG CAG GCA GAA GAG ATG AG	AGG GAT GAT GGG TAG GTT GTG
Bmp2	TGG GTT TGT GGT GGA AGT G	TCGTTTGTGGAGCGGATG
Nog	GCC AGC ACT ATC TAC ACA TCC	CAG CAG CGT CTC GTT CAG
Alpl	GTG GGC ATT GTG ACT ACC	GGT GGC ATC TCG TTA TCC
Bglap	TCT CTC TGC TCA CTC TGA	GTC TGT TCA CTA CCT TAT TGC
Spp1	AAC TCT TCC AAG CAA TTC C	TCT CAT CAG ACT CAT CCG
Dlx5	TCA GGA ATC GCC AAC TTT G	CCA TAA GAA GCA GAG GTA GG
Runx2	CCG CCA CCA CTC ACT ACC	GAT AGG ATG CTG ACG AAG TAC C
Gapdh	TTC AAC GGC ACA GTC AAG G	TCT CGC TCC TGG AAG ATG G

5.2.2.2 Alkaline Phosphatase Activity

Changes in alkaline phosphatase specific activity were used as an outcome measure of osteoblast differentiation. Wild type, Sh-Pdia3 and Sh-VDR cells were treated as described above. At the end of the 12 hour BMP2 treatment, the medium was replaced by full medium for another 12 hours. The cell layers were washed twice with cold PBS and were lysed in 0.05% Triton X-100. Alkaline phosphatase specific activity was measured as the release of *p*-nitrophenol from *p*-nitrophenylphosphate at pH 10.2 as described previously (30).

5.2.3 3D Culture Model

5.2.3.1 PCL/collagen 3D Scaffold Preparation

PCL scaffolds were prepared as previously described (27,31). Sheets (100x100x9 mm) of medical grade poly ε-caprolactone (Osteopore International, Singapore) with 85% porosity were cut with a 5 mm internal diameter biopsy punch to yield a cylindrical scaffold. The scaffolds were treated briefly with 5M sodium hydroxide in order to roughen the surface to facilitate cell attachment; the scaffolds were then washed three times with sterile water; and sterilized overnight via 70% ethanol evaporation. Sterile PCL scaffolds were washed three times with excess sterile water and then were placed into a sterile custom mold. Sterilized rat tail type I collagen solution (Trevigen, Gaithersburg, MD) was diluted with sterile filtered 0.05% acetic acid to 1.5 mg/mL, neutralized with sterile filtered 1M sodium bicarbonate, and aseptically pipetted into the mold to occlude the pores of the scaffold. The PCL/collagen gel constructs were then placed in a -80°C freezer for one hour prior to being lyophilized overnight. Using a sterile scaffold holder, the lyophilized constructs were placed into 24-well low-attachment cell culture plates (Corning, Lowell, MA); they were then wrapped

with parafilm and stored at room temperature until cell seeding.

5.2.3.2 3D Cell Culture

In order to study mineralization in this 3D system, WT, Sh-Pdia3 and Sh-VDR MC3T3-E1 cells were plated at 20,000 cells/cm^2 in T75 flasks with full medium (α-MEM supplemented with 10% FBS 1%P/S with or without 2.0ug/ml puromycin). At confluence, cells were trypsinized, counted, and reconstituted in full medium at a density of 3 x 10^4 cells/μL. 100μL of the cell suspension were pipetted onto the tops of the PCL/collagen constructs and cells were allowed to attach to the surface. After a one-hour incubation period, full medium was added to the culture wells so that the cell-scaffold constructs were submerged. After 24 hours, cultures were treated with vehicle (ethanol) or 10^{-8}M 1α,25(OH)2D3 in full medium for 15 minutes. The medium was changed to osteogenic medium consisting of α-MEM supplemented with 16% FBS (Atlanta Biologics, Lawrenceville, GA), 1% penicillin-streptomycin, 50 μg/mL ascorbic acid 2-phosphate (Sigma-Aldrich), 6 mM beta-glycerophosphate (Sigma-Aldrich), and 1 nM dexamethasone (Sigma-Aldrich). One half of the cultures were treated with 50ng/mL recombinant human BMP2 (Sigma-Aldrich). The osteogenic medium $\pm$ BMP2 was changed three times weekly during cell culture. At each change, the same 15 minute transient treatment of 1α,25(OH)2D3 was applied. Cell/scaffold constructs were cultured dynamically on an orbital shaker (Stovall Life Scientific, Greensboro, NC) at the rate of 6.5 RPM in a CO_2 (5%) incubator. At 4 and 8 weeks, mineralized matrix of the cell/scaffold constructs was determined via micro-CT imaging. At the end of 8 weeks, samples were fixed in 10% neutral buffered formalin for 24 hours twice and further processed for scanning electron microscopy (SEM) and surface analysis by X-ray photon microscopy (XPS) as described below.

5.2.4 Analysis of 3D Constructs

5.2.4.1 Micro-CT Imaging

In order to determine the volume of mineralized matrix, cell-scaffold constructs were removed aseptically from culture at 4 and 8 weeks and placed in custom tubes for micro-CT scanning. Mineralized matrix of the cell/scaffold constructs was determined by using a VivaCT scanner (Scanco Medical, Brüttisellen, Switzerland) at 55 kVp, 109 mA, 1024 mu scaling, and a 200 ms integration time. The constructs were evaluated with a threshold of 80 with a filter width of 1.2 and a filter support of 1.0. The total volume of the mineralized matrix was then determined.

5.2.4.2 Scanning Electron Microscopy

In order to study the morphology of the mineralized matrix, the constructs were first sectioned in half, coated with gold (thickness ≈ 8 nm) and the cut surface was imaged using a Hitachi 4700 scanning electron microscope (SEM, Hitachi High Technologies America, Inc., USA) with an accelerating voltage of 12 kV.

5.2.4.3 X-ray Photoelectron Spectroscopy

The chemical composition of the cut surface was determined by XPS. Adult mouse femoral bone was used as a positive control. XPS (Thermo K-Alpha, Thermo Fisher Scientific Inc., MA) was used under ultra-high vacuum (less than 10^{-9} Torr) with a monochromatic Al Kα X-ray source (hv = 1486.6 eV, 90° take-off angle). The XPS spectra were evaluated with the Thermo Advantage 4.43 software package. The distribution of Ca (347 eV) and P (133 eV) on the surface of the constructs was obtained by XPS chemical mapping.

5.2.5 Statistical Analysis

The data presented are from a single representative experiment. Each data point represents the means ± standard error for six independent cell cultures. Significance was determined by one-way analysis of variance and post hoc testing performed using Bonferroni's modification of Student's t-test for multiple comparisons. $P \leq 0.05$ was considered significant. All experiments were repeated at least once to ensure the validity of the data.

Treatment/control ratios were used to compare the effect of treatment in groups with different baseline levels. The value for each sample in the treated group was divided by the mean of the control group. Each data point represents the means ± standard error for six normalized values and a dashed line with value equal to one represented the control. Due to the non-normal distribution, significance was determined using the Mann Whitney test. $P \leq 0.05$ was considered significant.

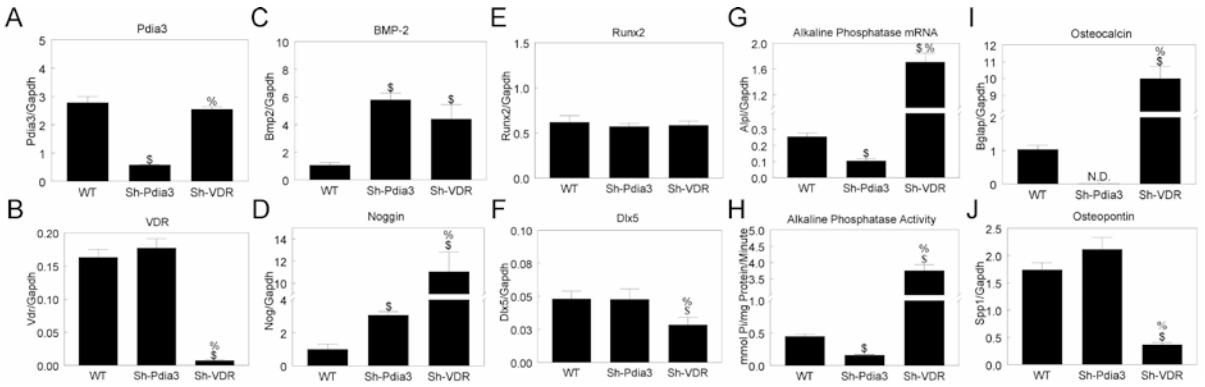

Fig. 5-1 Effect of silencing Pdia3 or VDR on gene expression. Wild type, Sh-Pdia3 and Sh-VDR MC3T3-E1 cells were treated with full medium containing the 1α,25(OH)2D3 vehicle (ethanol) for 15 minutes followed by replacing the medium with medium containing vehicle. mRNA was harvested 12 hours later and real-time PCR was performed: Pdia3 (A), Vdr (B), Bmp2 (C), Nog (D), Runx2 (E), Dlx5 (F), Alpl (G), Bglap (I), and Spp1 (J). Alkaline phosphatase activity was measured at 24 hours (H). $ $p<0.05$, Sh-Pdia3 or Sh-VDR vs. Wild type; % $P<0.05$, Sh-VDR vs. Sh-Pdia3.

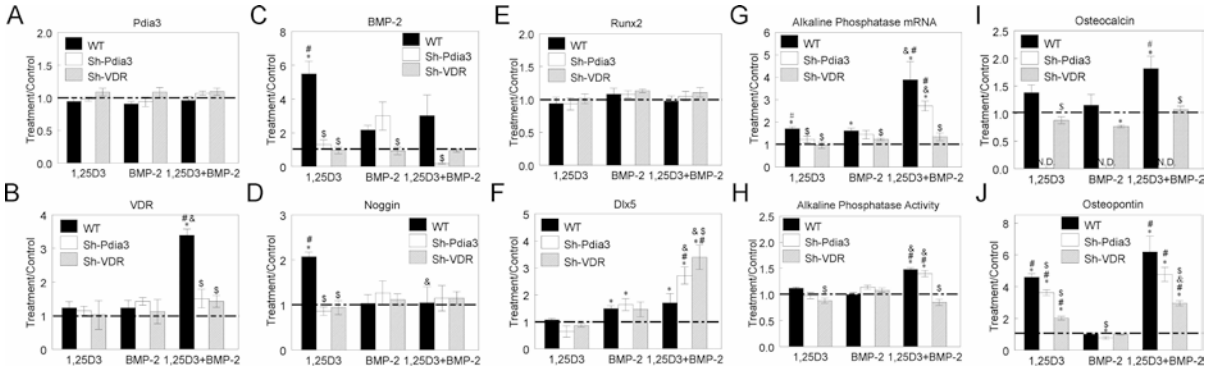

Fig. 5-2 Effect of 1α,25(OH)2D3 and BMP2 on gene expression in wild type, Sh-Pdia3 and Sh-VDR MC3T3-E1 cells. Wild type, Sh-Pdia3 and Sh-VDR MC3T3-E1 cells were treated with full medium containing the 1α,25(OH)2D3 vehicle (ethanol) or 10^{-8}M of 1α,25(OH)2D3 for 15 minutes followed by replacing the medium with medium with vehicle (ethanol) or 50ng/ml of BMP2. mRNA was harvested 12 hours later and real-time PCR was performed: Pdia3 (A), Vdr (B), Bmp2 (C), Nog (D), Runx2 (E), Dlx5 (F), Alpl (G), Bglap (I), and Spp1 (J). Alkaline phosphatase activity was measured at 24 hours (H). $ $p<0.05$, Sh-Pdia3 or Sh-VDR vs. Wild type. To evaluate the effect of the treatments independently of differences in baselines, values from treated groups [1α,25$(OH)_2D_3$, BMP2 or both] were divided by values from the vehicle only control group. Data presented are the resulting treatment/control ratios: * $p<0.05$, treatments [1α,25$(OH)_2D_3$, BMP2 or 1α,25$(OH)_2D_3$+BMP2] vs. control; # $p<0.05$, [1α,25(OH)2D3 or 1α,25$(OH)_2D_3$+BMP2] vs. BMP2 alone; & $p<0.05$, 1α,25$(OH)_2D_3$+BMP2 vs. 1α,25(OH)2D3 alone.

5.3 Results

5.3.1 Gene Expression

Baseline mRNA expression differed among the 3 cell lines. Silencing Pdia3 reduced Pdia3 expression by 80 % compared to wild type MC3T3-E1 cells (Fig. 5-1a) but had no effect on expression of Vdr (Fig. 5-1b). Similarly, silencing VDR had no effect on Pdia3 expression but reduced Vdr levels by 90 %. Bmp2 levels increased in Sh-Pdia3 cells by 500% and in Sh-VDR cells by 300% (Fig. 5-1c). Expression of Nog was also affected in the silenced cells. There was a 200% increase in Sh-Pdia3 cells and a 1000% increase in Sh-VDR cells (Fig. 5-1d). Baseline levels of mRNAs for Runx2 were unaffected by silencing either Pdia3 or VDR (Fig. 5-1e). Whereas Dlx5 did not change in Sh-Pdia3 cells compared to WT, expression was reduced in the Sh-VDR cells (Fig. 5-1f). Baseline levels for mRNAs associated with osteoblast differentiation were sensitive to silencing of specific receptors for 1α,25(OH)2D3. Sh-Pdia3 cells had reduced levels of Alpl whereas Alpl was increased in Sh-VDR cells (Fig. 5-1g). Alkaline phosphatase specific activity was affected in a comparable manner (Fig. 5-1h). No mRNA for Bglap was detected in Sh-Pdia3 cells but expression was markedly increased in Sh-VDR cells (Fig. 5-1i). In contrast, silencing Pdia3 had no effect on Spp1 but expression in Sh-VDR cells was markedly reduced compared to WT (Fig. 5-1j).

mRNA levels were differentially affected by 1α,25(OH)2D3 and BMP2, either alone or in combination. Regardless of whether cells were silenced for Pdia3 or VDR, no treatment altered Pdia3 expression compared to their baseline levels (Fig. 5-2a). Similarly, neither treatment with 1α,25(OH)2D3 alone nor BMP2 alone altered Vdr, but the combination caused a greater than 2 fold increase in Vdr expression in WT cells but had no effect on the silenced cells (Fig. 5-2b). 1α,25(OH)2D3 alone increased BMP2 expression in WT cells whereas BMP2 had no effect on any of the cell lines (Fig. 5-2c). Similarly, 1α,25(OH)2D3 increased Nog expression in WT cells only and BMP2 had no

effect (Fig. 5-2d). Expression of Runx2 was not affected by any of the treatments in any of the cell lines (Fig. 5-2e). Dlx5 was not affected by 1α,25(OH)2D3 alone but BMP2 caused a small increase in WT and Sh-Pdia3 cells. When BMP2 was used following 1α,25(OH)2D3 treatment, Dlx5 was increased in WT cells and to a greater extend in both of the silenced cell lines (Fig. 5-2f). Both 1α,25(OH)2D3 and BMP2 alone caused small increases in Alpl expression in WT cells and there was a synergistic increase in Alpl in WT and Sh-Pdia3 cells when the combination treatment was used (Fig. 5-2g). This was correlated with increased activity in the WT and Sh-Pdia3 cells treated with the combination of 1α,25(OH)2D3 and BMP2 (Fig. 5-2h). Bglap expression was increased over baseline only in cultures treated with 1α,25(OH)2D3 plus BMP2 (Fig. 5-2i). It was absent in Sh-Pdia3 cells regardless of treatment and reduced compared to baseline in Sh-VDR cells. Spp1 was increased by 1α,25(OH)2D3 in WT cells and Sh-Pdia3 cells and to a comparable extent in WT and Sh-Pdia3 cells treated with 1α,25(OH)2D3 plus BMP2 (Fig. 5-2j). 1α,25(OH)2D3 also increased Spp1 in Sh-VDR cells but to a lesser extent. By itself BMP2 had no effect on Spp1.

5.3.2 Mineralization in 3D Scaffolds

3D reconstruction of micro-CT scans of the cell/scaffold constructs showed that mineral deposition was regulated by 1α,25(OH)2D3 and BMP2 in a differential manner depending on cell type (Fig. 5-3). Although wild type constructs were not mineralized at 4 weeks, Sh-Pdia3 constructs were well mineralized at that time. Treatment with 1α,25(OH)2D3 alone had no effect on wild type and Sh-Pdia3 cells but reduced mineral deposition in Sh-VDR cells. BMP2 increased mineral deposition in the WT constructs and the Sh-VDR constructs, but did not increase mineral deposition in Sh-Pdia3 constructs. Treatment of the constructs with BMP2 and 1α,25(OH)2D3 had no additional

effect but Sh-VDR constructs exhibited reduced mineral content compared to the constructs treated with BMP2 alone.

At 8 weeks, these effects were more pronounced. WT constructs were more mineralized than at 4 weeks; this was increased by BMP2 alone. 1α,25(OH)2D3 and BMP2 together generated a synergistic increase in mineral deposition. Sh-Pdia3 constructs had the greatest mineral content and this was not affected by treatment with 1α,25(OH)2D3 alone, BMP2 alone or both factors. Sh-VDR constructs also exhibited greater mineral deposition at 8 weeks but this was reduced by treatment with 1α,25(OH)2D3. Treatment with BMP2 increased mineral deposition over that seen in untreated Sh-VDR cells and it also reduced the inhibitory effect of 1α,25(OH)2D3.

These qualitative observations were confirmed by measurement of mineralized volume. At 4 week, there was no evidence of mineral in WT cultures and only low levels of mineral in Sh-VDR cultures, whereas Sh-Pdia3 cultures was well calcified (Fig. 5-4a). At 8 weeks, mineralized volume of the WT scaffolds was low whereas calcium phosphate deposits in Sh-Pdia3 cultures and Sh-VDR cultures were extensive and to a comparable extent (Fig. 5-4b). Treatment with 1α,25(OH)2D3 reduced mineralized volume in WT and Sh-VDR constructs at 4 weeks (Fig. 5-4c), whereas BMP2 increased mineralized volume in these same culture. 1α,25(OH)2D3 and BMP2 in combination caused a synergistic increase in WT constructs only. At 8 weeks, 1α,25(OH)2D3 continued to suppress mineralized volume of sh-VDR constructs (Fig. 5-4d). BMP2 increased mineral in WT constructs and caused a small increase over baseline in Sh-VDR constructs. However 1α,25(OH)2D3 and BMP2 in combination resulted in a synergistic increase in WT constructs but the stimulatory effect of BMP2 on Sh-VDR constructs was abrogated.

Cell Type	WT		Sh-Pdia3		Sh-VDR	
mm^3	Control	1,25D3	Control	1,25D3	Control	1,25D3
4W Control	 0.00±0.00	 0.00±0.00	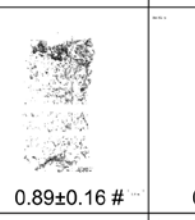 0.89±0.16 #	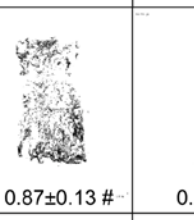 0.87±0.13 #	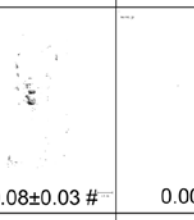 0.08±0.03 #	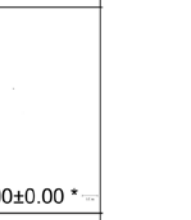 0.00±0.00 *
4W BMP-2	 0.11±0.03 &	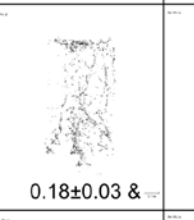 0.18±0.03 &	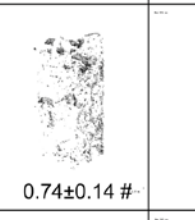 0.74±0.14 #	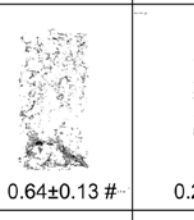 0.64±0.13 #	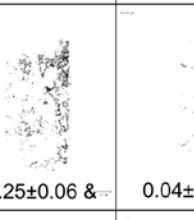 0.25±0.06 &	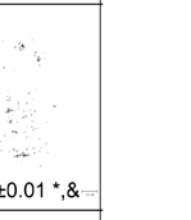 0.04±0.01 *,&
8W Control	 0.10±0.02	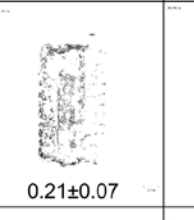 0.21±0.07	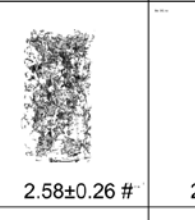 2.58±0.26 #	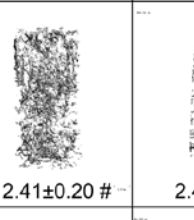 2.41±0.20 #	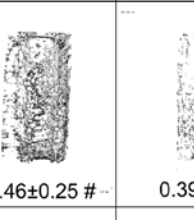 2.46±0.25 #	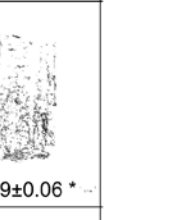 0.39±0.06 *
8W BMP-2	 1.12±0.17 &	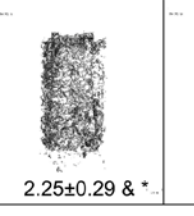 2.25±0.29 & *	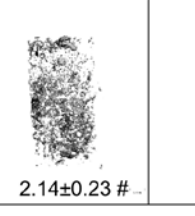 2.14±0.23 #	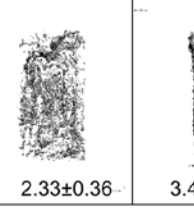 2.33±0.36	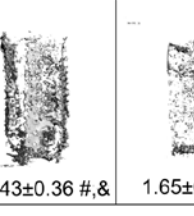 3.43±0.36 #,&	 1.65±0.24 *,&

Fig. 5-3 Effect of 1α,25(OH)2D3 and BMP2 on mineralized volume in 3D PCL scaffolds (image). Cells were cultured and treated as previously described. At 4 and 8 weeks, micro-CT was used to measure the mineralized volume. An image of the representative sample that had the closest value to the mean, is shown. The mean mineralized volume ± SEM for the group is provided under the image. # P<0.05, Sh-Pdia3 and Sh-VDR vs. wild type under same treatment; & P<0.05, BMP2 vs. control; * P<0.05, 1α,25(OH)2D3 vs. control.

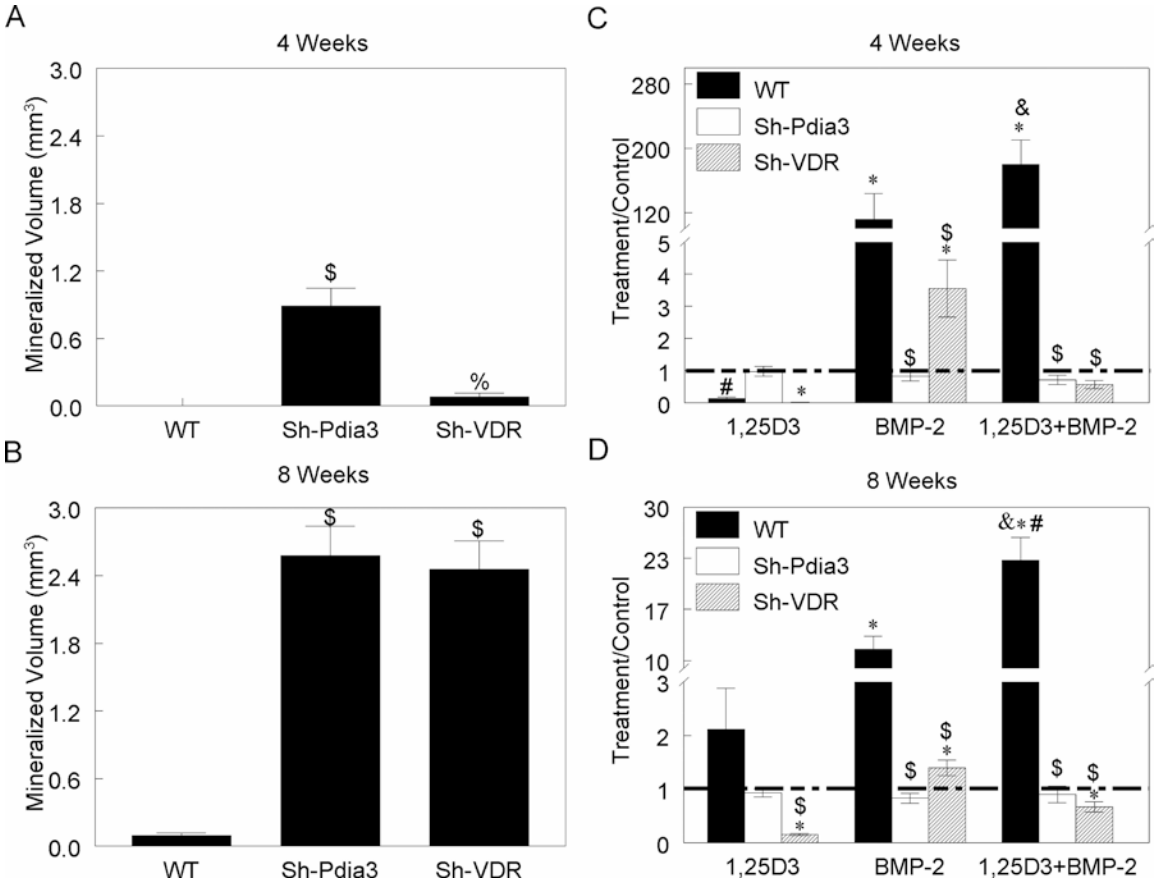

Fig. 5-4 Effect of 1α,25(OH)2D3 and BMP2 on mineralized volume in 3D PCL scaffold. Cells were cultured and treated as described above. At 4 and 8 weeks, micro-CT was used to measure the mineralized volume. The mineralized volumes without treatment are shown in panels A (4 weeks) and B (8 weeks). To evaluate the effect of the treatments independently of differences in baselines, values from treated groups [1α,25$(OH)_2D_3$, BMP2 or both] were divided by values from the vehicle only control group. Data presented are the resulting treatment/control ratios for 4 weeks (C) and 8 weeks (D): * $p<0.05$, treatments [1α,25$(OH)_2D_3$, BMP2 or 1α,25$(OH)_2D_3$+BMP2] vs. control; # $p<0.05$, 1α,25(OH)2D3 or 1α,25$(OH)_2D_3$+BMP2 vs. BMP2 alone; & $p<0.05$, 1α,25$(OH)_2D_3$+BMP2 vs. 1α,25(OH)2D3 alone.

The morphology of the 3D cultures varied with the cell line and treatment regimen. Low magnification SEMs of the bisected scaffolds showed that cells and extracellular matrix were present throughout (Fig. A-5). Wild type cells generated a smooth plate-like structure compared to the very porous net-like structures that were seen in both Sh-Pdia3 and Sh-VDR constructs. High magnification SEMs of the bisected surface of scaffolds containing wild type cells treated with 1α,25(OH)2D3 or BMP2 showed that aggregated clusters were randomly distributed (Fig. 5-5). In contrast, wild type cells that were treated with both 1α,25(OH)2D3 and BMP2 exhibited a morphology with mineralized areas under 1μm of length evenly covering all of the surface. Globular aggregated features approximately 10~15μm in diameter were observed in most of the scaffolds containing Sh-Pdia3 cells. Scaffolds containing Sh-VDR cells had densely packed spherical features embedded in continuously formed layers similar to those seen in Sh-Pdia3 constructs, whether the cells were treated with vehicle or 1α,25(OH)2D3. SEM images of decalcified Sh-Pdia3 constructs exhibited a fibrous matrix structure without any globular features, indicating that these structures might be mineral deposits (Fig. A-6).

Oxygen (O), carbon (C), nitrogen (N), and calcium (Ca), and phosphorus (P) were detected in all samples as well as in native bone (Fig. A-7). Ca/P ratios for all constructs varied from 0.8 to 0.9, similar to native bone. Interestingly, there was a difference in the distribution of the deposited elements. Wild type constructs exhibited localized deposits of Ca and P. The locations of Ca and P were partially overlapping. The distribution was not changed whether they were treated with BMP2 alone or with 1α,25(OH)2D3 and BMP2. The Sh-Pdia3 constructs had more diffuse and more colocalized Ca and P deposits throughout compared to wild type constructs with or without BMP2 treatment (Fig. A-7b). The deposits of Ca and P in the femur were also more diffused compared to wild type constructs.

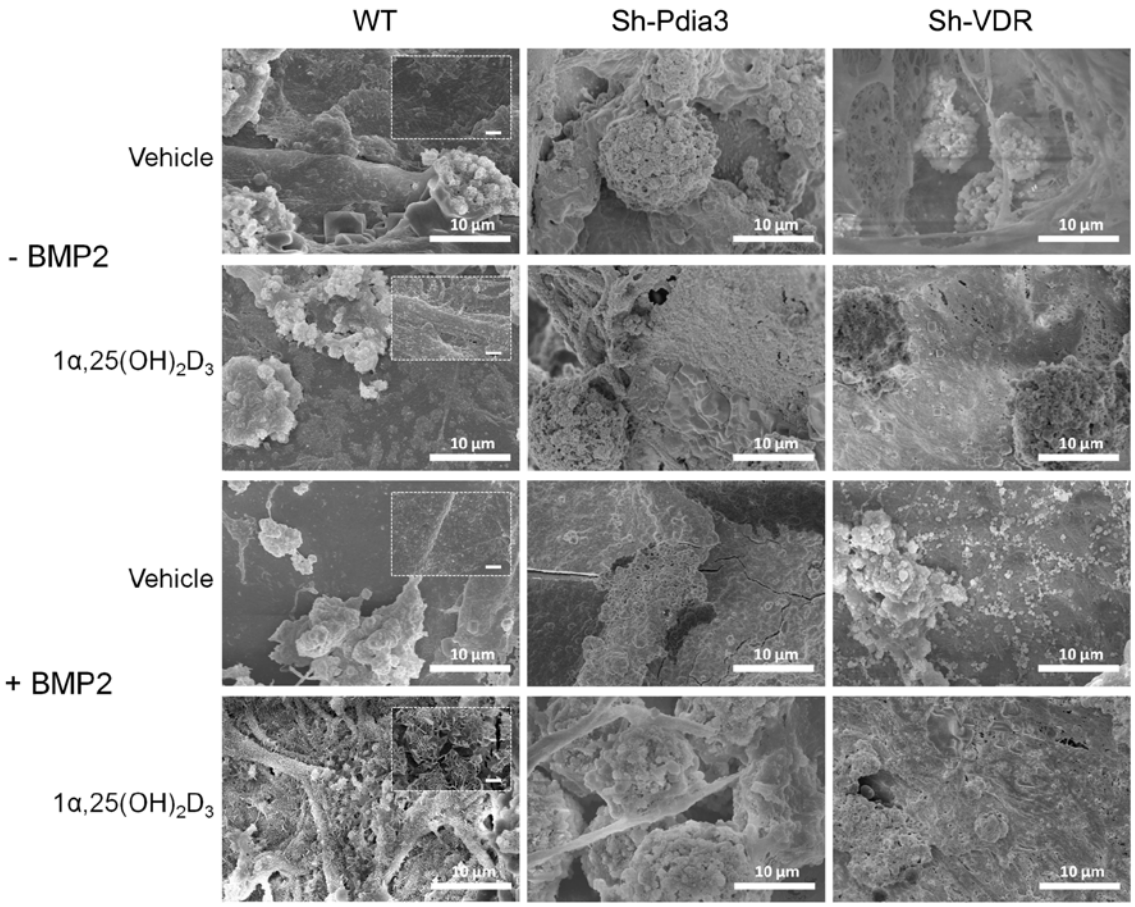

Fig. 5-5 Effect of 1α,25(OH)2D3 and BMP2 on morphology of the mineralized matrix at high magnification. Cells were cultured and treated as described previously. At 8 weeks, the constructs were bisected and the cut surface examined by SEM (magnification= 2K). The images were digitally enlarged from the original image to show the details. The scale bar represents 1μm.

5.4 Discussion

The results of this study demonstrate that BMP2 and 1α,25(OH)2D3 act in concert to enhance osteoblast differentiation in both 2D and 3D cultures. The intent of the experimental design was to examine the potential role of rapid responses to 1α,25(OH)2D3 in osteoblast differentiation by exposing the cultures to a 15 minute pulse of the secosteroid at each change of medium. This is different from the previous work where osteoblast differentiation was primed by exposure to BMP2 prior to 24 hours treatment with 1α,25(OH)2D3 (32). We found that even short duration treatment with 1α,25(OH)2D3 was sufficient to stimulate osteoblast differentiation in 2D culture and regulate mineralization in 3D culture, indicating that membrane-associated rapid signaling was involved.

As anticipated, Sh-Pdia3 cells had reduced levels of Pdia3 mRNA and Sh-VDR cells had reduced levels of Vdr. Moreover, reduced expression of one receptor did not have an appreciable effect on expression of the other receptor. In contrast, diminished levels of both receptors caused marked increase in Bmp2 and its inhibitor Nog. Furthermore, baseline levels of mRNAs for osteoblast marker genes varied with the cell line. Whereas cells silenced for Pdia3 had reduced expression of mRNAs for alkaline phosphatase and osteocalcin compared to wild type MC3T3-E1 cells, VDR-silenced cells had higher levels of these mRNAs. In contrast, Sh-Pdia3 cells had normal levels of mRNA for osteopontin whereas Sh-VDR cells had markedly reduced levels of mRNAs for this extracellular matrix protein. These observations suggest that signaling pathways mediated by these receptors differentially regulate these mRNAs, potentially via ligand binding by low levels of 1α,25(OH)2D3 (10^{-11} to 10^{-13} M) present in the medium due to the fetal bovine serum (33), and this may have been sufficient to stimulate cell response (34). Even so, the marked differences between the two cell lines indicate different roles for each receptor, which are evident when only one receptor is functional.

The 2D culture studies demonstrated that the rapid signaling pathways activated by 1α,25(OH)2D3 involve both receptors. Wild type MC3T3-E1 cells exhibited increased mRNAs for Alp, Bglap, and Spp1. Importantly, Bmp2 and Nog were also upregulated. Others have shown that expression of Bmp2 can be upregulated by PKC activators, PMA and phorbol ester (35). Given the fact that 1α,25(OH)2D3 causes a rapid increase in PKC in MC3T3-E1 cells (7), it is likely that 1α,25(OH)2D3 increased Bmp2 expression through PKC-dependent rapid responses.

Reduced expression of either Pdia3 or Vdr blocked the stimulatory effects of the secosteroid on all mRNAs examined, except Spp1. Expression of osteopontin is under regulation of vitamin D response element (VDRE) (36), thus it is not surprising that the effect on Spp1 was greater in Sh-VDR cells than in Sh-Pdia3 cells, but in neither cell line was 1α,25-(OH)2D3-dependent Spp1 expression completely inhibited. Reduced expression of Pdia3 completely abrogated expression of mRNAs for osteocalcin. These observations suggest that Pdia3 action is downstream of VDR for Spp1 but upstream of VDR signaling for Bglap expression and that at least some of the stimulatory effects of 1α,25(OH)2D3 on osteoblast differentiation may be mediated by BMP2. Interestingly, neither Runx2 nor Dlx5 was affected by 1α,25(OH)2D3 although both have been associated with BMP2 signaling (28).

Our results based on 2D cultures demonstrate that 1α,25(OH)2D3 and BMP2 enhance osteoblastic differentiation, as has been shown by others (37), but data also exist showing that BMP2 can act to inhibit 1α,25(OH)2D3-stimulated osteocalcin expression (38). BMP2 dose is a critical element in determining the outcome. We used a low dose of 50 ng/ml, whereas the latter study used a 10-fold high concentration of 500 ng/ml.

By itself, BMP2 had no effect on expression of Pdia3, Vdr, Bmp2, or Nog in wild

type cells or in either of the silenced cell lines. Similarly, BMP2 did not affect expression of Runx2, Bglap or Spp1. In contrast, BMP2 caused a small but significant increase in Dlx5, and the effect was comparable in wild type, Sh-Pdia3, and Sh-VDR cells. BMP2 also caused a small increase in Alp in wild type cells, but not in alkaline phosphatase activity. Even though BMP2 did not stimulate Bglap in wild type cells, levels of this mRNA were actually reduced in Sh-VDR cells. Taken together these observations suggest that under the experimental conditions used for the 2D cultures, BMP2 exposure alone was insufficient to stimulate osteoblastic differentiation to the extent normally associated with BMP2 action unless the cells are first primed with 1α,25(OH)2D3.

The synergistic increase in Alp and alkaline phosphatase activity observed when wild type cells were primed with 1α,25(OH)2D3 and then treated with BMP2 supports this hypothesis. This was most likely due to the synergistic increase in Vdr expression, indicating that enhanced response to 1α,25(OH)2D3 precedes enhanced response to BMP2. The combination treatment did not affect expression of Pdia3, Nog, Runx2, or BMP2 expression. The expression of Dlx5 in the wild type cells with the combined treatment was comparable to Dlx5 in cells treated with BMP2 alone. We did not assess expression of BMP2 receptor subunits or of components of the BMP2-dependent SMAD signaling pathway, so it is possible that Bmp2 was increased, but the cells might not have been competent to respond to endogenously generated protein.

Importantly, Vdr expression was not sensitive to BMP2 in the Sh-Pdia3 cells or in the Sh-VDR cells, either when treated with BMP2 alone or in combination with 1a,25(OH)2D3. Vdr expression is regulated via VDR directly (39) and via mechanisms resulting in activation of the ERK1/2 ERK1/2 family of mitogen activated protein kinases (MAPK), such as those due to Pdia3 dependent signaling (40). Even when VDREs are

present in the promoter, as they are for osteocalcin and osteopontin (36,41), Pdia3 signaling plays an important role in regulating their expression by 1α,25(OH)2D3 either alone or in combination with BMP2.

The loss of a differentiated osteoblast phenotype in Sh-Pdia3 cells may be due in part to its effect on Vdr expression. Reduced levels of Pdia3 blocked the increase in Vdr caused by the combination treatment and reduced Bmp2 expression to levels below baseline, although even baseline levels of BMP2 were significantly greater in the Sh-Pdia3 cells than in WT. However, reduced levels of VDR also reduced Bmp2, indicating that the interaction of the two signaling pathways is complex. Interestingly, VDR was found to interact with Pdia3 to initiate rapid responses in fibroblasts (42).

There appears to be feedback involved as well. To our surprise, in MC3T3-E1 cells treated with 1α,25(OH)2D3 and BMP2, Dlx5 levels in Sh-Pdia3 were increased 0.5 fold over levels in wild type cells and 2.7 fold over baseline; in Sh-VDR cells Dlx5 was increased 1 fold over wild type and 3.4 fold over baseline. This result suggests that Dlx5 is normally suppressed by 1α,25(OH)2D3 via Pdia3 and VDR dependent pathways. The reverse is true for alkaline phosphatase. Alp expression depends on both Pdia3 and VDR, but the stimulatory effect of the combination on enzyme activity is mediated by VDR only.

Taken together, our results support the hypothesis that there is cross talk between the signaling pathways activated by each ligand. 1α,25(OH)2D3 activates Pdia3 dependent PKC, PLC and PLA2 signaling in osteoblasts (43-45), as well as ERK1/2 MAPK (40). Others have shown that 1α,25(OH)2D3 can enhance BMP2 signaling by increasing the phosphorylation of receptor-regulated Smads through PKC alpha (46,47) and MAPKs may also interact with Smads to modulate the interaction of BMP2 and 1α,25(OH)2D3 pathways. In addition, VDR mediates the regulation of

osteoblasts including VDRE-dependent gene expression as well as rapid activation of transcaltachia at the plasma membrane via voltage gated ion channels, providing another means of modulating rapid responses to 1α,25(OH)2D3 and downstream responses to BMP2.

The 3D cell culture model enabled us to examine the interactive effects of 1α,25(OH)2D3 and BMP2 on biomineralization. We used the same experimental design as for the 2D cultures, exposing the cultures to a 15 minute pulse of 1α,25(OH)2D3 at each medium change prior to adding BMP2. FBS was present in the cultures to ensure that the cells could proliferate. Because of the low levels of 1,25(OH)2D3 in the media due to the FBS, it is not possible to ascribe the effects of the hormone, either alone or in combination with BMP2, to rapid responses per se. Even with this shortcoming, however, the study shows definitively that mineral deposition is regulated by 1α,25(OH)2D3 and BMP2 in an interactive manner.

By itself, BMP2 treatment increased mineral deposition in wild type constructs and this effect was enhanced by the pulse treatment with 1α,25(OH)2D3. The medium used for these studies contains beta-glycerophosphate, a substrate for alkaline phosphatase. Alkaline phosphatase was upregulated by both factors, thereby releasing free phosphate and increasing the potential for calcium phosphate deposition (48). Interestingly, 1α,25(OH)2D3 alone inhibited mineral deposition in the wild type cultures supporting previous studies showing that 1α,25(OH)2D3 blocks terminal differentiation of osteoblasts (21-23).

Others have observed enhanced osteogenic potential in 2D cultures of osteoblasts from VDR knockout mice (49). In our study, we found that suppression of either Pdia3 or VDR resulted in a dysregulation of mineral deposition in the 3D cultures. In the Sh-Pdia3 constructs, the amount of mineral was greater than in either wild type or in Sh-VDR constructs at 4 weeks and more mineral was present in the Sh-VDR

constructs at 4 weeks than in WT constructs. At 8 weeks, mineral volume in Sh-Pdia3 constructs and Sh-VDR constructs was comparable and more than 20-fold greater than in wild type cultures. The increase in mineral in the Sh-Pdia3 cultures may have been due to increased Alp expression and corresponding increase in enzyme activity, resulting in an increase in inorganic phosphate production due to hydrolysis of beta-glycerophosphate (50). In addition, Sh-Pdia3 cultures lacked Bglap expression and osteocalcin provides an inhibitory control on crystal size during calcium phosphate deposition in the extracellular matrix (51). Reduced levels of osteocalcin may have played a role in the Sh-VDR constructs as well. These data suggest that by depletion of either of the two receptors, osteoblasts can escape from the inhibitory effect of 1α,25(OH)2D3 on their terminal differentiation and mineralization.

The 20-fold increase in mineralized volume seen in 3D cultures of Sh-Pdia3 and Sh-VDR cells compared to wild type cell constructs was greater than the 10-fold increase in mineral seen in cultures treated with BMP2. This was an unexpected finding. These data suggest that the inhibition in calcium phosphate deposition due to 1α,25(OH)2D3 may be a more dominant regulatory control than BMP2-dependent stimulation of mineral formation. If this is the case, mineral content of constructs cultured under the combination regimen should not be greater than in the constructs treated with the secosteroid alone. This is the case. At 4 weeks in the absence of BMP2, Sh-Pdia3 constructs were mineralized to a comparable extent, whether they were treated with 1α,25(OH)2D3 or not. Treatment with BMP2 alone or BMP2 + 1α,25(OH)2D3 increased mineral deposition in wild type and Sh-VDR cultures, but the amount of mineral did not exceed that seen in Sh-Pdia3 constructs. These relationships were also evident at 8 weeks. However, 1α,25(OH)2D3 enhanced mineral in wild type cultures and decreased it in Sh-VDR cultures. These results provide strong

circumstantial evidence that both receptors are required for the cross-talk with BMP2 to occur. Interestingly, in Sh-VDR cells, 1α,25(OH)2D3 had a strong inhibitory effect on mineralization at both 4 and 8 weeks unlike what was seen in wild type cells. We believe that these data suggest the existence of a 1α,25(OH)2D3 induced VDR independent inhibitory pathway in mineralization.

With regard to BMP2, our data demonstrated that the effect of BMP2 treatment remained intact in Sh-VDR cells. Therefore, as expected, VDR does not participate in effects induced by BMP2 alone. However, to our surprise, in Sh-Pdia3 cells, not only is the synergistic increase absent but also the stimulatory effect of BMP2 does not take place. These results suggest that Pdia3 may be important to the proper functioning of BMP2 in osteoblast mineralization.

In summary, we found that the combination treatment of 1α,25(OH)2D3 and BMP2 combined treatment synergistically increased osteoblast associated gene expression in the 2D culture. This effect is mediated through both VDR and Pdia3 with VDR having a dominant role. In the 3D study, wild type cells treated with both factors also exhibited a synergistic increase in the mineralized volume, and a difference in morphology of the mineral deposition. Silencing of either receptor strongly increased the basal level of mineralization. Silencing Pdia3 resulted in no response to both factors, whereas silencing VDR caused a significant decrease in mineralized volume after 1α,25(OH)2D3 treatment, which reveals the different nature of the two receptors in mediating osteoblast mineralization. Based on these results, we believe that 1α,25(OH)2D3 may be a valuable additive to BMP2, which is already used clinically. Moreover, due to the dominating role of Pdia3 and VDR in regulating osteoblast mineralization, they may serve as potential targets to promote osteogenesis and mineralization for bone tissue engineering purposes.

5.5 References

1. Holick, M. F. (2006) *J Clin Invest* **116**, 2062-2072
2. Holick, M. F. (2007) *N Engl J Med* **357**, 266-281
3. Lee, C. S., Chen, J., Wang, Y., Williams, J. K., Ranly, D. M., Schwartz, Z., and Boyan, B. D. (2011) *Bone* **49**, 419-427
4. Chen, J., Lee, C. S., Coleman, R. M., Yoon, J. Y., Lohmann, C. H., Zustin, J., Guldberg, R. E., Schwartz, Z., and Boyan, B. D. (2009) *Calcif Tissue Int* **85**, 134-145
5. Huhtakangas, J. A., Olivera, C. J., Bishop, J. E., Zanello, L. P., and Norman, A. W. (2004) *Mol Endocrinol* **18**, 2660-2671
6. Walters, M. R., Rosen, D. M., Norman, A. W., and Luben, R. A. (1982) *J Biol Chem* **257**, 7481-7484
7. Chen, J., Olivares-Navarrete, R., Wang, Y., Herman, T. R., Boyan, B. D., and Schwartz, Z. (2010) *J Biol Chem* **285**, 37041-37050
8. Boyan, B. D., Bonewald, L. F., Sylvia, V. L., Nemere, I., Larsson, D., Norman, A. W., Rosser, J., Dean, D. D., and Schwartz, Z. (2002) *Steroids* **67**, 235-246
9. Mizwicki, M. T., Keidel, D., Bula, C. M., Bishop, J. E., Zanello, L. P., Wurtz, J. M., Moras, D., and Norman, A. W. (2004) *Proc Natl Acad Sci U S A* **101**, 12876-12881
10. Zanello, L. P., and Norman, A. W. (2004) *Proc Natl Acad Sci U S A* **101**, 1589-1594
11. Kraichely, D. M., and MacDonald, P. N. (1998) *Front Biosci* **3**, d821-833
12. Breen, E. C., van Wijnen, A. J., Lian, J. B., Stein, G. S., and Stein, J. L. (1994) *Proc Natl Acad Sci U S A* **91**, 12902-12906
13. Li, Y. C., Pirro, A. E., Amling, M., Delling, G., Baron, R., Bronson, R., and Demay, M. B. (1997) *Proc Natl Acad Sci U S A* **94**, 9831-9835
14. Yoshizawa, T., Handa, Y., Uematsu, Y., Takeda, S., Sekine, K., Yoshihara, Y., Kawakami, T., Arioka, K., Sato, H., Uchiyama, Y., Masushige, S., Fukamizu, A., Matsumoto, T., and Kato, S. (1997) *Nat Genet* **16**, 391-396
15. Amling, M., Priemel, M., Holzmann, T., Chapin, K., Rueger, J. M., Baron, R., and Demay, M. B. (1999) *Endocrinology* **140**, 4982-4987
16. Boyan, B. D., Sylvia, V. L., McKinney, N., and Schwartz, Z. (2003) *J Cell Biochem* **90**, 1207-1223
17. Wang, Y., Chen, J., Lee, C. S., Nizkorodov, A., Riemenschneider, K., Martin, D., Hyzy, S., Schwartz, Z., and Boyan, B. D. (2010) *J Steroid Biochem Mol Biol* **121**, 257-260
18. Matsumoto, T., Igarashi, C., Takeuchi, Y., Harada, S., Kikuchi, T., Yamato, H., and Ogata, E. (1991) *Bone* **12**, 27-32
19. Halvorsen, Y. D., Franklin, D., Bond, A. L., Hitt, D. C., Auchter, C., Boskey, A. L., Paschalis, E. P., Wilkison, W. O., and Gimble, J. M. (2001) *Tissue Eng* **7**, 729-741
20. Matsumoto, T., Kawanobe, Y., Morita, K., and Ogata, E. (1985) *J Biol Chem* **260**, 13704-13709

21. Slater, M., Patava, J., and Mason, R. S. (1994) *J Bone Miner Res* **9**, 161-169
22. Lynch, M. P., Stein, J. L., Stein, G. S., and Lian, J. B. (1995) *Exp Cell Res* **216**, 35-45
23. Ecarot, B., and Desbarats, M. (1999) *Endocrinology* **140**, 1192-1199
24. Bonewald, L. F., Harris, S. E., Rosser, J., Dallas, M. R., Dallas, S. L., Camacho, N. P., Boyan, B., and Boskey, A. (2003) *Calcif Tissue Int* **72**, 537-547
25. Boyan, B. D., Bonewald, L. F., Paschalis, E. P., Lohmann, C. H., Rosser, J., Cochran, D. L., Dean, D. D., Schwartz, Z., and Boskey, A. L. (2002) *Calcif Tissue Int* **71**, 519-529
26. Bonewald, L. F., Kester, M. B., Schwartz, Z., Swain, L. D., Khare, A., Johnson, T. L., Leach, R. J., and Boyan, B. D. (1992) *J Biol Chem* **267**, 8943-8949
27. Dosier, C. R., Erdman, C. P., Park, J. H., Schwartz, Z., Boyan, B. D., and Guldberg, R. E. (2012) *J Mech Behav Biomed Mater* **11**, 112-122
28. Lee, M. H., Kim, Y. J., Kim, H. J., Park, H. D., Kang, A. R., Kyung, H. M., Sung, J. H., Wozney, J. M., and Ryoo, H. M. (2003) *J Biol Chem* **278**, 34387-34394
29. Ulsamer, A., Ortuno, M. J., Ruiz, S., Susperregui, A. R., Osses, N., Rosa, J. L., and Ventura, F. (2008) *J Biol Chem* **283**, 3816-3826
30. Martin, J. Y., Schwartz, Z., Hummert, T. W., Schraub, D. M., Simpson, J., Lankford, J., Jr., Dean, D. D., Cochran, D. L., and Boyan, B. D. (1995) *J Biomed Mater Res* **29**, 389-401
31. Peister, A., Deutsch, E. R., Kolambkar, Y., Hutmacher, D. W., and Guldberg, R. E. (2009) *Tissue Eng Part A* **15**, 3129-3138
32. Schwartz, Z., Sylvia, V. L., Liu, Y., Dean, D. D., and Boyan, B. D. (1998) *Endocrine* **9**, 273-280
33. Schwartz, Z., Brooks, B., Swain, L., Del Toro, F., Norman, A., and Boyan, B. (1992) *Endocrinology* **130**, 2495-2504
34. Schwartz, Z., Schlader, D. L., Ramirez, V., Kennedy, M. B., and Boyan, B. D. (1989) *J Bone Miner Res* **4**, 199-207
35. Helvering, L. M., Sharp, R. L., Ou, X., and Geiser, A. G. (2000) *Gene* **256**, 123-138
36. Nishikawa, J., Matsumoto, M., Sakoda, K., Kitaura, M., Imagawa, M., and Nishihara, T. (1993) *J Biol Chem* **268**, 19739-19743
37. Jorgensen, N. R., Henriksen, Z., Sorensen, O. H., and Civitelli, R. (2004) *Steroids* **69**, 219-226
38. Kawasaki, K., Aihara, M., Honmo, J., Sakurai, S., Fujimaki, Y., Sakamoto, K., Fujimaki, E., Wozney, J. M., and Yamaguchi, A. (1998) *Bone* **23**, 223-231
39. Zella, L. A., Meyer, M. B., Nerenz, R. D., Lee, S. M., Martowicz, M. L., and Pike, J. W. (2010) *Mol Endocrinol* **24**, 128-147
40. Schwartz, Z., Ehland, H., Sylvia, V. L., Larsson, D., Hardin, R. R., Bingham, V., Lopez, D., Dean, D. D., and Boyan, B. D. (2002) *Endocrinology* **143**, 2775-2786
41. Owen, T. A., Bortell, R., Yocum, S. A., Smock, S. L., Zhang, M., Abate, C., Shalhoub, V., Aronin, N., Wright, K. L., van Wijnen, A. J., and et al. (1990) *Proc Natl Acad Sci U S A* **87**, 9990-9994
42. Sequeira, V. B., Rybchyn, M. S., Tongkao-On, W., Gordon-Thomson, C., Malloy,

P. J., Nemere, I., Norman, A. W., Reeve, V. E., Halliday, G. M., Feldman, D., and Mason, R. S. (2012) *Mol Endocrinol* **26**, 574-582
43. Boyan, B. D., Sylvia, V. L., Dean, D. D., Pedrozo, H., Del Toro, F., Nemere, I., Posner, G. H., and Schwartz, Z. (1999) *Steroids* **64**, 129-136
44. Schwartz, Z., Gilley, R. M., Sylvia, V. L., Dean, D. D., and Boyan, B. D. (1999) *Bone* **24**, 475-484
45. Schwartz, Z., Sylvia, V. L., Luna, M. H., DeVeau, P., Whetstone, R., Dean, D. D., and Boyan, B. D. (2001) *Steroids* **66**, 683-694
46. Lee, H. J., Ji, Y., Paul, S., Maehr, H., Uskokovic, M., and Suh, N. (2007) *Cancer Res* **67**, 11840-11847
47. Lee, H. J., Wislocki, A., Goodman, C., Ji, Y., Ge, R., Maehr, H., Uskokovic, M., Reiss, M., and Suh, N. (2006) *Mol Pharmacol* **69**, 1840-1848
48. Hiwada, K., and Wachsmuth, E. D. (1974) *The Biochemical journal* **141**, 283-291
49. Sooy, K., Sabbagh, Y., and Demay, M. B. (2005) *J Cell Biochem* **94**, 81-87
50. Anagnostou, F., Plas, C., Nefussi, J. R., and Forest, N. (1996) *J Cell Biochem* **62**, 262-274
51. Romberg, R. W., Werness, P. G., Riggs, B. L., and Mann, K. G. (1986) *Biochemistry* **25**, 1176-1180

CHAPTER 6. Summary

6.1 The role of Pdia3 in rapid responses to 1α,25(OH)2D3 in osteoblasts.

In chapter 2, we show that 1α,25(OH)2D3 stimulates phospholipase A_2 (PLA_2)-dependent rapid release of *prostaglandin* E_2 (*PGE_2),* activation of protein kinase C (PKC), and regulation of bone related gene transcription and mineralization in osteoblast-like MC3T3-E1 cells (WT) via a mechanism involving Pdia3. Pdia3 was present in caveolae based on co-localization with lipid rafts and caveolin-1. In Pdia3-silenced (Sh-Pdia3) cells, 1α,25(OH)2D3 failed to stimulate PKC and PGE_2 responses; in Pdia3-overexpressing cells (Ov-Pdia3), responses to 1α,25(OH)2D3 were augmented. Downstream mediators of Pdia3, PLA_2 activating protein (PLAA) and arachidonic acid, stimulated similar PKC activation in wild type, Sh-Pdia3 and Ov-Pdia3 cells supporting the hypothesis that Pdia3 mediates the membrane action of 1α,25(OH)2D3. Treatment of MC3T3-E1 cells with 1α,25(OH)2D3 for 9minutes stimulated rapid phosphorylation of extracellular signal-regulated kinases 1 and 2 (ERK1/2) and increased expression of alkaline phosphatase, MMP-13, and osteopontin but decreased expression of osteocalcin, osteoprotegerin (mRNA and protein) and smad2. These effects were attenuated in Sh-Pdia3 cells. Sh-Pdia3 cells produced higher numbers of von Kossa-positive nodules and alizarin red-positive nodules compared to WT cells with or without 1α,25(OH)2D3 treatment while Ov-Pdia3 did not show any mineralization. Our data suggest Pdia3 is an important initiator of 1α,25(OH)2D3 stimulated membrane signaling pathways, which have both genomic and non genomic effects during osteoblast maturation.

6.2 The relative role of the two plasma membrane receptors of 1α,25(OH)$_2$D$_3$, Pdia3 and VDR

In chapter 3, we found that Pdia3 co-localized with VDR and the caveolae scaffolding protein, caveolin-1 on the surface of MC3T3-E1 osteoblasts. Immunoprecipitation showed that both Pdia3 and VDR interacted with caveolin-1. Pdia3 further interacted with phospholipase A2 activating protein (PLAA), whereas VDR interacted with c-Src. 1α,25$(OH)_2D_3$ also changed the interactions and transport of the two receptors and rapidly activated phospholipase A2 (PLA2) and c-Src. Silencing either receptor or caveolin-1 inhibited both PLA2 and c-Src, indicating the two receptors function interdependently. The two receptor dependent rapid responses to 1α,25$(OH)_2D_3$ also regulated gene expression, proliferation and apoptosis of MC3T3-E1 cells. The data demonstrate the importance of both receptors and caveolin-1 in mediating membrane responses to 1α,25$(OH)_2D_3$ and subsequently regulating osteoblast biology.

6.3 The molecular mechanism of Pdia3 as plasma membrane receptor of 1α,25(OH)2D3

In chapter 3, we mutated three amino acids (AAs lysine 214, arginine 282 and cystine 406), which are important for the chaperone function of Pdia3 in the endoplasmic reticulum, and examined their role in the response to 1α,25$(OH)_2D_3$. We also created constructs to overexpress Pdia3 with or without the ER retention signal KDEL to investigate the requirement for plasma membrane Pdia3. Finally, we determined if palmitoylation was involved in translocating Pdia3 to the plasma membrane. We found that AAs K214 and R282 in the calreticulin interaction site and C406 in the isomerase catalytic site were all important to the receptor function of Pdia3. Overexpressing the Pdia3 mutants changed the plasma membrane presence of phospholipase A2 activating protein (PLAA), c-Src, and caveolin-1. Overexpressing Pdia3-KDEL increased plasma membrane localization and augmented baseline protein kinase C (PKC) activity but the

stimulatory effect of 1α,25$(OH)_2D_3$ on PKC was comparable to that seen in wild type cultures. In contrast, 1α,25$(OH)_2D_3$ increased PGE2 release in Pdia3±KDEL cells. Palmitoylation was not required for the plasma membrane association of Pdia3 and was also not important to rapid response. These data indicate that the chaperone functional domain of Pdia3 and subcellular location of Pdia3 are both important to its role in rapid membrane response to 1α,25$(OH)_2D_3$.

6.4 The role of Pdia3 and VDR in 3D mineralization

In chapter 4, we treated wild type, Pdia3-silenced (Sh-Pdia3) and VDR-silenced (Sh-VDR) pre-osteoblastic MC3T3-E1 cells with either 1α,25(OH)2D3 or BMP2, or 1α,25(OH)2D3+BMP2 and measured osteoblast marker expression in 2D culture and mineralization in a 3D poly ε-caprolactone/collagen scaffold model. Quantitative PCR showed silencing Pdia3 or VDR had a differential effect on baseline expression of osteoblast markers. 1α,25(OH)2D3+BMP2 caused a synergistic increase in osteoblast marker expression in WT cells, while silencing either Pdia3 or VDR attenuated this effect. 1α,25(OH)2D3+BMP2 also caused a synergistic increase in Dlx5 in both silenced cell lines, potentially via loss of 1α,25(OH)2D3-dependent inhibition of BMP2-induced osteoblast differentiation. Micro-CT showed the mineralized volume of untreated Sh-Pdia3 and Sh-VDR 3D cultures was greater than WT. 1α,25(OH)2D3 reduced mineral in WT and Sh-VDR cultures; BMP2 increased mineralization; and 1α,25(OH)2D3+BMP2 caused a synergistic increase but only in WT cultures. SEM showed that mineralized matrix morphology in 3D cultures differed for silenced cells compared to WT cells. These data indicate a synergistic cross talk between 1α,25(OH)2D3 and BMP2 toward osteogenesis and mineral deposition, involving both VDR and Pdia3.

6.5 Conclusions

In this thesis, we first mapped out a detailed mechanism of 1α,25$(OH)_2D_3$ stimulated rapid response in osteoblasts. The importance of Pdia3 to the mechanism was shown by silencing and overexpressing Pdia3. The function of Pdia3 in the first step of our pathway was demonstrated. By establishing the role of Pdia3 in 1α,25$(OH)_2D_3$-dependent gene transcription, protein secretion and mineralization, we showed that the proposed Pdia3 signaling pathway has significant physiological relevance.

Second, we found Pdia3 and another proposed membrane receptor, VDR, separately formed complexes with the scaffolding protein caveolin1 and their own downstream mediators PLAA and c-Src, respectively, which were then activated by 1α,25$(OH)_2D_3$ via changing protein-protein interaction with their receptors. These two complexes interact in a way that losing either one of the receptors or the scaffolding proteins would result in an abolishment of the dynamic response to 1α,25$(OH)_2D_3$. The transient 1α,25$(OH)_2D_3$ treatment stimulated differentiation, proliferation and a reduction of apoptosis, which are all mediated through VDR, Pdia3 and caveolin1 receptor complexes.

Third, for the molecular mechanism, we for the first time showed specific amino acids in the chaperone domain of Pdia3 are important for rapid responses possibly through changing the complex formation with its downstream mediators. Deletion of the ER retention signal can increase plasma membrane associated Pdia3 and affect rapid membrane responses to 1α,25$(OH)_2D_3$. Moreover, we found Pdia3 did not associate with plasma membrane through palmitoylation.

Last, we found that the combination treatment of 1α,25(OH)2D3 and BMP-2 synergistically increased osteoblast associated gene expression in the 2D culture. This effect is mediated through both VDR and Pdia3. In the 3D study, wild type cells treated with both factors also exhibited a synergistic increase in the mineralized volume, and a

difference in morphology of the mineral deposition. Silencing of either receptor strongly increased the basal level of mineralization.

Based on these results, we believe that 1α,25(OH)2D3 may be a valuable additive to the BMP-2, which is already used clinically. Moreover, due to the dominating role of Pdia3 and VDR in regulating osteoblast mineralization, they may serve as potential targets to promote osteogenesis and mineralization for bone tissue engineering purposes.

6.6 Discussion and significance

It has been 8 years since the gene identity of this novel membrane receptor was revealed to be Pdia3 (1). However, regardless of the increasing attention on vitamin D, Pdia3 is still not well accepted. This is partially because the supporting evidence for Pdia3 involvement in membrane responses is mainly serum blocking experiments using Pdia3 antiserum (2-6), which has the problem of nonspecificity. In this thesis, we used various molecular approaches including silencing, overexpression, targeted subcellular localization, and site-directed mutagenesis, and we found that all these changes have significant effects on the rapid responses of 1α,25$(OH)_2D_3$. This evidence offers strong support for involvement of Pdia3 by excluding the possibility of nonspecific side effects.

Another reason that Pdia3 is not well accepted as receptor is because its molecular mechanism of action is not fully clear. Pdia3 does not have a traditional 1α,25$(OH)_2D_3$ binding pocket. However, because ligand binding property is the most important feature of a receptor, it is an inevitable problem for discussion. Early studies showed that basal lateral membranes from chicken intestinal epithelium and matrix vesicles from chondrocytes have saturable binding to 1α,25$(OH)_2D_3$ and Pdia3 was found as a major protein in these fractions (5, 7). However, with the existence of other components in these crude fractions, these data are not conclusive. A more recent

report showed that whole cell lysates from Pdia3 (-/-) intestinal cells lost the ability to bind to 1α,25$(OH)_2D_3$ (8). But it is not clear if this is caused by a disruption on direct binding of Pdia3 and 1α,25$(OH)_2D_3$, or by an indirect effect of knocking out Pdia3 on other proteins. The second explanation seems more plausible because in this thesis, we show that Pdia3 is required for the proper function of VDR as well.

X-ray crystallography and nuclear magnetic resonance could give direct evidence of ligand-binding on its receptor in crystal or soluble forms. However, so far, neither of these methods have been able to show that 1α,25$(OH)_2D_3$ binds to Pdia3. Instead of these experimental approaches, we made an effort to computationally predict the binding site of 1α,25$(OH)_2D_3$ on Pdia3 from its resolved 3D structure with the help of Dr. Jeffrey Skolnick and Dr. Hongyi Zhou from the Georgia Institute of Technology, School of Biology. Unfortunately, using this method we were unable to find 1α,25$(OH)_2D_3$ binding sites in Pdia3 (data not shown). Because no current evidence supports direct binding, Pdia3 may play an indirect role in plasma membrane binding to 1α,25$(OH)_2D_3$.

Although Pdia3 may not directly bind with 1α,25$(OH)_2D_3$, we demonstrated it assembles a VDR-involved receptor complex and its chaperone property is required in the rapid response to1α,25$(OH)_2D_3$. These data indicate Pdia3 may serve as a scaffolding protein on the plasma membrane. In the chaperone function study of Pdia3, it was shown to bind with many important plasma membrane proteins (9), which supports the molecular basis that it is a scaffold for large protein complex assembling. In this study, we showed it forms a complex with important 1α,25$(OH)_2D_3$ signal molecules, caveolin1, PLAA and classical VDR. These interactions change in response to 1α,25$(OH)_2D_3$. Moreover, changing a single amino acid in Pdia3 with mutagenesis largely affect these interactions. These data indicate the scaffolding function of Pdia3 is specific and responsive to treatment. It is very different from the traditional view of a chaperone protein, which serves a quality control step in ER and is not involved in

signaling transduction. Interestingly, recent studies in other systems showed that chaperone proteins are also important regulators for receptor function (10-12), which further supports our model.

Overall, this thesis is novel in its proposal of Pdia3 as a scaffolding protein in 1α,25$(OH)_2D_3$ receptor complexes and could have a broad impact in the field of rapid responses to 1α,25$(OH)_2D_3$. First, we used various molecular approaches, which have high specificity, to demonstrate the requirement of Pdia3, helping to increase the awareness and acceptance of Pdia3 in the field. Second, this thesis provides a mechanism by which Pdia3 and VDR interact to elicit rapid responses. This could explain why previous reports separately demonstrated both Pida3 and VDR are required for rapid responses and solve the long time argument over the identity of the membrane receptor for 1α,25$(OH)_2D_3$. Third, this study demonstrates that the chaperone property of Pdia3 is important and gives insight into how the molecular structure of a chaperone protein could be involved in 1α,25$(OH)_2D_3$ receptor complexes. Moreover, our unpublished data indicates Pdia3 may function in other receptor systems besides 1α,25$(OH)_2D_3$, which if confirmed, will have a fundamental impact on understanding the role of chaperone function in receptor associated signal transduction.

As mentioned in the background, 1α,25$(OH)_2D_3$ raises more and more attention because its newly uncovered functions in a broad range of tissues and conditions including cartilage, bone, muscle, brain, immune system, diabetes, cancer and multiple sclerosis. Many of these effects are mediated through the rapid responses to 1α,25$(OH)_2D_3$. Although this thesis only shows the Pdia3 associated receptor complex in osteoblasts, another project in our lab shows this mechanism also exists in chondrocytes (13). Due to the presence of Pdia3 in almost every tissue and the similarity in the reported rapid responses in various models, it is very likely this mechanism is conserved

across cell types and could be applied to most of the aforementioned 1α,25$(OH)_2D_3$ effects.

6.7 References:

1. Nemere I, Farach-Carson MC, Rohe B, Sterling TM, Norman AW, Boyan BD, et al. Ribozyme knockdown functionally links a 1,25(OH)2D3 membrane binding protein (1,25D3-MARRS) and phosphate uptake in intestinal cells. Proc Natl Acad Sci U S A.101:7392-7. 2004.
2. Sequeira VB, Rybchyn MS, Tongkao-On W, Gordon-Thomson C, Malloy PJ, Nemere I, et al. The Role of the Vitamin D Receptor and ERp57 in Photoprotection by 1alpha,25-Dihydroxyvitamin D3. Mol Endocrinol. 2012.
3. Nemere I, Safford SE, Rohe B, DeSouza MM, Farach-Carson MC. Identification and characterization of 1,25D3-membrane-associated rapid response, steroid (1,25D3-MARRS) binding protein. J Steroid Biochem Mol Biol.89-90:281-5. 2004.
4. Boyan BD, Bonewald LF, Sylvia VL, Nemere I, Larsson D, Norman AW, et al. Evidence for distinct membrane receptors for 1 alpha,25-(OH)(2)D(3) and 24R,25-(OH)(2)D(3) in osteoblasts. Steroids.67:235-46. 2002.
5. Nemere I, Schwartz Z, Pedrozo H, Sylvia VL, Dean DD, Boyan BD. Identification of a membrane receptor for 1,25-dihydroxyvitamin D3 which mediates rapid activation of protein kinase C. J Bone Miner Res.13:1353-9. 1998.
6. Pedrozo HA, Schwartz Z, Rimes S, Sylvia VL, Nemere I, Posner GH, et al. Physiological importance of the 1,25(OH)2D3 membrane receptor and evidence for a membrane receptor specific for 24,25(OH)2D3. J Bone Miner Res.14:856-67. 1999.
7. Nemere I, Dormanen MC, Hammond MW, Okamura WH, Norman AW. Identification of a specific binding protein for 1 alpha,25-dihydroxyvitamin D3 in basal-lateral membranes of chick intestinal epithelium and relationship to transcaltachia. J Biol Chem.269:23750-6. 1994.
8. Nemere I, Garbi N, Hammerling GJ, Khanal RC. Intestinal cell calcium uptake and the targeted knockout of the 1,25D3-MARRS (membrane-associated, rapid response steroid-binding) receptor/PDIA3/Erp57. J Biol Chem.285:31859-66. 2010.
9. Elliott JG, Oliver JD, High S. The thiol-dependent reductase ERp57 interacts specifically with N-glycosylated integral membrane proteins. J Biol Chem.272:13849-55. 1997.
10. Wanamaker CP, Green WN. Endoplasmic reticulum chaperones stabilize nicotinic receptor subunits and regulate receptor assembly. J Biol Chem.282:31113-23. 2007.
11. Ramos RR, Swanson AJ, Bass J. Calreticulin and Hsp90 stabilize the human insulin receptor and promote its mobility in the endoplasmic reticulum. Proc Natl Acad Sci U S A.104:10470-5. 2007.
12. Razandi M, Pedram A, Levin ER. Heat shock protein 27 is required for sex steroid receptor trafficking to and functioning at the plasma membrane. Mol Cell Biol.30:3249-61. 2010.
13. Doroudi M, Schwartz Z, Boyan BD. Phospholipase A(2) activating protein is required for 1alpha,25-dihydroxyvitamin D(3) dependent rapid activation of protein kinase C via Pdia3. J Steroid Biochem Mol Biol.132:48-56. 2012.

Appendix

Table A-1. Sequences of real-time PCR primers. Primers were designed by Beacon Designer 7.0 software.

Gene	Forward Primer	Reverse Primer
ALP	GTG GGC ATT GTG ACT ACC	GGT GGC ATC TCG TTA TCC
BSP	TGG AGA CGG CGA TAG TTC	GAG AGT GTG GAA AGT GTG G
GAPDH	TTC AAC GGC ACA GTC AAG G	TCT CGC TCC TGG AAG ATG G
ITPKA	ACC GCC TAC AGC AGA TCC	CCA CAC ACC AGC ACG ATG
MMP13	CTG GTC TTC TGG CAC ACG	TGG GCA GCA ACA ATA AAC AAG
OCN	TCT CTC TGC TCA CTC TGA	GTC TGT TCA CTA CCT TAT TGC
OPN	AAC TCT TCC AAG CAA TTC C	TCT CAT CAG ACT CAT CCG
OTN	GCT GCT CGC CTC TAA ACC	ATG ATG CTG GGA ACT CTC G
PDIA3	CGA TGT GTT GGA ACT GAC G	TTC ATA CTC AGG GGC AAG C
RUNX2	CCG CCA CCA CTC ACT ACC	GAT AGG ATG CTG ACG AAG TAC C
SMAD2	CTC CTC ATC CCA TTC CTG TTC	TGC CCA CAC AAA CCT TTC C
VDR	AGG CAG GCA GAA GAG ATG AG	AGG GAT GAT GGG TAG GTT GTG
OPG	CGC CAA CAT TTG CTT TCG	TGC TCC CTC CTT TCA TCA

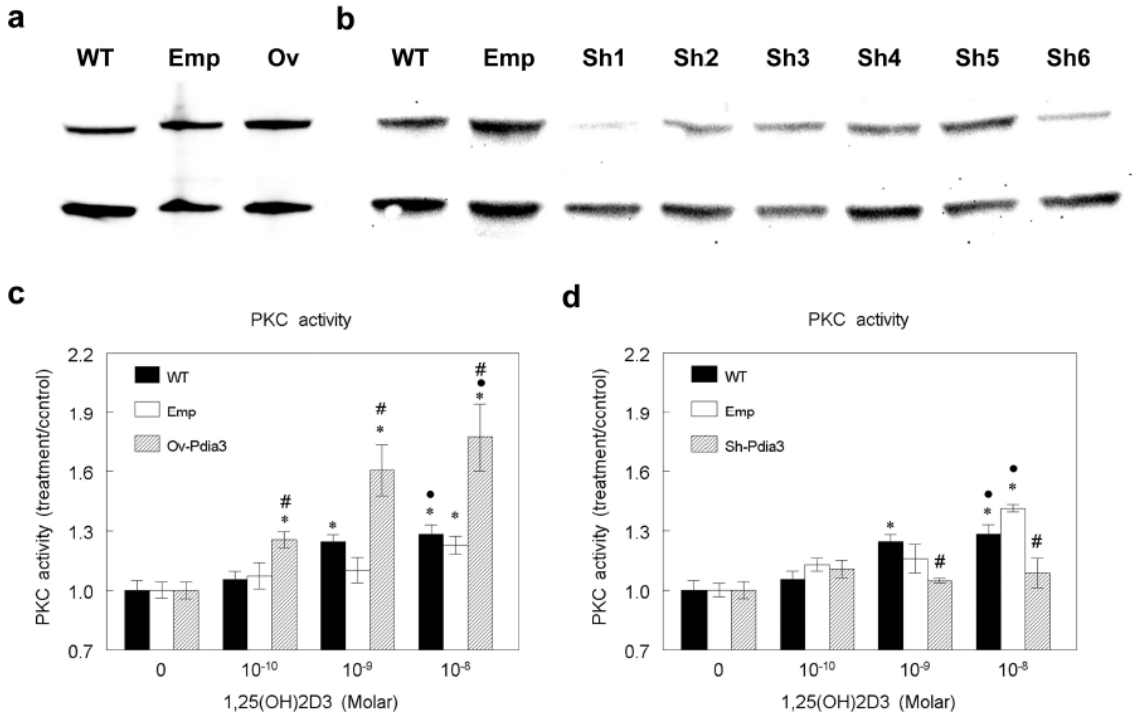

Figure A-1. Western blot of Pdia3 and effect of 1α,25$(OH)_2D_3$ on PKC activity in MC3T3-E1 cells transduced or transfected with empty vector controls for Sh-Pdia3 and Ov-Pdia3. 3a: Western blot of Pdia3 for wild type, empty vector control and Ov-Pdia3 cells. 3b: Western blot of Pdia3 for wild type, empty vector control and vectors containing five different short hairpin RNA sequences. Sh1 was chosen as Sh-Pdia3. 3c: PKC activity for wild type, empty vector control and Ov-Pdia3 cells 3d: PKC activity for wild type, empty vector control and Sh-Pdia3 cells. * $p<0.05$, treatment vs. control; • $p<0.05$, 10^{-8} and 10^{-9} vs. 10^{-10}; # $p<0.05$ Sh-Pdia3 and Ov-Pdia3 vs. WT for the same treatment.

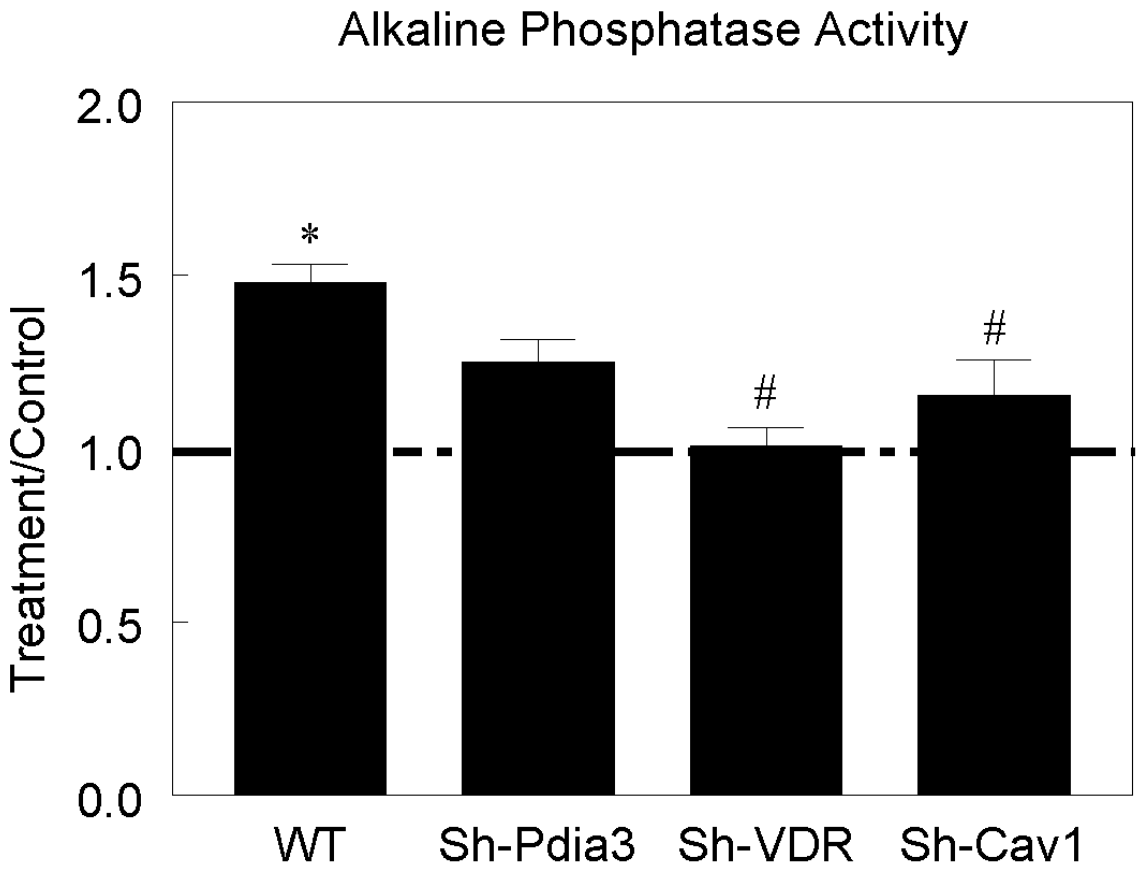

Figure A-2. The role of Pdia3, VDR and caveolin-1 in 1α,25$(OH)_2D_3$ stimulated alkaline phosphatase activity. Wild type cells were treated with vehicle (ethanol) or 10^{-7}M 1α,25$(OH)_2D_3$ for 15 minutes. Cell layers were harvested at 24 hours and lysed. Alkaline phosphatase activity in the cell layer lysate was normalized to total protein. Treatment over control ratios were calculated. The line represents vehicle, which equals to 1. *: $p<0.05$, 1α,25$(OH)_2D_3$ vs. control; #: $p<0.05$, Sh-Pdia3, Sh-VDR and Sh-Cav1 vs. WT.

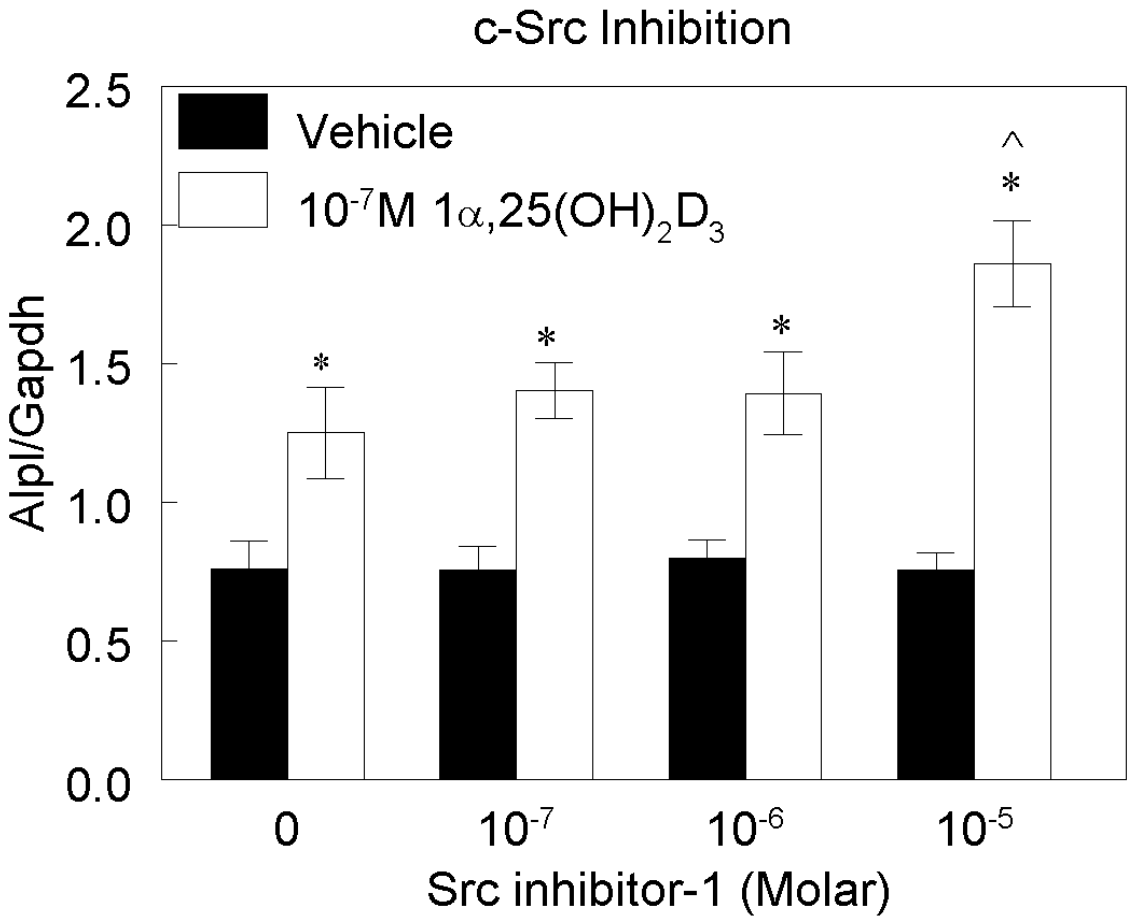

Figure A-3. The effect of c-Src inhibitor-1 on 1α,25$(OH)_2D_3$-stimulated Alpl expression. Wild type cells were treated with vehicle (DMSO) or with 10^{-7}, 10^{-6} or 10^{-5} M c-Src inhibitor-1 (dissolved in DMSO) 30 minutes before and maintained during 15 minutes of 1α,25$(OH)_2D_3$ treatment. mRNA was harvested at 8 hours. Alpl mRNA was normalized to Gapdh. *: $p<0.05$, 1α,25$(OH)_2D_3$ vs. control; ^: $p<0.05$, inhibitor vs. control.

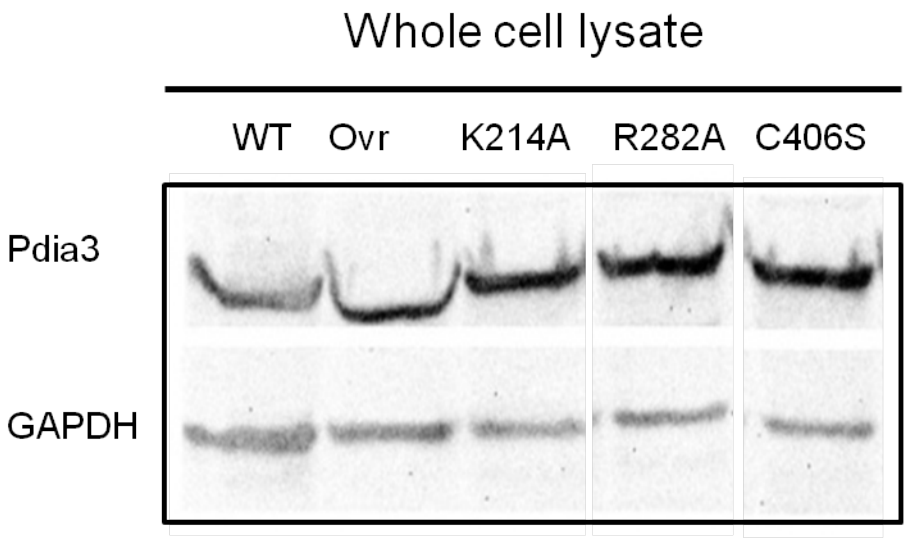

Figure A-4. Overexpression of Pdia3 and its mutants in MC3T3-E1 cells. 10 days after plating, the whole cell lysates of wild type, Ovr, K214A, R282A, and C406S MC3T3-E1 cells were harvested. Western blots against Pdia3 and internal loading control Gapdh were performed.

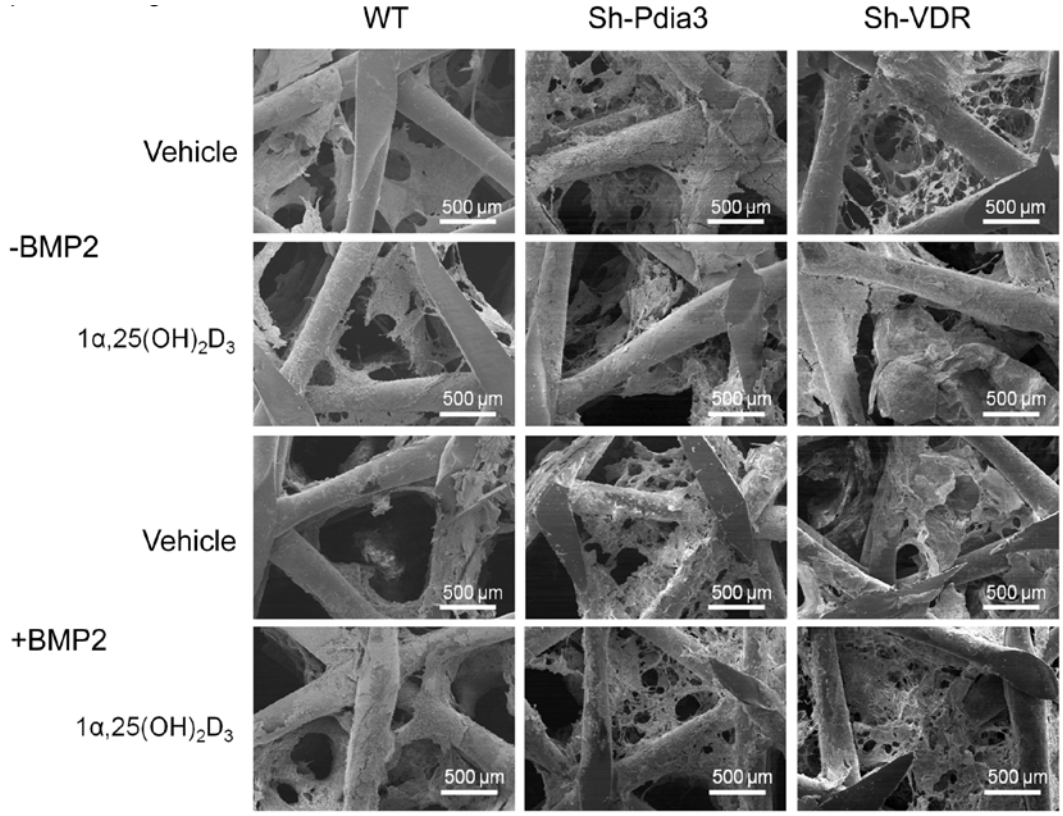

Figure A-5 Effect of 1α,25(OH)2D3 and BMP-2 on the morphology of mineralized matrix at low magnification. Cells were cultured and treated as described previously. At 8 weeks, SEM was used to examine the morphology with magnification of 25.

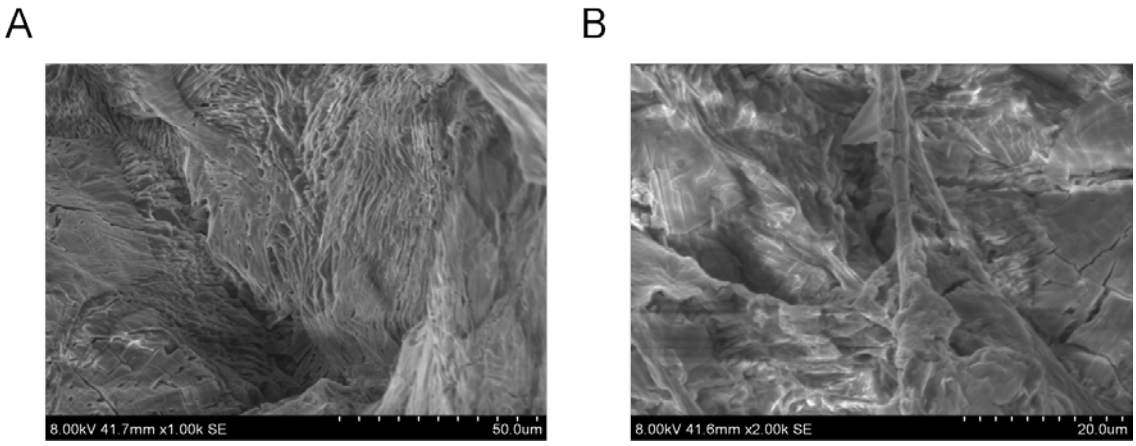

Figure A-6 Effect of decalcification on the morphology of mineralized matrix. Cells were cultured and treated as previously described. At 8 weeks, the mineralized scaffolds were decalcified in EDTA solution for two weeks. SEM was used to examine the morphology with magnification of 2K.

A

Cell	Treatment	Atomic %, O	C	N	Ca	P	Ca/P
WT	BMP-2	17.9	71.8	3.6	2.7	3.1	0.9
WT	1,25D3+BMP-2	22.0	56.4	4.3	3.9	4.7	0.8
Sh-Pdia3		26.6	45.1	8.4	4.5	5.6	0.8
Sh-Pdia3	BMP-2	26.2	41.0	5.1	5.0	6.4	0.8
Mouse Femur		26.6	51.3	10.8	4.4	4.8	0.9

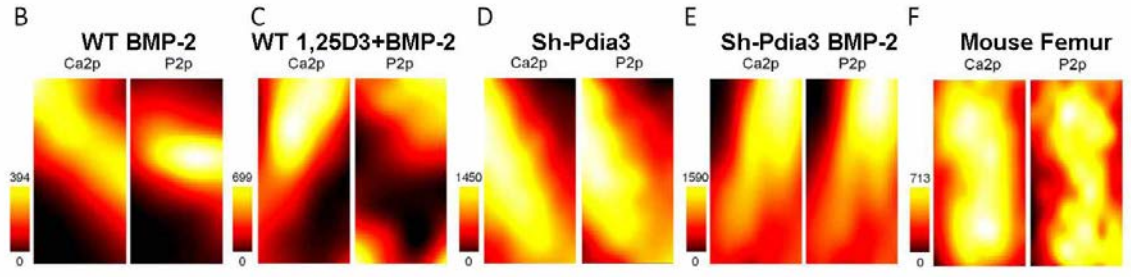

Figure A-7 Effect of 1α,25(OH)2D3 and BMP-2 on Ca and P deposition. Cells were cultured and treated as previously described. At 8 weeks, the general survey (A) and chemical mapping (B to F) were performed using X-ray photoelectron spectroscopy.